Investigation of working memory representations bridging perception & action in the somatosensory domain

Dissertation
zur Erlangung des akademischen Grades
Doktorin der Naturwissenschaften (Dr. rer. nat.)

am Fachbereich Erziehungswissenschaft und Psychologie
der Freien Universität Berlin

vorgelegt von
Lisa Alexandria Velenosi, M. Sc.

Berlin, 2023

Erstgutachter: Prof. Dr. Felix Blankenburg
Zweitgutachter: Prof. Dr. Ryszard Auksztulewicz
Datum der Disputation: 21.12.2023

Acknowledgements

This dissertation would not have been possible without the invaluable help and support from advisors, colleagues, friends, and family.

First of all, I'd like to thank Prof. Felix Blankenburg for his support and guidance as my PhD supervisor, for allowing me the opportunity to explore new ideas and methods, and for creating an open-minded and friendly work environment. I am also grateful to Prof. Ryszard Auksztulewicz for kindly agreeing to evaluate my dissertation. I am incredibly thankful to the Bernstein Center for Computational Neuroscience Berlin for both supporting me financially as well as providing me with a career path after science. The friends and experiences that I gained as a student in the doctoral program have been profound and will not be soon forgotten.

An important thank you to all the current and former members of the NNU: Alex, Christian, Daniela, Evgeniya, Isil, Jakub, Jan, Kathrin, Miro, Pia, Sam, Simon, Till, Timo, Yuan-hao, and Lilla. Without all of you, your motivation, stimulating discussions, but also the fun we had playing volleyball, lab dances, and on coffee breaks, I am certain that I would not have completed this PhD.

Finally, a huge thank you to my friends and family. Your constant reminders and push to "just write" were never appreciated but were nevertheless helpful. Special thanks go to Jojo, Garret, Marina, and the members of the Sanderstraße WG. Of course, this PhD would not have been possible without Richard, who never stopped encouraging me to finish, one way or another. Lastly, a thank you to my family: Ross, Jill, Matthew, Zoe, Addy, Peyton, and Gecko. The goal of becoming "Dr. Venomous" is one step closer to reality.

September 2023

Table of Contents

Abbreviations

ANS	Approximate number system
BOLD	Blood-oxygen level dependent
cvMANOVA	Cross-validated multivariate analysis of variance
DMTS	Delayed-match-to-sample
DMTC	Delayed-match-to-category
EEG	Electroencephalography
fMRI	Functional magnetic resonance imaging
FEF	Frontal eye fields
M1	Primary motor cortex
MFG	Middle frontal gyrus
MT	Middle temporal visual area
MVPA	Multivariate pattern analysis
IPS	Intraparietal sulcus
IFG	Inferior frontal gyrus
LIP	Lateral intraparietal sulcus
NHP	Non-human primate
PMC	Premotor cortex
dPMC	Dorsal premotor cortex
mPMC	Medial premotor cortex
vPMC	Ventral premotor cortex
PFC	Prefrontal cortex
dlPFC	Dorsolateral prefrontal cortex
vlPFC	Ventrolateral prefrontal cortex
PPC	Posterior parietal cortex
RDM	Random dot motion
S1	Primary somatosensory cortex
S2	Secondary somatosensory cortex
SMA	Supplemental motor area
SVR	Support vector regression
WM	Working memory

Abstract

This dissertation comprises original experimental work exploring the intermediate stages of the perception-action loop in the somatosensory domain. The stages correspond to the maintenance of working memory (WM) content, the goal-directed manipulation of the content, and the formation of memory-based decisions. Concurrently, the thesis addresses ongoing debates in cognitive neuroscience, specifically, the localization of the respective WM- and decision-making content. For both debates, the central issue rests with the extent of influence that experimental design has on the localization of the resulting representations.

This dissertation consists of four empirical works which were designed to address these discussions. The works probe the localization of maintained and manipulated somatosensory WM content in humans using functional magnetic resonance imaging (fMRI) in combination with advanced multivariate analysis techniques. In the first study, we explored the WM maintenance of numerosities, an abstract quantity. By employing uncountable somatosensory stimuli, we were able to show that numerosities are maintained by frontal regions in a likely domain-general manner. Secondly, we asked how the manipulation of WM content would change the representational space underlying the content. Indeed, we found that WM representations in the intraparietal sulcus changed with the cognitive demands of the task. In the final two studies comprising this dissertation, we shifted the focus to the localization of the ensuing decision variable, the final WM stage before an action is performed. To this end we improved upon the standard frequency-discrimination task to decouple the decision variable from the sensory-motor features of the task. The third and fourth studies were

identical except for the motor output. In the third study, decisions were communicated via saccade and decision-content was identified in the frontal eye fields, whereas in the fourth, via button press and content was found in the premotor cortex. Therefore, we identified a dissociation with decision-specific information identified in motor-specific regions, providing evidence in favour of the Intentional Framework for perceptual decision making.

Thus, the studies comprising this thesis were designed to provide insight into the intermediate stages of the somatosensory perception-action loop and associated debates. By taking advantage of modifications of experimental paradigms, advanced whole-brain data analysis techniques, and the extensive literature in the somatosensory domain, the dissertation provides evidence in favour of the distributed representation of WM content. The distribution of WM representations is not limited to either frontal or sensory regions. Indeed, the fronto-parietal network - specifically the intraparietal sulcus, inferior frontal gyrus, and the premotor cortex - is necessary for the successful performance of the intermediate stages of the perception-action loop. Therefore, the maintenance of WM content, the manipulation and maintenance of the resulting content, and the computation of the decision variable, all take place in a network consisting primarily of frontal and parietal regions with the specific distribution of WM content depending on the experimental paradigm. The dissertation concludes with a detailed exploration of the stages underlying each of the four empirical studies and discusses the implications of the results for the greater field of cognitive neuroscience.

Zusammenfassung

Diese Dissertation befasst sich mit experimentellen Arbeiten zur Erforschung der Phasen der Wahrnehmungs-Aktions-Schleife im Bereich der Somatosensorik. Die Phasen entsprechen der Aufrechterhaltung von Arbeitsgedächtnisinhalten (WM), der zielgerichteten Manipulation der Inhalte und der Bildung gedächtnisbasierter Entscheidungen. Gleichzeitig greift die Arbeit aktuelle Debatten in der kognitiven Neurowissenschaft auf, insbesondere die Lokalisierung der jeweiligen WM- und Entscheidungsinhalte. Für beide Debatten steht die Frage im Mittelpunkt, inwieweit das experimentelle Design Einfluss auf die Lokalisierung der resultierenden Repräsentationen hat.

Diese Dissertation besteht aus vier empirischen Arbeiten, die diese Diskussionen aufgreifen sollen. Die Arbeiten untersuchen die Lokalisierung von beibehaltenen und manipulierten somatosensorischen WM-Inhalten beim Menschen mit Hilfe der funktionellen Magnetresonanztomographie (fMRI) in Kombination mit fortgeschrittenen multivariaten Analyseverfahren. In der ersten Studie haben wir die WM-Aufrechterhaltung von Zahlenwerten als einer abstrakten Größe untersucht. Durch den Einsatz von nicht zählbaren, somatosensorischen Reizen konnten wir zeigen, dass Zahlenwerte von frontalen Regionen auf eine wahrscheinlich domänenübergreifende Weise aufrechterhalten werden. Zweitens haben wir untersucht, wie die Manipulation von WM-Inhalten den Repräsentationsraum verändern würde, der den Inhalten zugrunde liegt. In der Tat haben wir herausgefunden, dass sich die WM-Repräsentationen im intraparietalen Sulcus mit den kognitiven Anforderungen der Aufgabe veränderten. In den letzten beiden Studien dieser Dissertation haben wir den

Schwerpunkt auf die Lokalisierung der anschließenden Entscheidungsvariablen verlagert, der letzten WM-Phase vor der Ausführung einer Handlung. Zu diesem Zweck verbesserten wir die Standardaufgabe zur Frequenzdiskriminierung, um die Entscheidungsvariable von den sensorisch-motorischen Merkmalen der Aufgabe zu entkoppeln. Die dritte und vierte Studie sind bis auf den motorischen Output identisch. In der dritten Studie wurden die Entscheidungen über Sakkaden mitgeteilt und der Entscheidungsinhalt wurde in den frontalen Augenfeldern identifiziert, während in der vierten Studie die Entscheidungen über Tastendruck mitgeteilt wurden und der Inhalt im prämotorischen Kortex gefunden wurde. Wir haben daher eine Dissoziation festgestellt, bei der entscheidungsspezifische Informationen in motorspezifischen Regionen identifiziert wurden, was für das Intentional Framework für die perzeptuelle Entscheidungsfindung spricht.

Die in dieser Arbeit durchgeführten Studien sollten also einen Einblick in die Phasen der somatosensorischen Wahrnehmungs-Aktions-Schleife und die damit verbundenen Debatten geben. Durch die Nutzung von Modifikationen experimenteller Paradigmen, fortschrittlicher Ganzhirn-Datenanalysetechniken und der umfangreichen Literatur im somatosensorischen Bereich liefert die Dissertation Belege für die verteilte Repräsentation von WM-Inhalten. Die Verteilung der WM-Repräsentationen ist weder auf frontale noch auf sensorische Regionen beschränkt. Tatsächlich ist das fronto-parietale Netzwerk - insbesondere der intraparietale Sulcus, der inferiore frontale Gyrus und der prämotorische Kortex - für die erfolgreiche Ausführung der Zwischenstufen der Wahrnehmungs-Aktions-Schleife notwendig. Die Aufrechterhaltung von WM-Inhalten, die Manipulation und Aufrechterhaltung der resultierenden Inhalte und die Berechnung der Entscheidungsvariablen finden also alle in einem Netzwerk statt, das hauptsächlich aus frontalen und parietalen Regionen besteht, wobei die spezifische Verteilung der WM-Inhalte vom experimentellen Paradigma abhängt. Die Dissertation schließt mit einer detaillierten Untersuchung der Phasen, die jeder der vier empirischen Studien zugrunde liegen, und diskutiert die Implikationen der Ergebnisse für den größeren Bereich der kognitiven Neurowissenschaft.

List of Original Research Articles

1. Uluç I, **Velenosi LA**, Schmidt TT, Blankenburg F (2020). Parametric representation of tactile numerosity in working memory. *Eneuro*, *7*(1).

2. **Velenosi LA**, Wu YH, Schmidt TT, Blankenburg F (2020). Intraparietal sulcus maintains working memory representations of somatosensory categories in an adaptive, context-dependent manner. *NeuroImage*, *221*, 117146.

3. Wu, YH, **Velenosi LA**, Schröder P, Ludwig, S, Blankenburg, F (2019). Decoding vibrotactile choice independent of stimulus order and saccade selection during sequential comparisons. *Human brain mapping*, *40(6)*, 1898 - 1907.

4. Wu, YH, **Velenosi, LA**, Blankenburg F (2021). Response modality-dependent categorical choice representations for vibrotactile comparisons. *NeuroImage*, *226*, 11759.

1. Introduction

The simplest neural network is the stimulus-response network wherein a sensory neuron directly impinges on a motor neuron. Spinal reflexes present a classic example of this simple system. A doctor's reflex hammer to the knee activates a sensory neuron which activates the motor neuron downstream, causing the muscle to contract and the leg to raise. This stereotypical behaviour is extremely limited in that it occurs regardless of the current situation, previous experiences, or the individual's current desires. If the hammer hits the sensory nerve in the knee, the leg will raise. The world, however, is a complicated dynamical system. As a result, any organism that can adapt its motor response to a stimulus based on the current situation, previous experiences, and their current goals has an increased chance of survival. Indeed, it has been suggested that the neocortex has evolved for exactly this purpose (Wolpert et al., 2011).

The inclusion of intermediary neurons within the stimulus-response network endows the system with the ability to both select an appropriate response from an array of possibilities as well as the ability to remember. While the original stimulus may no longer be perceived by the organism, the intermediary neurons continue to pass information related to the stimulus, thereby maintaining a memory of the perceived stimulus. This information may be stored in long-term memory or kept for a short period of time until a decision is made and the appropriate motor plan has been selected and performed. This short-term, goal-oriented memory is called working memory (WM, Baddeley, 2010). Moreover, by increasing the number of neurons between the sensory and motor neurons, the range of possible motor responses to a specific stimulus

increases at an exponential rate. For the past several decades, cognitive neuroscientists have taken it upon themselves to understand and map the cortex's complicated network of stimulus-response contingencies. Researchers have systematically studied the components of WM and have unified the various components through the concept of the perception-action or action-perception loop (Buzsáki, 2021).

In the following sections of this introduction, I provide an overview of the stages of the perception-action loop, before exploring the frequency discrimination and Delayed-Match-To-Sample (DMTS) tasks and multivariate pattern analysis (MVPA) techniques in combination with functional magnetic resonance imagery (fMRI). The tasks, together with fMRI-MVPA, provide an ideal means for probing the intermediate representations of the perception-action loop. To this end, the novel experimental studies comprising this dissertation employed modifications of the tasks, in combination with fMRI-MVPA, to localize and manipulate the intermediate stages of the perception-action loop in the somatosensory system. After the introduction, I summarize the main findings from the four empirical experiments which comprise the novel work in this dissertation. Finally, I conclude the dissertation by exploring the significance of the results within the established literature and contemplate the implications for the current understanding of the perception-action loop and the wider field of human cognitive neuroscience.

1.1. The Perception-Action Loop

It is the transformation of a perceived stimulus, through several intermediate representations, into an action, which underlies behaviours commonly associated with intelligence (D'Esposito & Postle, 2015). For example, during an oral exam, you need to (1) perceive the words spoken by the examiners, (2) remember and combine the individual words to form the question, (3) use your previous knowledge, experience, and current situation to understand and properly respond to the question, (4) decide on the correct answer, (5) before finally preparing and voicing your answer to the question. Indeed, WM acts as a bridge, spanning the gap between the perception of the initial sensory stimulus and the resulting motor output, and is therefore responsible for all intermediate stages between perception and action.

Buzsáki, in his book “The brain from inside-out” (2021) summarizes the history of the perception-action loop, referring to it as an outside-in perspective, originating with Aristotle and having been expanded upon by David Hume. According to this outside-in perspective, all knowledge results from mapping cause-and-effect relationships with a focus on perception. Importantly, Buzsáki points out that this logic, which underlies Western philosophy, requires that WM act as a sort of internal homunculus which decides what to perceive, remember, and how to act. Instead, Buzsáki argues for an inverted action-focused, inside-out, view. By focusing on action instead of perception, a system can learn the mappings between an action and perception, thereby shifting the underlying mechanism from a homunculus to a learning rule. Thus, with an action-focused interpretation of the perception-action loop, and human behaviour more generally, the brain, via intermediary WM representations, can experiment with and learn the consequences of various actions and their resulting effects on perception. As a result, the perception-action loop, with an inside-out focus, enables the evolution of complex behaviours without the need for the inclusion of an internal homunculus (Buzsáki, 2021).

The term WM was proposed in 1960 by Miller, Galanter, and Pribram in their revolutionary book “Plans and Structure of Behavior”. Today, as nicely summarized by van Ede and Nobre (2023), WM is broadly understood as a collective term wherein internally directed selective attention is employed to perform dozens of actions including: protecting representations from decay and interference, reconfiguring neural codes, changing representational states, among others. It is this ability to reconfigure and manipulate stimulus representations that differentiates WM from other memory formats. Moreover, it is the maintenance of WM representations, their manipulation, and transformation into a decision, which is the central focus of this dissertation. In the following sections, the different WM stages of interest, and relevant background information, will be explored in more detail.

1.1.1. Maintenance of Information in Working Memory

The maintenance of information in WM refers to bridging the gap between the perception of the stimulus and eventual motor response. Returning to the oral exam example, maintenance refers to the ability to remember the individual words spoken by

the examiners for a sufficient amount of time such that the question can be understood and an answer prepared. Indeed, the maintenance of information in WM is the most basic, and may be considered, the most important function of WM (Nyberg & Eriksson, 2016).

Interestingly, long-before the concept of WM had been introduced, researchers had already begun to untangle the neural basis of WM maintenance (Marois, 2015). In the 1930s, researchers were attempting to ascribe a role to the prefrontal cortex (PFC). To this end, Jacobsen and colleagues bilaterally lesioned the PFC in non-human primates (NHPs) and revealed deficits in the delayed-response task (Jacobsen, 1935; Jacobsen et al., 1936). The delayed-response task is a staple in WM research and a large portion of the modern literature is a direct result of variations on this simple task. In the classic version of the task, a trial begins with the presentation of a stimulus, which is then removed for a short period of time, before a target stimulus is presented and participants indicate if the target matched the original stimulus. To perform the task, a representation of the original stimulus must be maintained in WM, bridging the gap between the presentation of the original and target stimuli. Thus, Jacobsen and colleagues demonstrated that the PFC is necessary for the WM maintenance of stimuli.

Almost four decades later, two independent groups identified the supposed neural activity underlying WM maintenance. The groups described neurons in the lateral PFC of NHPs which exhibited sustained activity during the WM delay in the delayed-response task (Fuster & Alexander, 1971; Kubota & Niki, 1971). Moreover, trials when the NHPs made a mistake were often associated with a lack of delay-activity in the PFC. Importantly, Goldman-Rakic (1995) later demonstrated that the sustained activity of PFC neurons was specific to the content of WM. Goldman-Rakic and colleagues revealed that PFC neurons possessed a stimulus-specific selectivity profile, meaning they would only exhibit delay-activity when a preferred stimulus or stimulus property was to-be-remembered. As a result, the researchers concluded that these delay-active neurons in the PFC were the single-cell correlates of WM maintenance. However, delay-active neurons are not isolated to the PFC. In fact, delay-activity had also been described in other parts of the cortex (Chelazzi et al., 1998; Fuster & Jervey, 1981). Thus began the debate regarding where and how information is maintained in WM, a debate which

continues to this day and was heavily influenced by the results from Jacobsen, Fuster, and Goldman-Rakic.

1.1.2. Goal-directed Manipulation of Working Memory Information

Whereas the maintenance of WM information specifically refers to the storage of WM content for a short delay, the goal-directed manipulation of WM content can refer to a broad range of mechanisms. Generally, WM manipulation refers to a conscious, goal-oriented change in the WM content and corresponding reconfiguration of the neural code (Veltman et al., 2003). Returning to the oral exam example, the examiners may ask you to perform some mental arithmetic, such as "1 + 2". To answer the question, you will need to manipulate the information perceived (1, 2) to arrive at the correct response (3). As a brief tangent, the dynamic coding hypothesis of WM maintenance suggests that WM content in the PFC is maintained in a stable but dynamic neural representation (Stokes et al., 2013). Note that, according to this theory, the representational state of the neural code is changing whereas the representation remains stable. Thus, because the representation remains stable, dynamic coding does not constitute a form of WM manipulation. To summarize, maintenance refers to a stable WM representation with a potentially dynamic code, and manipulation refers to a change in the WM representation and code for a specific goal or purpose.

The manipulation of WM content inherently encompasses a wide variety of experimental paradigms. Classically, paradigms required participants to mentally reorder lists of stimuli (D'Esposito et al., 1999; Koenigs et al., 2009), compare stimuli with previously presented stimuli (n-back tests, Owen et al., 2005), rotate mental images (Shepard & Metzler, 1971), among many other tasks. Similar to results from the maintenance WM literature, the results from decades of research suggest that the frontal cortex, particularly the PFC, and the superior parietal cortex, are responsible for the goal-directed manipulation of WM content (Nyberg & Eriksson, 2016). Importantly, these studies often don't consider the location of the WM content per se, but instead likely identify the top-down control systems which manipulate the WM content.

The goal-directed manipulation of WM content can be further understood to include the formation of a category or label (Seger & Miller, 2010). In these studies, participants are often asked to classify a stimulus according to a previously known or

newly learned rule (Freedman & Assad, 2016). Studies exploring the formation of a category label often distort the boundary between WM manipulation and the final WM stage in the perception-action loop, the formation of a decision. Indeed, some researchers have suggested a common mechanism underlying categorization and perceptual decision making (Freedman & Assad, 2011). Perceptual decision-making entails forming a decision, often based on WM content, and the localization of the resulting decision will be discussed in the following section of the dissertation. Thus, decision formation is itself a form of WM manipulation, in that it requires the modification of maintained WM representation for the completion of a specific goal.

1.1.3. Memory-based Perceptual Decision Making

Memory-based perceptual decision making refers to the final WM stage in the perception-action loop. Indeed, this stage corresponds to the point, after all relevant information has been collected and manipulated, when a final decision is formed. The decision enables an appropriate motor plan to be prepared and communicated by downstream regions. Returning to the oral exam example, once the question has been comprehended and the appropriate manipulations have been performed (1 + 2), a decision (3) has been reached and can be communicated. Where and how these decisions are formed has been a central neuroscientific and scholarly research topic more generally (see Glimcher, 2003 for a comprehensive historical review).

Classically, signal detection experiments in combination with statistical decision theories such as Signal Detection Theory (Green & Swets, 1966; Macmillan & Creelman, 2004) or Sequential Sampling Methods (Ratcliff et al., 2016), have been employed to probe perceptual decision making (Gold & Shadlen, 2001; Shadlen et al., 1996; Shadlen & Newsome, 1998). Theories of sequential sampling suggest that participants gain evidence in favour of a decision by repeatedly sampling the perceptual stimulus. Then, once sufficient evidence has been collected, a decision boundary is reached and a decision is formed (O'Connell et al., 2018; Ratcliff et al., 2016). The Random Dot Motion (RDM) task has proven to be particularly powerful in localizing decision-specific signals in the visual domain. In the task, participants are presented with randomly moving dots on a screen, some of which are moving in a coherent direction, and participants must identify the direction of motion. Importantly, the amount of coherent motion can be

varied independently of the motion direction, thereby enabling researchers to decouple the decision from the trial-wise sensory information (Parker & Newsome, 1998).

Shadlen, Newsome, and colleagues, having substantial evidence for the middle temporal visual area (MT) to accumulate sensory evidence for the direction of motion in RDM tasks, proceeded to identify the locus of perceptual decision-making. Decisions in the RDM task were communicated by saccades to a pre-determined location. Thus, the researchers chose to focus their search for a perceptual decision-making region to regions already known to be important for the performance of saccades, specifically the lateral intraparietal area (LIP), the frontal eye fields (FEF), and the superior colliculus. When the sensory evidence favoured a saccade to a target within the recorded LIP neuron's receptive field, Shadlen and Newsome identified a gradual increase in LIP neuronal firing rates during stimulus presentation which was maintained until the saccade, the downstream motor plan, was completed. In contrast, when the saccade was away from the receptive field, the firing rate decreased (Shadlen & Newsome, 1996; 2001). The authors proposed that this systematic activity in LIP represented the accumulation of evidence in favour of a decision, as well as the formation of the decision itself, in the RDM task.

Importantly, several features suggest that the activity patterns of LIP neurons represent the accumulation of sensory evidence in favour of a decision instead of merely motor preparation behaviour (Wutz et al., 2001). The change in neuronal firing rate scales with the trial-wise sensory coherence, which, the stereotypical motor preparation is independent of (Shadlen & Newsome, 1998; 2001). Moreover, in a follow-up study, the researchers allowed the NHPs to respond freely. Previously, the NHPs were only able to communicate their decision during a pre-defined decision period. Researchers aligned the trial-wise data according to the initiation of the saccade and found that the ramping in LIP continued to a specific criterion, independent of the trial-wise motion coherence, before a saccade was triggered (Roitman & Shadlen, 2002). Finally, quantitative modelling provides evidence for the sensory evidence, encoded in MT population firing rates (Mazurek et al., 2003), to be temporally integrated and represented by the average firing rate of LIP neurons (Shadlen & Newsome, 1996; Shadlen et al., 1998). Interestingly, similar decision-making behaviour has been identified in other oculomotor

regions such as the FEF (Ding & Gold, 2012; Hanes & Schall, 1996; Kim & Shadlen, 1999), and the superior colliculus (Horwitz & Newsome, 1999; Ratcliff et al., 2003).

The combination of modelling and neurophysiological recordings has been critical for generating testable hypotheses regarding the neural networks and computations underlying memory-guided perceptual decision making (Hanks & Summerfield, 2016). Indeed, the identification of oculomotor regions' involvement in evidence accumulation and decision-making in visual perceptual decision-making tasks has resulted in the so-called Intentional Framework for decision making (Cisek & Kalaska, 2010; Gold & Shadlen, 2007). The Intentional Framework states that the decision variable for a particular perceptual decision will be computed in regions upstream from the eventual motor effector. As per the RDM example with saccade decision-responses, oculomotor regions LIP and FEF integrate the temporal evidence from motion-direction sensitive region MT until a decision criterion is reached and the downstream saccade effectors can be engaged. Whether perceptual decisions are computed in a single, general decision-making region or whether decisions are formed in a task-relevant region, as suggested by the Intentional Framework, remains an open question.

1.2. The Tasks: Frequency Discrimination & Delayed-Match-to-Sample

A short historical detour, the frequency-discrimination task evolved from the simple sensory-discrimination task. The sensory-discrimination task was introduced by Vernon Mountcastle and colleagues (Lamotte & Mountcastle, 1975; Mountcastle et al., 1972; 1990) to enable the differentiation and identification of neural correlates of the perception-action loop. The sensory-discrimination task was itself a modification of the classic delayed-response task wherein a stimulus is presented and then removed for a short period of time and participants must remember the stimulus during the delay to correctly complete the task (Jacobsen, 1935).

In the frequency-discrimination task, Mountcastle and colleagues presented two sequential tactile stimuli vibrating at different frequencies to the index fingers of NHPs while recording neurophysiological data from several regions hypothesized to be involved in the perception and evaluation of somatosensory stimulation. The task

required that the NHPs indicate whether a vibrotactile comparison frequency (f2) was higher or lower than a base frequency (f1). The task can be sub-divided into several individual components which are necessary for its successful completion: (1) NHPs must perceive the base stimulus f1, (2) encode and maintain f1 in WM, (3) perceive the comparison frequency f2, (4) form a decision by comparing f2 against the memory-trace of f1, before finally (5) communicating their decision via a motor response. One of Mountcastle's students, Ranulfo Romo, used extensive variations of the frequency-discrimination task to gradually decipher the somatosensory perception-action loop in NHPs (e.g., Romo et al., 1998; 1999; 2000; 2004; Romo & Salinas, 2003). As described by Romo, the vibrotactile variant of the sensory-discrimination task is ideal for identifying the neural correlates of sensory processing because (1) humans and NHPs perform similarly on the task, (2) the different stages of cognitive processing are spread out in time, and (3) the same neural populations are consistently activated by the vibrotactile stimulus (Romo et al., 2012).

The original frequency-discrimination task was modified after an important observation was made by Romo and colleagues. Originally, the base frequency, f1, was held constant across trials within a run (LaMotte & Mountcastle, 1975; Mountcastle et al., 1990). Romo and colleagues realized that, if the base frequency didn't change, the task could be performed without having to maintain f1 in WM. By performing additional follow-up experiments, they showed that the NHPs were not comparing f2 against f1 but simply classifying f2 as high or low without taking f1 into consideration. Romo and colleagues showed that, by changing f1 on each trial, NHPs could learn to correctly perform the vibrotactile discrimination task, as evidenced by close inspection of the experimental psychophysics (Hernández et al., 1997). As noted by the authors, no matter how well designed a task may seem, participants may develop alternative strategies to complete the task in an unexpected manner (Romo & de Lafuente, 2013). As a result of Romo and colleagues' careful inspection of their experimental data, the vibrotactile discrimination task became, and remains, a powerful tool for the investigation of the neural correlates of the perception-action loop (Romo & de Lafuente, 2013).

While Romo and colleagues have accumulated an invaluable and extensive literature on the neural mechanisms underlying the somatosensory frequency-

discrimination task, a few issues with the experimental design remained. Firstly, with human neuroimaging data, it is not possible to dissociate the WM representation of the first stimulus (f1) from the original perceptual representation of f1. To address this issue, the paradigm was modified such that two separate sensory stimuli are sequentially presented and a retro-cue indicates which of the two stimuli should be encoded in WM (Christophel et al., 2012; Harrison & Tong, 2009; Lepsien et al., 2005; Oberauer & Kliegl, 2001). Moreover, the task no longer requires a comparison of the two initially presented stimuli. Instead, participants decide whether the cued stimulus matches a target stimulus which is presented after the end of the WM delay period. This retro-cue variant of the sensory-discrimination task is commonly used in human WM research because it allows for the dissociation of the maintained WM content from neural processes occurring in parallel, such as perception and motor preparation. Researchers are additionally able to use the "to-be-forgotten" stimulus as a negative control in their analyses, thereby providing an experimental test of the specificity of their WM analyses.

To summarize, the frequency discrimination and DMTS tasks were developed so that researchers could reliably differentiate and investigate the representations underlying the various stages of the perception-action loop. Importantly, by controlling the durations, onsets, and correlations between the different task stages, it is possible to decouple and probe the neural processes underlying the various stages of the perception-action loop. For this reason, all four empirical studies comprising this dissertation employed modifications of the classic task designs. In the following sections of this sub-chapter, I present relevant results from NHP studies. The relevant results from humans are described in the following sections.

1.2.1. Maintenance of Information in Working Memory

Romo and colleagues have employed the frequency-discrimination task, the precursor to the DMTS task, to investigate the neural basis of WM maintenance in the somatosensory domain. Following the literature and their detailed knowledge of the somatosensory perception-action loop pathway, the researchers decided to record neurophysiological data from the primary somatosensory cortex (S1), the secondary somatosensory cortex (S2), as well as frontal regions including the inferior convexity of the PFC – analogous to the dorsolateral prefrontal cortex in humans (dlPFC, Levy &

Goldman-Rakic, 2000), the ventral premotor cortex (vPMC), the dorsal premotor cortex (dPMC), the supplemental motor area (SMA), and the primary motor cortex (M1). Romo and colleagues have shown that the firing rate of neurons in S1 was only modulated by the stimulus during stimulus presentation. In contrast, all downstream regions: S2, PFC, vPMC, dPMC, SMA, and M1, demonstrated a more complicated response profile. The researchers found that all regions downstream from S1, including M1, were modulated by the first frequency and maintained the frequency-specific information in WM during the delay (Barak et al., 2010; Brody et al., 2003; Hernández et al., 2010; Jun et al., 2010; Machens et al., 2005; 2010). Moreover, using the region-specific neuronal latencies, the researchers were able to map the somatosensory processing pathway, beginning in contralateral S1 and continuing to bilateral S2, PFC, vPMC, and finally dPMC & SMA (Hernández et al., 2010). Thus, using the frequency-discrimination task, Romo and colleagues provided striking evidence for all frontal regions, as well as somatosensory and motor regions, to maintain vibrotactile frequency information in WM.

1.2.2. Goal-directed Manipulation of Working Memory Information

Expanding on their previous work, Romo and colleagues used a modification of the frequency-discrimination task design to explore the WM representation of vibrotactile categories (Rossi-Pool et al., 2016). In this study, researchers presented NHPs with two sequential stimuli comprising temporal patterns of electrical stimulation to the wrist. The NHPs needed to decide whether the two patterns were identical. The researchers recorded the neurophysiological activity from neurons in both contralateral S1 and the dPMC, a region which the researchers knew maintained WM representations of stimuli and hypothesized may encode more complicated WM dynamics as well (Hernández et al., 2010). Indeed, they found that, while firing rates in S1 were only modulated by the stimulus during stimulus presentation, the dPMC displayed a more sophisticated response profile. The dPMC firing rates were modulated by the specific trial type, such that it was possible to differentiate whether the stimuli were identical as well as the specific trial-wise ordering of the stimuli. This led the researchers to conclude that the WM information was manipulated and information relating to both the stimulus identities and trial type were maintained in the firing rates of dPMC neurons.

In the visual domain, Freedman and colleagues (2001) performed an important experiment on image categorization with NHPs. The researchers presented the participants with image morphs which had been manipulated so that they were a statistical mixture of a cat and dog. The NHPs were trained to decide which category, cat or dog, the image belonged to. Importantly, because the category-information in the image was independent of the category label, the researchers could differentiate stimulus features from the category label in the neurophysiological recordings. Freedman and colleagues identified category-specific information in the PFC. Ten years later, in two follow-up studies employing categorized directions of motion (Swaminathan & Freedman, 2012) and arbitrary groupings of visual stimuli (Fitzgerald et al., 2012), Freedman and colleagues found that the category-specific WM information was more pronounced in the posterior parietal cortex (PPC), specifically the LIP, than PFC neurons.

The use of arbitrary groupings is especially significant. Arbitrary stimulus groupings do not employ feature-specific categorization rules but are instead taught to participants. Thus, the use of arbitrary groupings provides a means of exploring both the formation and maintenance of novel WM manipulation rules and category representations in WM, without relying on sensory features or previous knowledge. Moreover, in both follow-up studies, the same LIP neurons maintained information on both categories, motion direction and arbitrary groupings. Freedman and colleagues concluded that, not only is the category information identified in LIP unlikely to have originated in the PFC, as previously believed, but that LIP neurons are capable of learning new category information. Therefore, the researchers provided compelling evidence for LIP neurons to manipulate WM content, in this case form a category label, and then feed the manipulated content forward to the PFC (Swaminathan & Freedman, 2012).

1.2.3. Memory-based Perceptual Decision Making

The decision in the frequency-discrimination task, the comparison of two frequencies, takes place after the second vibrotactile frequency (f2) has been presented. Interestingly, during presentation of the second stimulus, all downstream regions recorded by Romo and colleagues, including S2, frontal regions (PFC, vPMC, dPMC,

SMA), and M1, showed a multiplexed modulation of their firing rates which resulted from a combination of neurons modulated by f1 or f2, partially differentiated modulations by the two frequencies, as well as fully differentiated modulations of the neuronal firing rates (Romo & de Lafuente, 2013). Romo and colleagues suggested that the partially and fully differentiated neuronal modulations result from a subtraction operation where neurons with opposing response properties are contrasted. The result of this subtraction is evident in the modulation of the PMC firing rates which scale with the difference in frequency between f2 and f1 (Hernández et al., 2002; 2010; Romo & Salinas, 2003; Romo et al., 2004). Thus, the authors proposed that decisions in the vibrotactile frequency-discrimination task are made by subtracting the first frequency from the second (f2 – f1) and the resulting sign reflects the decision (higher -vs- lower). This was further evidenced by evaluating error trials where the neuronal activity in PMC and other frontal regions correlated with the decision, and not with the stimulus (Hernández et al., 2010).

One major short-coming with the work completed by Romo and colleagues is their focus on the frontal cortex. This is in contrast to Shadlen and Newsome who, while employing the RDM task, had a wider cortical focus. As previously introduced, the RDM is the visual correlate of the tactile frequency-discrimination task in that visual stimuli of randomly moving dots are presented and participants must indicate, either the direction of the motion, or which of two stimuli has more coherent motion. In the RDM task, decisions were often communicated by saccades and Shadlen and Newsome identified a gradual increase of evidence for a specific decision in LIP neuronal firing rates which was maintained until the saccade was completed (Shadlen & Newsome, 1998; 2001).

The Intentional Framework for perceptual decision making, which states that the decision variable for a particular memory-based decision will be in regions upstream from the eventual motor effector (Cisek & Kalaska, 2010; Gold & Shadlen, 2007), aligns well with results from both the RDM and frequency-discrimination tasks. As per the RDM example with saccade decision-responses, oculomotor regions LIP and FEF integrate the temporal evidence from motion-direction sensitive region MT until a decision criterion is reached and the downstream saccade effectors can be engaged (Shadlen & Newsome, 1996; 2001). Whereas Romo and colleagues employed manual responses in their frequency-discrimination tasks and identified memory-based decision

content in the PMC, a region upstream from manual motor-control regions such as M1 (Romo & de Lafuente, 2013).

1.3. Functional Magnetic Resonance Imaging & Multivariate Pattern Analysis

Neurophysiological recordings, as used by Romo, Freedman, Gold, Shadlen, and their colleagues, are an incredibly powerful data set which enable conclusions on the spatial and temporal resolution level of single neurons and circuits to be drawn. At the same time, fMRI, which enables the mapping of specific cognitive functions to neuronal regions, was becoming more common and gaining in popularity. In contrast to neurophysiological data, fMRI data is much slower but allows the simultaneous non-invasive recording of the entire brain, thereby providing a means to conduct neuroscientific research in healthy humans. Experiments with humans additionally benefit from a faster training period (days vs. months) as well as from a post-experiment debriefing session wherein participants describe, to the best of their abilities, what cognitive strategies they employed to complete the task. Furthermore, the simultaneous recording of whole-brain fMRI data facilitated a novel analysis technique known as multivariate pattern analysis (MVPA, also known as multi-voxel pattern analysis, Haxby, 2012; Haxby et al., 2014).

Standard, or univariate, fMRI data analysis treats each voxel in the brain as an isolated individual unit and tests whether the measured Blood-Oxygen-Level-Dependent (BOLD) signal in each voxel significantly varies with the experimental variables being tested (Friston et al., 1995). For example, whether there is an increased BOLD signal during the maintenance of a specific stimulus in WM. MVPA, in contrast, takes into consideration that voxels are part of an inter-dependent system and searches for patterns across the system of neighbouring voxels (Haynes & Rees, 2006; Tong & Pratte, 2012). The idea stems from the assumption that the brain represents information according to a population coding method, which is inherently distributed in space (Pouget al., 2000). Distributed coding presumes that when a stimulus is presented, a subset of neurons in a population will fire in response. This subset of neurons is distributed in space and the pattern is detectable with MVPA, but may not be visible with univariate analysis pipelines (Haynes & Rees, 2006). Accordingly, an increased BOLD

response during WM does not mean that the area is maintaining WM content but may instead reflect ongoing processes which are required for WM, such as attention (Riggall & Postle, 2012). Indeed, fMRI in combination with MVPA (known as fMRI-MVPA) has proven itself to be a powerful technique for identifying and localization information maintained in the brain, even when no difference in BOLD signal is apparent (Haynes, 2015). Thus, due to the powerful nature of the non-invasive analysis pipeline, studies employing fMRI-MVPA have been used to localize information at various stages of the perception-action loop. Consequently, fMRI-MVPA, in combination with modifications of the frequency discrimination and DMTS experimental paradigms, was used in all four empirical studies comprising this dissertation.

1.3.1. Maintenance of Information in Working Memory

Armed with a new and powerful data analysis technique, researchers returned to the DMTS task to localize maintained WM content using fMRI-MVPA. Following tradition in human cognitive neuroscience, researchers began by presenting visual stimuli to participants, then expanded to stimuli across all sensory modalities. In contrast to the majority of previous fMRI studies which had relied on univariate analysis methods, researchers employing fMRI-MVPA identified visual WM content in the early visual cortices (Christophel et al., 2012; Riggall & Postle, 2012). Expanding to other sensory modalities, WM content of vibrotactile stimuli was identified in the somatosensory cortices (Schmidt et al., 2017), and studies identified auditory WM content in auditory cortices (Uluç et al., 2018; Yu et al., 2021). Importantly, the observation that sensory WM content is maintained in regions essential for the initial perception of the sensory content features supported the idea of grounded cognition (Barsalou, 2008). Indeed, researchers suggested that sensory WM likely relies on cortical areas necessary for the perceptual processing of the stimuli, culminating in the feature-specific memory stores theory of WM (Pasternak & Greenlee, 2005). Both grounded cognition and feature-specific memory stores fit well with the influential multicomponent model of WM proposed by Baddeley and Hitch (1974).

The original multicomponent model of WM consisted of a visuospatial sketchpad and a phonological loop, each able to maintain specific content, visuospatial or verbal, respectively, in WM, as well as a central executive. The model was later updated to

include an episodic buffer for maintaining episodic memories in WM (Baddeley, 2000). Baddeley and Hitch proposed that the central executive selected and coordinated what information entered the various memory stores, which acted as slaves of the central executive (Baddeley & Hitch, 1974). The Baddeley and Hitch multicomponent model of WM has been incredibly influential in WM research and there have been ongoing efforts to discover and localize the underlying neural implementation of the various model components (Andrade, 2002).

In accordance with the Baddeley and Hitch model, the feature-specific memory stores theory of WM, and later, the Sensory-Recruitment theory of WM (D'Esposito, 2007; D'Esposito & Postle, 2015), suggest that WM is not a unitary system localized in the PFC but instead results from the combined activity of a network of brain regions. The WM content is stored in sensory regions and the PFC acts as a control mechanism, analogous to the central executive (Awh & Jonides, 2001; D'Esposito, 2007; Jonides et al., 2005; Postle, 2006). Christophel and colleagues (2017) summarized the plethora of results from WM studies, from both the neurophysiological and fMRI-MVPA fields, exploring the maintenance of content-specific information in WM. The resulting maps for the neurophysiological and human data are surprisingly concurrent and provide strong evidence for the wide-spread maintenance of WM content across the cortex, including the PFC and PPC. Interestingly, studies employing more abstract stimuli, such as language characters (Corrreia et al., 2014; Yan et al., 2021), numerosity (Nieder et al., 2002; Nieder, 2012; 2016), and analogue properties (Spitzer et al., 2014), have identified WM content in a broad network including the PFC. The results suggest that the more complicated or abstract the stimulus, the more wide-spread the distribution of WM content and involvement of higher-order brain regions, particularly the PFC and PPC (Christophel et al., 2017).

Finally, there are also researchers who argue that only the PFC is capable of maintaining WM content (Constantinidis et al., 2018), or only higher-order brain regions such as the PFC and PPC (Xu, 2017; Xu, 2018). The researchers contend that sensory regions are not able to protect WM representations from distractors and that the activity in sensory regions likely reflects feedback mechanisms from the PFC and PPC (Xu, 2017). Moreover, proponents of these theories argue that the various alternative explanations for WM fail to explain the experimental results (Constantinidis et al., 2018).

As a result, the proponents argue that WM content resides in regions which have evolved specifically for the purpose of maintaining information in a stable and robust manner, such as the PFC and PPC (Haller et al., 2018). The debate regarding the role of sensory regions in WM, and the localization of WM content generally, is ongoing. As a result, several camps have formed: those arguing in favour of representations in sensory cortices (Scimeca et al., 2018), those in favour of an intermediate resolution with distributed WM representations across both sensory and higher-order regions (Christophel et al., 2017), and those in favour of higher-order only representations of WM content (Constantinidis et al., 2018; Xu, 2018).

One means for addressing this debate is to explore the maintenance of abstract numerosities in WM. As with all stimuli, numerosities are initially perceived bound to a set of sensory features, for example, a number of dots presented on a screen will have visual (location, size, colour, etc.) and verbal (number, etc.) features. However, by engaging the approximate number system (ANS) in combination with a clever task design, it is possible to extract the numerosity estimate away from the sensory features and thereby explore the grounding of WM content in sensory regions, when the features are no longer bound to the content.

In WM, a fronto-parietal network comprising the PFC and intraparietal sulcus (IPS) has been shown to display numerosity-selective activity (Jacob et al., 2018, Nieder, 2012). Moreover, evidence in humans has found that beta-band activity in the right PFC was modulated by numerosity (Spitzer et al., 2014). Thus, Spitzer and colleagues have provided evidence for the maintenance of abstract numerosity WM content in the PFC, however issues with localizing electrophysiological (EEG) signals, as well as the possibility of additional, distributed numerosity-related WM representations, makes the maintenance of numerosity WM content an attractive avenue for exploration. Thus, the first study comprising this dissertation employs a somatosensory DMTS task, in combination with an fMRI-MVPA analysis pipeline, to localize maintained WM representations of numerosities with the goal of addressing the debate surrounding the localization of maintained WM content.

1.3.2. Goal-directed Manipulation of Working Memory Information

As suggested by the Sensory-Recruitment theory of WM (D'Esposito, 2007; D'Esposito & Postle, 2015), manipulated WM content is hypothesized to be maintained in a grounded fashion, meaning in regions responsible for the perception of the content features. In contrast, previous work analysing univariate fMRI results had identified the PFC and PPC as responsible for the manipulation of WM content (Nyberg & Eriksson, 2016). However, it is unclear whether the activity identified relates to the manipulated WM content per se, or the mechanism by which the WM content is manipulated. Moreover, it is difficult to determine with certainty whether the manipulated WM content is truly independent from the presented stimulus and associated sensory features with human neuroimaging data. Therefore, to draw conclusive inferences regarding the nature of manipulated WM content, it is necessary to divorce the content from the underlying perceptual and sensory features.

Several methods have been implemented to prevent any contamination of perceptual activity into WM analyses. Some researchers employ a perceptual mask, consisting of a noisy stimulus, presented after the stimulus-of-interest has been removed, in an attempt to overwhelm the sensory cortex and erase any perceptual residues from the stimulus-of-interest (Christophel et al., 2012; Schmidt et al., 2017; Uluç et al., 2018). Another means is to abstract the desired WM representation away from the sensory features, either via categorization or arbitrary grouping (Seger & Miller, 2010).

A pivotal study by Lee, Kravitz, and Baker (2013) employed experimental context to dissociate the involvement of various brain regions in human WM. The experiment consisted of separate blocks of trials where participants were asked to encode either the visual features of an object or the object as a whole. The researchers found a clear dissociation between the blocks. On trials where the visual features were encoded in WM, the content was identified in visual cortices, whereas on object-specific trials, the WM content was additionally found in the lateral PFC. This study provided an important clue as to how experimental manipulation can further elucidate the regions involved in WM manipulation, and provided evidence for the maintenance of category-specific WM content in the PFC. However, the use of object categories inherently bound the WM content to the stimulus features. As previously discussed, arbitrary stimulus groupings,

which do not employ feature-specific categorization rules but are instead taught to participants, provide a means of exploring the formation and maintenance of novel group representations in WM without relying on sensory features (Seger & Miller, 2010).

Expanding on the study by Lee, Kravitz, and Baker (2013), the inclusion of separate experimental contexts provides an opportunity to explore, not only the differing localization of WM content across contexts, but also the representational nature of the WM content. Indeed, one limitation of fMRI data is the lack of information regarding the underlying neural code. However, by employing novel analysis methods such as Representational Similarity Analysis (Kriegeskorte et al., 2008) or cross-validated MANOVAs (cvMANOVA, Allefeld & Haynes, 2014), it is possible to probe the underlying neural code of WM with non-invasive human neuroimaging data. Importantly, these methods provide a means to begin answering questions regarding the relationship between, and purpose of, the posited distributed WM representations (Christophel et al., 2017).

To summarize, the use of arbitrary groupings and separate experimental contexts provides a means of both exploring the localization of manipulated WM content as well as providing insight into the representational nature of WM content across contexts. The second study in this dissertation addresses the question of whether manipulated WM content is bound to the sensory cortices, or whether there is sensory-independent WM content which is maintained in higher-order regions, such as the PFC. Indeed, my co-authors and I employed separate experimental blocks wherein participants were instructed to maintain either the individual stimulus or its arbitrarily defined group in combination with advanced fMRI-cvMANOVA data analysis techniques. With this experimental design and analysis pipeline, we were able to dissociate the WM content from the underlying physical features, and localize the abstracted, manipulated WM content across contexts.

1.3.3. Memory-based Perceptual Decision Making

The first study to investigate human vibrotactile decision making with fMRI reported a broad decision-making network consisting of prefrontal, posterior parietal, and sensorimotor regions (Preuschhof et al., 2006). Moreover, when the task difficulty was modulated, Pleger and colleagues (2006), found that regions in the left dlPFC, anterior

cingulate gyrus, and insula were modulated by the difficulty of the vibrotactile decisions. The dlPFC (Heekeren et al., 2004; 2006), inferior frontal gyrus (IFG, Liu & Pleskac, 2011; Filimon et al., 2013), and insula (Ho et al., 2009; Liu & Pleskac, 2011) have all been shown to be involved in perceptual decision-making in the visual domain. Indeed, results from human neuroimaging studies have suggested that the frontal and parietal regions act as domain-general evidence accumulation mechanisms (Heekeren et al., 2006; Ho et al., 2009; O'Connell et al., 2012). Unfortunately, due to the sluggish nature of the BOLD response, it is difficult to determine the specific role performed, or mechanism implemented, by any specific region (Mulder et al., 2014).

With EEG data, the faster timescale allows a more fine-tuned evaluation of the ongoing processes. Thereby permitting conclusions regarding the specific mechanisms underlying perceptual decision-making in humans to be drawn. Herding and colleagues found that the differential power of oscillations in the upper beta band reflected subjective perceptual choice (Herding et al., 2016; 2017). Moreover, in line with the Intentional Framework for perceptual decision-making (Cisek & Kalaska, 2010; Gold & Shadlen, 2007), Herding and colleagues identified a double dissociation: the SMA as the most likely source of the beta-band modulation when manual responses were employed (2016), and the FEF for saccadic responses (2017).

Importantly, most previous work exploring memory-based perceptual decision making in the vibrotactile frequency-discrimination task suffers from two issues with their experimental paradigms. Firstly, most previous work employed paradigms wherein the decision was fixed with respect to the presentation order of the stimuli. The paradigms required that f2 act as comparison stimulus against f1, the reference stimulus. This creates an issue similar to that previously identified by Romo and colleagues wherein they realized that, by holding f1 constant across a trial block, NHPs could perform the task without having to maintain f1 in WM (Romo & de Lafuente, 2013). By employing a fixed reference and comparison stimulus ordering, the decision is inherently bound to the presentation order of the stimuli. Thus, "higher" decisions will always be bound to a trial-wise increase in stimulus frequency and accordingly, "lower" is bound to a decrease in stimulus frequency.

Secondly, in most previous studies, both human and NHP participants had foreknowledge of the motor action required to communicate their decision. Thus, once

the participant had formed their decision after the presentation of the second stimulus, they could immediately prepare the specific motor response because they knew that, for example, a saccade to the left or left button press indicated a decision of “higher”. This fixed mapping between the decision and the motor response allowed the participant to prepare a motor response directly after having formed a decision. Thus, it is plausible that the results from previous frequency discrimination studies have not identified decisions per se, but a multiplexing of decision-related signals together with sensorimotor components (Park et al., 2014).

Finally, to my knowledge, the final two studies comprising this dissertation are the only studies which have employed fMRI-MVPA to explore memory-based perceptual decision making. In both studies we directly addressed the above-mentioned issues with the frequency-discrimination task experimental design. Specifically, we ensure that the reference and comparison frequency orderings are balanced and prevent the preparation of a motor plan. Furthermore, the studies provide a direct investigation of the Intentional Framework (Cisek & Kalaska, 2010; Gold & Shadlen, 2007). To this end, the studies were designed such that they were identical in nature other than the response modality: in the first study, participants respond via saccade whereas in the second, they respond via button press. Therefore, the final two studies of this dissertation provide a well-controlled analysis of the Intentional Framework for perceptual decision making in the somatosensory domain.

1.4. Aim of the Dissertation

This dissertation aims to explore the intermediate stages of the perception-action loop in the somatosensory domain. The stages correspond to the maintenance of WM content, the goal-directed manipulation of the content, and the formation of a decision based on the content. Concurrently, the dissertation addresses ongoing debates in cognitive neuroscience. Specifically, the localization of WM- and decision-making content. For both debates, the central issue rests with the extent of influence that the experimental design has on the resulting neural computations. For WM maintenance, the Sensory-Recruitment theory (D’Esposito, 2007; D’Esposito & Postle, 2015) says that localization depends on the stimulus features, whereas the opposing camp argues for all

content to be maintained in higher-order regions such as the PFC and PPC (Constantinidis et al., 2018; Xu, 2018). Furthermore, in the decision-making field, the Intentional Framework says that the localization of the decision variable depends on the motor output (Gold & Shadlen, 2007; Cisek & Kalaska, 2010), whereas the other side argues for a domain-general decision variable that is independent of experimental features (Heekeren et al., 2006; Ho et al., 2009; O'Connell et al., 2012).

This dissertation consists of four original experimental works which were designed to address these ongoing discussions. The works probe the localization of maintained and manipulated somatosensory WM content in humans using fMRI in combination with advanced multivariate analysis techniques. Additionally, all four studies make use of a modified somatosensory stimulus discrimination paradigm. After the WM and decision delay periods, participants were asked to respond to a target stimulus. This is significant because, during the delays, participants were unaware of their post-target motor decision and could not form a motor plan. Therefore, by analysing the delay-period BOLD activity, we were able to disentangle WM content from perception and motor variables to localize brain regions maintaining somatosensory WM content. Correspondingly, the decision variables are additionally not corrupted by WM content.

In the first study, we explored how the maintenance of an abstract quantity, such as numerosity, would be distributed in the brain. To this end, participants were presented an uncountable sequence of tactile pulses to the left median nerve and asked to estimate the number of pulses. Importantly, participants could not perform the task without having extracted the number because the target stimulus did not match the cued stimulus in any other feature. Thus, with this first study, we explored how maintaining numerosity content in WM would differ from simple vibrotactile somatosensory stimuli and whether numerosity content is maintained in a modality-specific or general manner.

In the second study, we asked whether the manipulation of WM content would affect the underlying representational code, an ability known as adaptive coding (Duncan, 2001). To this end, participants were taught arbitrary groupings of patterns of tactile stimuli and asked to maintain either the presented stimulus or the stimulus' group in WM. In this study, we were interested in identifying how the WM

representation changed across experimental conditions and whether any region would modify their representational space in accordance with experimental demands.

In the final two studies comprising this dissertation, we shifted the focus from the localization of WM content to the localization of the ensuing decision variable. As suggested by the Intentional Framework (Cisek & Kalaska, 2010; Gold & Shadlen, 2007), the localization of the decision variable should depend on the specific experimental context and manipulations. Thus, we modified the classic paradigm employed by Romo and colleagues to ensure that participants maintained a decision during the decision period which was not corrupted by trial-specific conditions such as the stimulus ordering or motor decisions. To this end, we performed two identical studies which only differed in the means of communication. In both studies, participants were presented with, and asked to compare, two sequential vibrotactile frequency stimulations (f1 and f2). In the third study, participants communicated their decisions via saccades, whereas in the fourth, manual button presses were recorded. Thus, if memory-based perceptual decision making adheres to the Intentional Framework, the localization of the decision variable should differ between the two studies.

To conclude, the studies comprising this dissertation were designed to provide insight into the intermediate stages of the somatosensory perception-action loop. Furthermore, by taking advantage of modifications of classic experimental paradigms, advanced whole-brain data analysis techniques, and the extensive literature in the somatosensory domain, the studies address ongoing debates regarding the underlying nature of WM and decision-making.

2. Summary of the Empirical Studies

In this section, I summarize the four empirical studies which comprise the novel work of this dissertation. All four studies explore the localization of task-relevant representations using variations of the frequency discrimination and DMTS experimental paradigms together with fMRI-MVPA data analysis techniques. Moreover, all four studies aim to expand beyond the simple, standard paradigms and instead explore how features of the experimental paradigm influence the maintenance and localization of the resulting task-relevant representations.

2.1. Parametric Representation of Tactile Numerosity in Working Memory

WM studies in humans and NHPs employing vibrotactile stimuli have provided initial evidence for the right lateral PFC to play a central role in maintaining magnitudes or quantities of a sensory stimulus, specifically the frequency (Romo et al., 1999; Schmidt et al., 2017; Uluc et al., 2018; Wu et al., 2018). Vibrotactile stimuli, wherein a specific frequency is presented and encoded, can be construed as an abstract quantity which must be extracted from the sensory stimulus. In a similar vein, the estimation of magnitudes or numerosities is also an abstract quantity which is hypothesized to be processed by the ANS.

The ANS provides a quick estimate of numerical quantities such as size, length, amount, etc. without relying on symbols or language and has been shown to exist in both humans and other animals (Dehaene et al., 1992; Spitzer et al., 2014). The ANS is employed when there is insufficient time to count the stimulus, given that the value in

question is larger than the subitizing threshold (Kaufman et al., 1949). Below this threshold, participants are able to determine an exact amount without effort in a very short period of time. This is in contrast to counting or algebraic operations which rely on language and symbolic representations of precise numbers. The estimation process employed by the ANS is hypothesized to resemble the perception of a continuous magnitude (e.g., frequency, Nieder & Dehaene, 2009; Piazza et al., 2004; Spitzer et al., 2014). Extensive literature on the function of the ANS in perception has been amassed and the consensus suggests a frontoparietal network, comprising the right ventrolateral PFC (vlPFC) and IPS in the PPC, underpins the ANS (Cantlon et al., 2006; 2009; Dehaene et al., 2004; Jacob & Nieder, 2009; Knops & Wilmes, 2014; Nieder, 2012; 2016; Piazza et al., 2004; 2007).

Although the ANS has been extensively investigated, only a few studies have focused on the mental representation of remembered numerosity estimates in WM. Specifically, the mechanisms underlying estimated numerosity in WM are unclear. Thus, in the first study of this dissertation, we aimed to determine the extent to which the estimated approximation of numerosities would be maintained in a manner similar to the numerosities extracted in the visual domain. Moreover, we wanted to explore to what extent the pattern of maintained numerosity information would overlap with other abstract WM content, such as frequencies, and whether the content is grounded in sensory cortex. Thus, we hypothesized that, in line with the parametric vibrotactile literature (Nieder, 2016; Spitzer et al., 2014; Uluç et al., 2018; Wu et al., 2018), we would identify numerosity-specific WM content in the right PFC.

In the present fMRI-MVPA study, we employed a DMTS paradigm where participants were required to match numerosity targets. To this end, we defined four numerosity stimuli which consisted of temporal patterns of electrical stimulation presented to the left medial nerve. Note that the number of pulses corresponded to the stimulus numerosity (7, 9, 11, or 13). The pulse duration and repetition rate were chosen such that participants were able to perceive each individual pulse instead of the pulses blurring into a single sensation, and the numerosities were large and presented quickly enough to prevent participants from counting. Moreover, to ensure that participants extracted the numerosity and not the spectral pattern from the stimulus, four alternative stimuli were created for each numerosity and employed as targets. Each

alternative consisted of a different duration and pattern of stimulation. Thus, to correctly identify the target, participants needed to extract the numerosity from the stimulus, encode the numerosity in WM, and use this information to identify the corresponding target.

For all thirty-eight participants, six runs of fMRI data were collected. The data were analysed using a searchlight multivariate support vector regression analysis (SVR). In this pipeline, a searchlight travels through the brain and explores whether, in each searchlight, the WM representations of the four numerosities follow a linear ordering, as would be expected if the memoranda were encoded as ordinal numbers. We anticipated that, the larger the difference in ordinal numbering, the more different the WM representations.

The results of the multivariate SVR analysis are shown in Figure 1. The analysis identified numerosity-specific WM information in the left PMC, left MFG, left SFG extending into bilateral SMAs, right SFG extending to the right frontal pole, and the right MFG extending into the pars triangularis of the right IFG. The results provide further evidence for the numerosity-selective (Nieder, 2016) and parametric stimulus maintenance properties of the PFC (Romo et al., 1999; Schmidt et al., 2017; Uluc et al., 2018; Wu et al., 2018). Moreover, we additionally identified members of the well-known task-positive network: MFG, SMA, PMC (Fox et al., 2005). This network is commonly involved in the attention-focused completion of tasks and regions belonging to the network have been shown to maintain a wide variety of WM-content (Christophel et al., 2017).

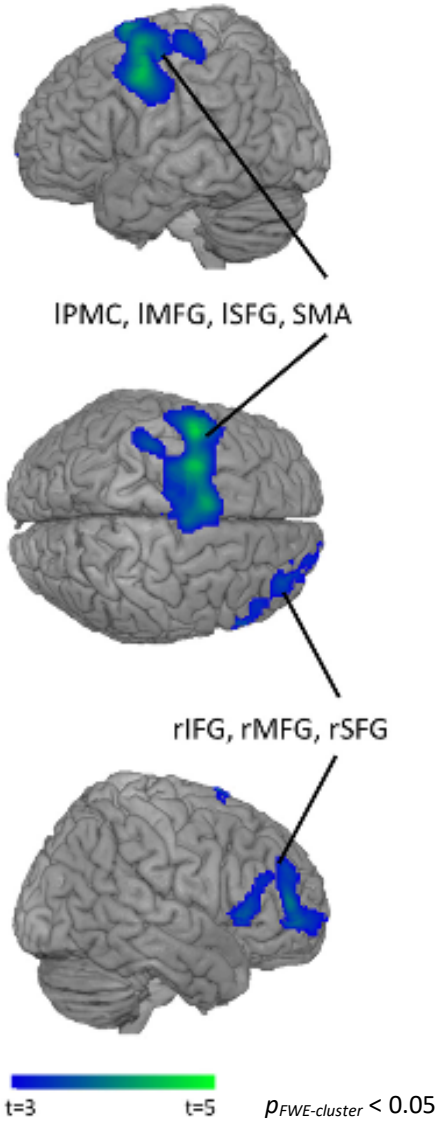

Figure 1: Brain regions coding information for memorized estimated numerosities. The figure was originally published in Uluç et al., 2020, available under CC BY 4.0

Therefore, the first empirical study of the dissertation demonstrated that, similar to other modalities, WM numerosity representations abstracted from tactile stimulation are also maintained in a distributed network spanning bilateral frontal cortices, and specifically the right PFC. This finding provides evidence in support of the hypothesis that the ANS, located in the right IFG (Nieder, 2016), is capable of maintaining numerosity WM content in a likely modality- and format-independent manner.

2.2. Intraparietal Sulcus Maintains Working Memory Representations of Somatosensory Categories in an Adaptive, Context-dependent Manner

In the second study comprising this dissertation, we explored the influence of task demands on the localization of manipulated WM representations. Specifically, how task demands can manipulate and modify the representational space underlying WM content. We were motivated by the work of Freedman and colleagues (2001; Fitzgerald et al., 2011; 2012; Freedman & Assad, 2016) who identified the neural signatures of visual categorical and arbitrary representations in PFC and LIP neurons, and Rossi-Pool and colleagues (2016) who identified tactile categorical-specific representations in the dPMC. Extending on these studies, and inspired by the Lee, Kravitz, and Baker (2013) task design, we designed a DMTS paradigm which enabled the dissociation of categorical labels from the underlying changes in stimulus features. This dissociation enabled conclusions regarding the location of stimulus and manipulated categorical WM information to be drawn.

To this end, we trained participants to form arbitrary groups of stimuli. The use of arbitrary groupings is significant because, while neurophysiological data enables the differentiation between stimulus-specific and category-specific neural information, the difference is more nuanced with fMRI data. Thus, we employed arbitrary groupings so that the groups would be independent from underlying stimulus features (Seger & Miller, 2010). Based on previous results (Fitzgerald et al., 2011; Fitzgerald et al., 2012; Freedman & Assad, 2016; Freedman et al., 2001; Rossi-Pool et al., 2016) we hypothesized that the manipulated group WM representations would be identified in the dPMC and IPS – the human LIP homologue (Grefkes & Fink, 2005).

To this end, we designed four stimuli inspired by those employed by Rossi-Pool and colleagues (2016). The stimuli, similar to those used in the first study, consisted of temporal patterns of bursts of electrical stimulation which were applied to the left medial nerve. The stimuli were identical for all participants and were chosen such that they were equally differentiable and recognizable, according to preliminary testing data. Four possible groupings of four stimuli exist, and participants were randomly assigned a grouping. Participants were trained on their specific grouping during a training session. After ensuring that participants had learned the groupings, four experimental runs of fMRI data were collected for each participant, with each run consisting of two experimental blocks: stimulus trials, and group trials. In the stimulus block, participants performed a standard DMTS trial in which they were asked, via retro-cue, to encode a presented stimulus and compare the resulting WM representation of the stimulus to a target. In the group block of trials, participants performed a so-called delayed-match-to-group task wherein they were instructed to encode both the cued stimulus together with its group member, and decide if the target was either of the encoded-group members.

Importantly, the resulting decision and motor outputs were additionally decoupled from the WM content. To this end, after the presentation of the target stimulus, participants were presented with two coloured circles. Each colour represented a decision which participants had been assigned. Moreover, the location of the coloured circles changed pseudorandomly on each trial and participants had to respond by choosing the location of the relevant colour. For example, if the participant was told to choose blue for correct and yellow for incorrect targets, they would first have to decide if the correct target was presented, locate the representative colour, and choose the motor output which corresponded to the location of the colour (left or right button press). Thus, it was not possible for participants to prepare a decision or motor plan during the WM delay.

In total, eight blocks of experimental trials, four of each condition, were collected from 36 participants. The fMRI data was analysed using a searchlight cross-validated MANOVA approach (Allefeld, 2016) which, unlike other MVPA methods, enables the evaluation of interaction analyses with multivariate data. The cvMANOVA results in a pattern distinctness value (Ds) which directly estimates the amount of multivariate

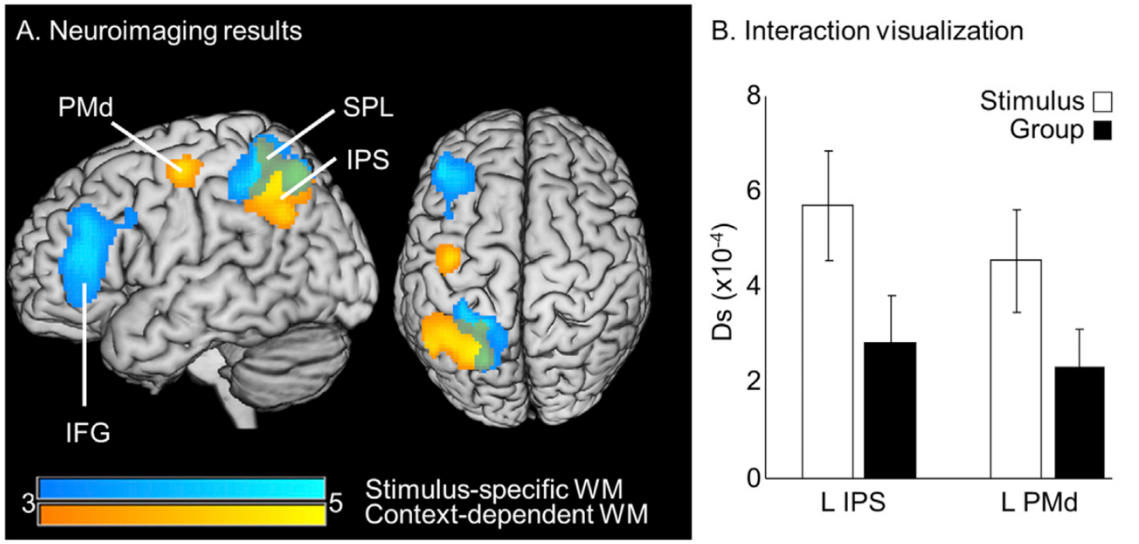

Figure 2: Neuroimaging cvMANOVA results. A. Colour-bars indicated respective voxel-wise T-statistic values. B. Error bars indicate standard error of the mean. The figure was originally published in Velenosi et al., 2020, available under CC BY 4.0

variance accounted for by the contrast. Thus, the Ds value indicates the dissimilarity of the WM representations. The results of the analyses are shown in Figure 2. In a first step, we identified condition-general stimulus-specific WM representations by performing a conjunction analysis across the two experimental conditions. This analysis identified stimulus-specific WM content in the left IFG and superior parietal lobule (blue regions in Figure 2A). Secondly, using an interaction analysis across experimental conditions, we demonstrated that the WM representations in the left IPS changed with changing task requirements (yellow regions in Figure 2A). The dPMC (referred to as PMd in the figure) did not reach significance but was included for completeness due to our strong a priori expectations.

Our interaction analysis identified a manipulation of the WM representations across experimental conditions (Figure 2B). The IPS represented the group members more similarly in the group condition (smaller Ds) than in the stimulus condition (larger Ds). Importantly, the analysis was controlled to ensure that, in both conditions, the same stimuli were contrasted. Thus, the results could not be attributed to differences in stimulus features. The dPMC, as shown in Figure 2B, did not show a statistical difference between the conditions.

To conclude, we provided novel evidence for the adaptive nature of somatosensory WM representations in the IPS. Importantly, we demonstrated

conclusively that the WM content maintained in the IPS was manipulated in accordance with the specific cognitive demands of the task.

2.3. Decoding Vibrotactile Choice Independent of Stimulus Order and Saccade Selection During Sequential Comparisons

In the previous study (Velenosi et al., 2020), we revealed that the parietal cortex adaptively maintains somatosensory WM content according to the context of the cognitive task demands. Interestingly, we did not identify any group-specific WM representations in the left dPMC, as had been previously shown by Rossi-Pool and colleagues (2016). In the discussion section of the publication, we hypothesized that this was due to our having successfully decoupled the decision and motor output variables from the WM content. Thus, we hypothesized, that due to the successful decoupling, we identified the stimulus and context-modulated WM content in WM-specific regions and not in the dPMC, a region involved in the preparation of motor plans (Nakayama et al., 2008; Yamagata et al., 2009; Yamagata et al., 2012). To further explore this hypothesis, the final two studies comprising this dissertation investigated the localization of memory-guided decision outcome variables in relation to the upcoming motor plan. We hypothesized that, in agreement with the Intentional Framework of decision-making (Cisek & Kalaska, 2010; Gold & Shadlen, 2007), the decision variable would be localized in brain regions which are required for creating and communicating the resulting motor decision.

To this end, we returned to the classic vibrotactile frequency decision making task. Previous studies using neurophysiological recordings in NHPs and EEG in humans found strong evidence for the perceptual choice to be encoded in a sensorimotor network spanning S2, PFC, and PMC (Haegens et al., 2011; Herding et al., 2016; 2017). However, we identified two confounds with the classic version of the experimental paradigm. These confounds resulted in the perceptual decisions being inherently coupled to the sensory and motor aspects of the task and thereby bring into question the validity of the literature results. Thus, in an effort to reaffirm the literature, we included two modifications to the classic paradigm to control for the confounds.

In the standard vibrotactile frequency decision-making task, participants decide whether the second frequency is higher or lower than the first frequency (f2 > or < f1). Thus, the decision is inherently tied to the ordering of the stimulus frequencies with a "higher" decision tied to increasing frequencies and "lower" with decreasing. To remove this dependency, we included a rule condition at the start of each trial which instructed participants which stimulus, the first or the second, should be used as the base frequency and which as the comparison. Thus, in half of the trials, participants would contrast the first stimulus against the second, and the opposite in the other half, thereby ensuring that the decision is decoupled from the presentation order of the stimuli.

Moreover, in previous studies, the decision was directly mapped to a specific motor output. For example, if decision higher - press the left button. Thus, once a decision has been made, participants could immediately translate the decision into a motor action plan instead of maintaining the abstract decision. Therefore, we decoupled the decision from the motor output by including a decision mapping cue. On each trial, participants were shown either an upward- or downward-facing arrow which indicated either "higher" or "lower" and participants had to decide whether they agreed with the arrow presented. For example, if participants were instructed to contrast the first frequency (Base - 12 Hz) against the second frequency (16 Hz), they would decide that the second frequency was higher. Then, after a delay, if an upward-pointing arrow was shown, they would decide that they agreed with the arrow and select the appropriate behavioural output to indicate a decision of "agree". Thus, importantly, during the delay after the second stimulus and before the presentation of the arrow, participants maintained the decision of "higher" or "lower". The formation of a final motor plan took place after the presentation of the arrow and participants communicated their decision via saccades.

Thus, by including these two modifications to the classic vibrotactile frequency discrimination paradigm, we were able to isolate the decision variable from the physical properties of the stimuli and the specific motor output. Based on previous research and according to the Intentional Framework of decision-making, we expected to identify decision-specific information in brain regions responsible for creating the motor plans for saccades, specifically the FEF.

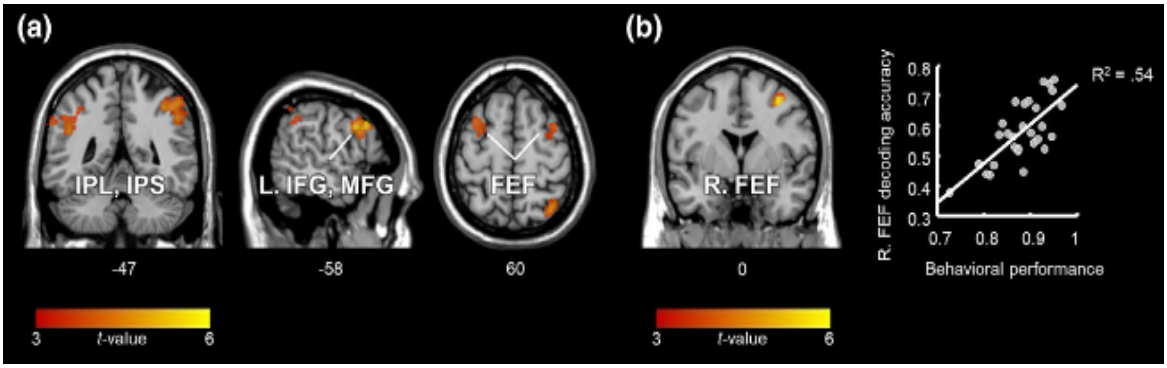

Figure 3: Neuroimaging results. Brain regions carrying choice information independent of the stimulus order and the direction of the ensuing saccade. The figure was originally published in Wu et al., 2019, available under license agreement 1448822-1 from John Wiley & Sons, Inc.

We collected six experimental runs of fMRI data from 30 participants and analysed the data using multivariate support vector classification. The results are shown in Figure 3. We identified choice-specific information, regardless of decision (f1 > or < f2), in the bilateral FEF, IPS, and left IFG and MFG. Moreover, we found that the participant-specific decoding accuracy in the right FEF, a region upstream from saccade control regions, was positively correlated with the participant's behavioural performance (Figure 3b). Thereby providing strong evidence for the involvement of the right FEF in memory-based perceptual decision making tasks when the decision is communicated via saccades. This empirical result provided strong evidence bridging the NHP results (Gold & Shadlen, 2007; Romo & de Lafuente, 2013) to humans.

To conclude, we provided evidence for decision-specific information in the somatosensory frequency discrimination task to be maintained in brain regions which are necessary for the planning and communication of the decision, commonly referred to as the Intentional Framework of perceptual decision making (Gold & Shadlen, 2007; Cisek & Kalaska, 2010). Moreover, we showed that choices are maintained in an intentional manner even when the choices are decoupled from sensory properties of the stimuli and the ensuing decision motor output.

2.4. Response Modality-dependent Categorical Choice Representations for Vibrotactile Comparisons

The final study comprising this dissertation consisted of a follow-up to the previous study. If indeed decision information is maintained in an effector-specific manner, then changing the motor effector should result in a corresponding change in the location of

the decision information. To this end we repeated the previous study and asked participants to respond with button-presses instead of saccades.

We again collected six runs of experimental data from 27 participants and analysed the data in a manner identical to the previous study. Indeed, when participants were asked to respond with a manual button press, the decision-specific information was located in the left dPMC and left IPS (Figure 4). Moreover, we did not find any statistically significant choice-specific information in the FEF. This dichotomy was further explored in a post-hoc analysis which confirmed the difference in localization of memory-guided choice-dependent information across the studies (Figure 4). Thus, we provided additional fMRI evidence for the coding of choice properties in human motor preparatory regions, even when choices are decoupled from action plans and maintained in an abstract form (higher – lower).

Finally, taken together, the third and fourth studies of this dissertation provide strong evidence for the representation of memory-guided perceptual decisions in human vibrotactile frequency discrimination tasks to be maintained in a response modality-dependent manner. To conclude, we replicated and extended the dissociation shown by Herding and colleagues (2016; 2017) with fMRI data and provide strong evidence in favour of the Intentional Framework of perceptual decision-making.

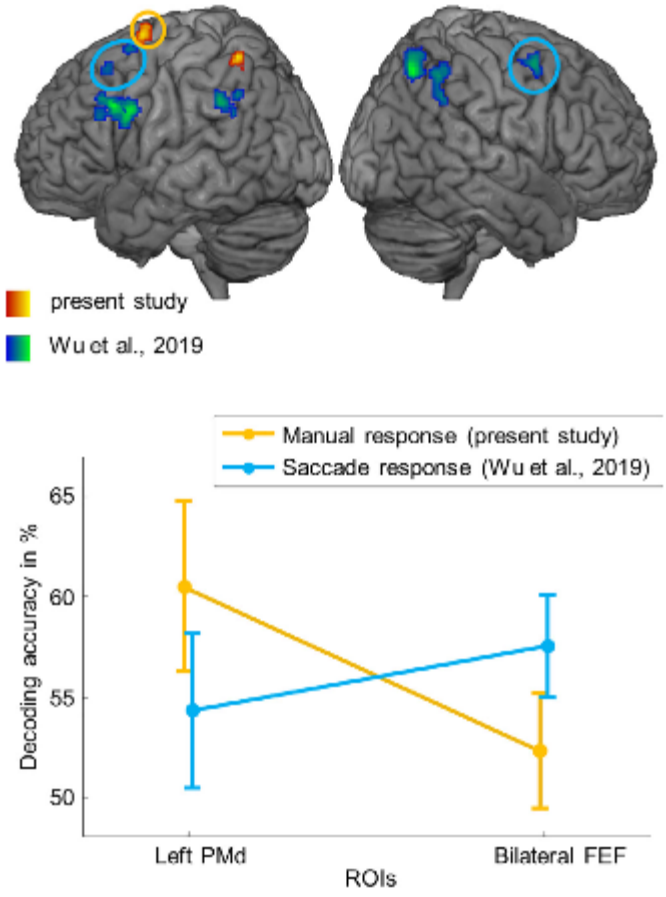

Figure 4: Comparison with results from saccade version of the task (Wu et al., 2019, n = 30). The figure was originally published in Wu et al., 2021, available under CC BY 4.0

3. General Discussion

In the final section of my dissertation, I present a synthesis of the empirical studies and suggest a unified somatosensory perception-action model of the brain.

The four empirical studies address questions relating to long-standing debates in the worlds of WM and memory-based perceptual decision making neuroscience. More specifically, the studies explore the influence of cognitive task-demands on the localization of neural representations. In the first study, Uluç et al., 2020, we showed that, similar to other forms of abstract WM content, approximated numerosities can be estimated from tactile stimulation and are maintained in a likely modality-independent manner in the PFC, specifically the right IFG. Secondly, in Velenosi et al., 2020, we showed that changing the experimental context resulted in a task-specific, adaptive modification of the WM representation in the IPS. Finally, in the two Wu et al., 2019; 2021, papers, we showed that simply changing the manner in which the decision is communicated results in a task-specific change in the localization of the decision content. There are several implications of the four empirical studies comprising this dissertation and these are discussed in detail below.

3.1. Localizing Maintained Information in Working Memory

The first aim of this dissertation was to localize WM representations underlying the initial WM processing stage after perception. In addition, to simultaneously address the ongoing debate regarding the localization of information maintained in WM. Indeed, as outlined in the introduction, this debate has been ongoing for decades with two main

opposing camps. One arguing that the specific qualities of the PFC make it ideal and uniquely able to maintain WM content (Goldman-Rakic, 1995), and another which argues that the qualities are not unique to the PFC and WM is maintained in sensory regions (Postle, 2006; Sreenivasan et al., 2014). Recently, a middle option has been introduced suggesting that the maintenance of WM content is a ubiquitous feature of the cortex (Christophel et al., 2017). In the first and second studies of this dissertation (Uluç et al., 2020; Velenosi et al., 2020), we directly addressed this debate by localizing the representations of content maintained in WM.

In the first study, participants extracted abstract numerosities from patterns of electrical pulses. The maintained WM content was identified in two frontal clusters spanning the IFG, MFG, SFG, SMA and PMC. In the second study, using similar stimuli as the first, WM content was also identified in the IFG, as well as the superior parietal lobule, including the IPS. Moreover, we included additional analyses in the supplemental material, specifically the distributed WM content maps for each experimental condition individually. The stimulus-specific WM content was maintained in a bilateral network spanning the IFG, PMC, PPC, middle temporal gyrus, and cerebellum. In contrast, the group-specific content was more localized and only identified in the bilateral MFG, left IFG, and left IPS. Thus, in both studies employing patterns of tactile electrical stimulation, the stimulus-specific WM content was maintained in the IFG. This provides additional evidence for the ability of the PFC to maintain abstract WM content in human fMRI studies. This is significant because, until recently, in contrast with neurophysiological recordings in NHPs, few human fMRI studies had identified WM content in the PFC (Riley & Constantinidis, 2016). Indeed, it appears as though the initial lack of findings of human WM content in the PFC was likely due to the nature of the stimulus, task, and analysis pipeline employed (Christophel et al., 2017).

In the overview compiled by Christophel and colleagues (2017), the authors compared the WM literature between human and NHPs and found that the majority of both species' cortices is able to maintain WM content. Generally, the more abstract the content, the more anterior the content is maintained. This gradient suggests that the localization of the WM content depends on the content itself, or more specifically, the method employed for encoding the content. For example, in both the first and second studies of this dissertation, the same stimuli were employed: temporal patterns of

electrical stimulation delivered to the median nerve. However, information outside of the frontal cortices was only found in the second study. There are several differences, both in the stimuli and study design, which may have contributed to the observed differences in localized WM representations. However, the conclusion is, depending on the experimental conditions and task-specific instructions, participants maintain differently distributed WM representations of the same stimulus across studies (Christophel et al., 2017). Thus, it is insufficient to draw general conclusions about the basis of WM maintenance from collections of studies which employ, for example, the same stimuli. Instead, specific details of the studies must be considered before conclusions can be drawn (van Ede & Nobre, 2023).

This conceptualization of WM can be extended to the central executive and slave module components of the Baddeley and Hitch (1974) multicompetent model of WM. In this extension, the entire cortex is the slave of the central executive. Indeed, the literature provides ample evidence for the ability of all cortical regions to maintain specific formats of WM content. Moreover, some researchers argue that the same neural circuits underlying long-term memory also subserve WM (Cowan, 2001; Oberauer & Hein, 2012; Desimone & Duncan, 1995). Thus, rather than localizing maintained WM content, it is preferable to consider the pragmatic utility of the content (van Ede & Nobre, 2023). What purpose do the distributed representations summarized by Christophel and colleagues (2017) serve? How do the regions support the various stages of processing between the perception of a stimulus and the motor output? How do the distributed WM representations enable behavioural flexibility? Do they represent independent processing stages along the perception-action loop (Christophel et al., 2017; Myers et al., 2017)? Or do they serve as back-up copies in case of distraction or neural damage? To this end, Romo and colleagues have provided evidence from NHPs based on the strength, dynamics, and latencies of neural responses that distributed regions in the frontal cortex maintain WM information (Hernández et al., 2010) but, to my knowledge, have yet to explore the relation between or the role of the distinct representations.

Romo and colleagues show that, while there is a temporal delay between the regions which can be used to map their connectivity, the entire set of six regions (S2, VPC, PFC, mPMC, dPMC, M1) maintain WM information. Due to the large energy costs

of multiple distinct WM representations, there must be an essential purpose for six regions to maintain potentially overlapping and duplicate information. Future studies are necessary to explore the relationship between and purpose of the parallel nature of the distributed WM representations (Christophel et al., 2017). By employing advanced analysis techniques such as representational similarity analysis (Kriegeskorte et al., 2008) or investigating the principal components of the representations (Rossi-Pool et al., 2017), it is possible to compare the maintained representations across regions. This would greatly benefit the field of cognitive neuroscience by extending the discussion from debating the localization of maintained WM content to investigating the role of the content in subserving the perception-action loop (van Ede & Nobre, 2023).

3.2. Localizing Goal-directed Manipulated Working Memory Content

A second aim of the dissertation was to explore the subsequent stage in the perception-action loop, the manipulation of WM content. As previously discussed, the concept of WM has evolved significantly over the past few years. Indeed, as nicely summarized by Myers and colleagues (2017), WM is a process which involves encoding stimuli, selecting the relevant information, reformatting the information, before finally transforming the information into an action plan. Thus, WM inherently contains manipulations and transformations of content. However, the goal-directed manipulation of WM content is not part of the standard WM pipeline per se. Instead, the manipulation of WM content involves an attempt to realise a specific goal via a transformation of the content. Thus, while the term WM maintenance, and WM more generally, has evolved to include various internal attention-demanding WM processes, including the transformations underlying the perception-action loop, I use the term WM manipulation to denote the conscious manipulation of WM content for the completion of a specific goal.

Indeed, the first two empirical studies comprising this dissertation directly speak to this aim as both studies required participants to manipulate tactile stimuli to perform the task. In Uluç et al., 2020, participants were required to extract a numerosity from the perceived stimulus. Whereas in Velenosi et al., 2020, participants were required to encode either the presented stimulus or abstract the stimulus to an associated group. In the first study, we were not interested in the manipulation of the WM content per se,

but in localizing the resulting abstract numerosity-specific WM content which we identified in two clusters in the frontal cortex. In the second study, we extended our focus to explore how the manipulation of WM content changes the representational space underlying the content. Indeed, by directly comparing across experimental conditions, we identified similarities between the distributed WM representations of the original and manipulated content. Whereas the original stimulus-specific information was identified across conditions in the left IFG and SPL including the IPS, the manipulated group-specific information was found in the IPS and IFG, and other than preliminary evidence for the dPMC, no frontal regions were found to maintain context-dependent manipulated WM content. Indeed, only the WM representations in the IPS were modified in accordance with the changing task demands.

In Velenosi et al., 2020, we had hypothesized that, by training participants to form groups of stimuli, the resulting WM representations would be modified such that group members would be represented more similarly to one another in the group condition than in the stimulus condition. Indeed, a multivariate interaction analysis allowed the identification of changing WM representations with experimental context in the IPS. This is significant because the majority of studies investigating WM manipulation have relied on univariate data analysis methods and have focused on identifying the likely top-down manipulation signals, which have been shown to originate from the PFC (D'Esposito et al., 1999; Wager & Smith, 2003; Royall et al., 2002). In contrast, our study extended the analysis of WM manipulation by localizing the manipulated WM content in the IPS.

In line with our findings, previous studies have shown that task-relevant representations in the IPS change with changing task-demands (Jackson & Woolgar, 2018; Liu & Hou, 2013; Woolgar et al., 2011) and that the IPS is central for grouping and categorizing stimuli (Freedman & Assad, 2016). Indeed, there is ample evidence for the involvement of the IPS in abstract cognitive functions including the representation of cognitive sets (Oristaglio et al., 2006; Stoet & Snyder, 2004), numerosity (Nieder et al., 2006; Nieder & Miller, 2004), and salience (Leathers & Olson, 2012), all of which comprise forms of categorization. Importantly, a study by Zhou and Freedman (2019), found that the LIP, the IPS homologue in NHPs (Grefkes & Fink, 2005), is necessary for the transformation of a stimulus representation into a more-abstract category label,

which is then passed to motor-selective neurons, also in the LIP. As a fitting summary of the literature, Freedman and Ibos (2018) have suggested a model which merges the various LIP functions into a single role: the identification of behaviourally relevant stimuli. To this end, the authors suggest that the nonlinear nature of responses observed in LIP neurons in DMTS tasks suggests the comparison and integration of incoming bottom-up sensory signals with top-down cognitive goals, likely from the PFC. Thus, taken across species, the IPS maintains WM representations indicating the current task goal. To conclude, the IPS likely acts as a central hub where manipulated WM content is computed, maintained, and shared with other downstream regions in the perception-action loop.

3.3. Localizing Memory-based Perceptual Decision-Making Content

The third goal of this dissertation was to localize the representations underlying memory-guided perceptual decision making. Moreover, in a similar vein as the WM localization debate, to simultaneously address the ongoing debate of whether domain-general regions compute the decision (Heekeren et al., 2006; Ho et al., 2009; O'Connell et al., 2012) or whether the regions change depending on the current task-demands, as per the Intentional Framework (Cisek & Kalaska, 2010; Gold & Shadlen, 2007). Indeed, our results from the third and fourth studies, Wu et al., 2019; 2021, directly address this goal. By performing two studies which were controlled for the sensory-motor features of the frequency discrimination task, and identical except for the motor output effector, our results directly speak to the debate. Indeed, we clearly show that, depending on the motor output effector, the location of the resulting decision-related information changes with the FEF maintaining the decision when communicated via saccades (Wu et al., 2019) and the PMC when by button presses (Wu et al., 2021). Thus, at first glance, the Intentional Framework (Cisek & Kalaska, 2010; Gold & Shadlen, 2007) appears to correctly explain our results. However, as is often the case in cognitive neuroscience, and with fMRI results specifically, the results are not so straightforward to interpret.

Undeniably, while the results show a clear dichotomy between the two experimental paradigms, this cannot be stated conclusively. Importantly, in both studies, multiple regions were found to maintain decision-specific information such as the IPS,

IFG, and MFG. In an analogous fashion to the maintenance of WM content, it is presently not known what purpose these additional distributed representations serve. Indeed, it may be possible that a general decision-making region lays upstream to both the FEF and the PMC where the decision was computed in both studies, such as the IPS, and communicated to the downstream regions necessary for producing the required motor behaviour (Freedman & Ibos, 2018; Zhou & Freedman, 2019). Unfortunately, our experimental paradigm does not provide the temporal resolution necessary to resolve such an interaction between regions. Thus, while our results provide evidence in favour of the Intentional Framework for perceptual decision making, we cannot state conclusively where the decision-related information was computed. Additional research, including connectivity studies in humans and neurophysiological work in NHPs, is necessary before a decisive conclusion between the two theories in memory-guided perceptual decision making can be drawn.

3.4. Comment on the Somatosensory Perception-Action Loop

Taken together, all four studies in this dissertation provide evidence for the localization of information underlying the intermediate stages of the perception-action loop in the somatosensory domain. Indeed, by considering the results from the four studies together with the extensive literature, it is possible to build a rudimentary model of the somatosensory perception-action loop.

Each trial begins with the perception of a somatosensory stimulus. This stimulus is converted into a perceptual representation which, based on previous findings from both the NHP and human literatures, occurs in contralateral S1 and bilateral S2 (Auksztulewicz et al., 2012; Romo & de Lafuente, 2013). Romo and colleagues demonstrated that tactile frequency information is transformed into a rate code by S1 (Hernández et al., 2000), which is expected to have occurred in all four of the studies comprising this dissertation. Indeed, all studies employed forms of vibrotactile stimulation: numbers of pulses, temporal patterns, and frequencies. Thus, based on the literature, we presume that, in all four studies, the contralateral S1 converted the tactile stimulation into a rate code which was then passed to downstream bilateral S2 regions.

Together, the contralateral S1 and bilateral S2 cortices establish the first representation of the stimulus (Auksztulewicz et al., 2012; Romo & Rossi-Pool, 2020; Schröder et al., 2019). Importantly, the accuracy of the initial stimulus representation has a significant influence on the outcome of the trial. As shown by Herding and colleagues (2016) and many others beginning with Hellström (1985), the trial-wise stimulus perception is biased by the subject's experimental history. Indeed, Herding and colleagues found that the representation of the stimulus on a trial will be biased towards the mean value of the previously perceived stimuli. Moreover, since all downstream transformations in the perception-action loop are computed using the initial perceptual representation, any errors or biases in the initial representation are perpetuated throughout the remaining stages, culminating in the evidence upon which a perceptual decision is based.

Following the initial perceptual representation, the information is distributed to a wide range of cortical regions. As shown by Romo and colleagues in the vibrotactile discrimination task, following activity in S2, the rate code information is passed to frontal regions, specifically the bilateral PFC and vPMC, and then with a short delay to the mPMC and dPMC (Hernández et al., 2010). Unfortunately, the research group did not consider the PPC in their experiments. Interestingly, all regions investigated by the Romo group were found to be actively involved in the perceptual decision-making task. This suggests a distributed network underlies the post-perception stages of the perception-action loop (Romo & de Lafuente, 2013).

Indeed, the regions reported by Romo and colleagues correspond well with the task-positive network (Fox et al., 2005) also known as the multiple-demand network (Duncan & Owen, 2000; Duncan, 2010). As indicated by the name, the network was identified due to the consistent activity of the regions during attention-demanding, externally orienting cognitive tasks. The task-positive network in humans is generally considered to consist of the lateral PFC, dorsal parietal cortex – especially the IPS, sensory-motor cortices, subcortical regions, and the cerebellum (Kim et al., 2010). Recently, a connectivity map between the regions comprising the multiple-demand network was completed (Camilleri et al., 2018). Camilleri and colleagues defined seed regions according to the multiple-demand network and computed both functional and resting-state connectivity between the regions. Using hierarchical clustering, they

identified separate clusters of regions. Of relevance to the current dissertation, the IPS, dPMC, inferior frontal junction, and inferior temporal gyrus were shown to be activated together, however the co-activation was dependent on the specific features of the task. The researchers did not include any sensorimotor regions other than the pre-SMA in their analysis and did not explore the temporal development of the network co-activations. Unsurprisingly, in all four of the empirical studies comprising this dissertation, regions belonging to the network were found to maintain task-relevant information: IFG, MFG, SMA, IPS, dPMC, and FEF. Moreover, in agreement with Camilleri and colleagues, the involvement of the specific regions was dependent on the task.

As defined by Kim and colleagues, the task-positive network consists of both sensory and motor regions. Thus, the network offers a transition from sensory representations to motor output. Indeed, it is likely that the initial sensory representations are transferred to the PPC and PFC for additional processing and manipulation, before being sent to motor regions for construction of the motor plan. Importantly, as stated by Christophel and colleagues in their review (2017), the location where task-relevant information is identified depends on the experimental design. Specifically, to what degree the participant is able to process the information along the perception-action loop for the successful completion of the task. In the following paragraphs, I explore each empirical study individually according to this distributed, task-dependent model of the somatosensory perception-action loop. Unfortunately, fMRI research does not lend itself to the investigation of temporal processes, thus, corroboration of the following sections with EEG in humans and neurophysiological recordings in NHPs is necessary.

Task-positive network maintains information in WM

Specifically, the sensory-motor and fronto-parietal regions comprising the task-positive network (Kim et al., 2010) maintain WM representations. In agreement with Christophel and colleagues (2017), the specific experimental design features, such as the stimulus, task, and motor output, will determine the localization of maintained information in WM for the particular experimental paradigm.

In the first study of this dissertation, participants extracted numerosity information from a repetitive tactile stimulus and used this information to make a perceptual decision, communicated using their right index and middle fingers. As previously discussed, the results of the multivariate SVR analysis identified two clusters of numerosity-specific WM information in the frontal cortex. One cluster in the right IFG, a region previously shown to be responsible for the extraction of numerosity-specific information (Nieder, 2016). The second cluster in the task-positive network member regions left SFG, MFG, and PMC.

Interestingly, only frontal regions and no somatosensory or parietal regions were found to maintain numerosity-specific WM information. This is likely due to the activity of the ANS which abstracts numerosity information from a stimulus, thereby dissociating the WM representation from the underlying somatosensory stimulus features and maintaining the information in the region responsible for the transformation. Moreover, if participants had been instructed to maintain the tactile sensation of the stimulus, then, based on somatosensory imagery results (Nierhaus et al., 2023; Schmidt et al., 2014), it is likely that the WM content would have additionally been maintained in somatosensory regions. Finally, the PMC is known to be necessary for the comparison of numerical quantities (Gruber et al., 2001; Nieder, 2005) and is also responsible for the preparation of manual motor commands (Nakayama et al., 2008; Yamagata et al., 2009; Yamagata et al., 2012).

Thus, I propose a complete perception-action loop description of this first experiment: S1 extracted the rate code from the tactile stimulus and passed the code to the ANS in the right PFC. The ANS isolated the numerosity information from the rate code, discarded the unnecessary sensory features, before sharing the information with bilateral downstream regions in the task-positive network (SFG, MFG). The contralateral PMC was the final processing stage before a decision could be made, and the ensuing motor plan computed. Due to participants having access to the WM information during the WM delay and not the test stimulus, a final decision could not be computed. Therefore, the WM information could not be processed further along the perception-action loop and formalized into a motor plan until after the presentation of the test stimulus, which is likely why no information was identified in M1.

In the second study, the experimental design was modified with the introduction of a second experimental condition, the group condition. In contrast to the first study where participants always extracted the numerosity, in the second study, participants extracted the group in half of the trials, whereas in the other half, they simply encoded and maintained the stimulus as presented. This experimental modification provided a means of contrasting the two experimental conditions. Indeed, we identified adaptive coding (Duncan, 2001) in the left IPS in that the WM representation changed depending on the experimental condition. Importantly, the IPS, like the PFC, is a core member of the task-positive network (Fox et al., 2005). Additionally, we identified stimulus-specific information in both the stimulus and group experimental conditions in the left IFG. Moreover, we did not identify any WM-specific information in somatosensory regions. We hypothesized that this was due to the nature of the stimuli and the experimental design. Participants were made very familiar with the stimuli during a training session and reported encoding them as auditory or verbal stimuli, which would be consistent with the representation identified in the IFG (Binder et al., 1997).

Importantly, in this second study, we did not identify any significant manipulated WM content in the PMC. We hypothesize that this was due to another crucial modification of the trial design. Whereas in the first study, participants were able to respond directly after presentation of the test stimulus (i.e., if stim 1 choose left, if stim 2 choose right), this was not possible in the second study. Indeed, after the target, two colour stimuli were presented, and participants had to choose the colour that corresponded with their decision. Moreover, the colours appeared randomly on either the left or right side. Thus, we argue that the PMC was not able to prepare a motor plan because participants had to first translate their WM representation into a decision, and then their decision into a colour, before a motor output could be computed. We suggest that this additional step further decoupled the WM information from motor regions such that the WM information was not present in motor regions and was instead maintained by the task-positive frontal-parietal regions: IFG and IPS. Indeed, we suggest that in this study, across both conditions, the IFG and IPS maintained stimulus-specific information in WM which was manipulated by the IPS during the group experimental condition. Due to the additional decoupling of the motor decision from the WM content, the information could not be processed further along the perception-action loop.

Task-positive network maintains memory-based perceptual decision representations

Transitioning to the final two decision-making experiments. The key difference between the two halves of the empirical studies comprising this dissertation is that the experimental focus shifts from the WM period to the period after the presentation of the test stimulus. Thus, in an identical fashion to the first two experiments, participants began by extracting and forming a perceptual representation which was transformed by the fronto-parietal task-positive network into a WM representation. Then, the test stimulus was presented and compared against the WM representation. The period between the presentation of the test stimulus and the completion of the motor action was the time period under investigation.

Importantly, the distinction between the two decision-making studies is the motor output effector, and this distinction is well-represented by the results. The fourth study, in an analogous fashion to the first and second, employed a manual button response with the right hand whereas the third study employed saccades as responses. Correspondingly, the decision-specific information was found in bilateral FEF (saccades) and the left PMC (right hand effector) respectively. Furthermore, the decoding accuracy in the FEF predicted the individual behavioural accuracy (Wu et al., 2019). Interestingly, additional regions in the fronto-parietal cortex were also identified during the saccadic response version of the task: the left MFG, left IFG, and inferior parietal lobule, which were not present in the manual response version of the task. It is likely that, due to the identical trial structure and task design, both studies required the same computations. However, due to differences in statistical power, only the third study was able to identify the decision-specific information in other frontal regions. This discrepancy highlights the necessity for well-powered studies so that robust conclusions can be drawn from the results.

Furthermore, similar to the first two studies of this dissertation, only fronto-parietal regions were found to maintain relevant information. Indeed, both the third and fourth studies identified memory-based decision-specific information in the left IPS, similar to the second study. Freedman and Assad have suggested that a common computational mechanism underlies both processes of decision making and categorization or grouping (Freedman & Assad, 2011; 2016). Thus, it is possible that the IPS computed the decision (higher -vs- lower) and this information was then conveyed to

downstream motor regions in an effector-specific manner. While this interpretation seemingly contradicts the Intentional Framework for decision making and appears to argue for a domain-general decision-making region, the third and fourth studies identified non-overlapping regions in the IPS as maintaining decision-specific information. Thus, it is possible that, due to the identical experimental features, similar but non-overlapping regions relevant for saccadic and motor downstream regions within the IPS computed the decision. Whereas a novel experimental paradigm with different stimuli, features, and task, would require the decision to be computed in a completely distinct region. Future research is necessary to determine whether the finding of distinct IPS regions is real or an artefact of statistical processing and power. Therefore, to conclude, studies employing computational modelling are necessary to determine whether a domain-general IPS, specific sub-regions of the IPS, or downstream motor regions such as the PMC and FEF compute the memory-based perceptual decision.

4. Conclusions and Open Questions

After having completed the research comprising this dissertation, it is possible to draw conclusions regarding the intermediate representations enabling the explosion of adaptive behaviours from the simple stimulus-response reflexes to the complex behaviours observed across species today. Indeed, the cortex has evolved a significant number of intermediate regions between the sensory and motor cortices and these regions have been found to support WM processes and representations. Sensory regions create and maintain perceptual representations, motor regions the motor action plans, and depending on the specific task-demands, a combination of sensory and

higher-order task-positive regions spanning the frontal and parietal cortices maintain, manipulate, and transform WM information. However, several open questions regarding this process remain.

First and foremost, a goal of cognitive neuroscience should be the description of the roles of the distributed representations underlying the intermediate stages of the perception-action loop. Neurophysiological recordings in combination with computational modelling is necessary to truly differentiate between the various representations. Indeed, Romo and colleagues have already provided invaluable information on the content of the representations in frontal regions, however it is necessary to look in more detail. What is the connectivity between the regions? Are the regions connected in a serial or parallel pathway, and does information feedback between regions? How does the information between the regions differ? Are all of the regions necessary or is there redundancy in the information maintained? What transformations take place along the pathway? What role does the PPC play? Finally, what oscillations contribute to or result from the various WM processes? While it is possible to address some of these questions using neuroimaging in humans in combination with RSA and other advanced techniques, neurophysiological data is necessary for drawing definitive conclusions. Indeed, only by determining the relation between, and purpose of, the various WM representations will it be possible to understand the progression of information along the perception-action loop.

Secondly, future studies should focus on predicting the localization of WM content, since such studies provide a strong basis upon which to draw conclusions regarding the nature and purpose of WM content. Expanding on the experimental paradigms of Lee and colleagues (2013) and ours (Velenosi et al., 2020), I suggest a paradigm consisting of two conditions wherein participants are instructed to use a specific method for encoding WM content. For example, in the first condition, participants are told to maintain the stimulus using a visual method, e.g., to imagine the stimulus in their mind's eye during the WM delay phase of the trial. Whereas, the second condition entails using a somatosensory method, e.g., to imagine feeling the stimulus during the WM delay. Thus, the same participants encode the same stimuli using two separate methods (visual, tactile) and, based on the Distributed Coding theory of WM (Christophel et al., 2017) a dichotomy between the experimental conditions

should be identified. Moreover, by analysing the data using MVPA as well as connectivity methods, it should be possible to localize the WM content and track the flow between regions. Moreover, repeating the study using EEG, and with a different response motor effector, would provide additional important temporal and oscillatory information about the influence of experimental design on the representations underlying the perception-action loop.

Finally, I would like to again highlight the central importance of the experimental design for the interpretation of results. As demonstrated by all four studies included in this dissertation, the particular details of the experimental design: the stimuli, task, and analysis pipeline, influence which brain regions maintain relevant information. While this may seem a trivial insight, I believe it to be a very important aspect of cognitive neuroscience research. Indeed, when comparing between experimental results, it is important to consider the minute differences in experimental designs as they may result in different results which hinder the development of a complete mapping of the cortex's complicated network of stimulus-response contingencies. Only with careful consideration of the experimental context and details, will cognitive neuroscience achieve the goal of describing the mechanisms underlying the ability of organisms to adapt their motor responses to a stimulus based on their current situation, previous experiences, and current goals.

Bibliography

Allefeld, C., & Haynes, J. D. (2014). Searchlight-based multi-voxel pattern analysis of fMRI by cross-validated MANOVA. *Neuroimage*, *89*, 345-357.

Andrade, J. (2002). Working memory in perspective. *Psychology Press.*

Auksztulewicz, R., Spitzer, B., & Blankenburg, F. (2012). Recurrent neural processing and somatosensory awareness. *Journal of Neuroscience*, *32*(3), 799-805.

Awh, E., & Jonides, J. (2001). Overlapping mechanisms of attention and spatial working memory. *Trends in cognitive sciences*, *5*(3), 119-126.

Baddeley, A. (2000). The episodic buffer: a new component of working memory? *Trends in cognitive sciences*, *4*(11), 417-423.

Baddeley, A. (2010). Working memory. *Current biology*, *20*(4), R136-R140.

Baddeley, A. D., & Hitch, G. (1974). Working memory. In *Psychology of learning and motivation*, *8*, 47-89.

Barak, O., Tsodyks, M., & Romo, R. (2010). Neuronal population coding of parametric working memory. *Journal of Neuroscience*, *30*(28), 9424-9430.

Barsalou, L. W. (2008). Grounded cognition. *Annual review of psychology*, *59*, 617-645.

Binder, J. R., Frost, J. A., Hammeke, T. A., Cox, R. W., Rao, S. M., & Prieto, T. (1997). Human brain language areas identified by functional magnetic resonance imaging. *Journal of Neuroscience*, *17*(1), 353-362.

Brody, C. D., Hernández, A., Zainos, A., & Romo, R. (2003). Timing and neural encoding of somatosensory parametric working memory in macaque prefrontal cortex. *Cerebral cortex*, *13*(11), 1196-1207

Buzsáki, G. (2021). The brain from inside out. *Oxford University Press.*

Camilleri, J. A., Müller, V. I., Fox, P., Laird, A. R., Hoffstaedter, F., Kalenscher, T., & Eickhoff, S. B. (2018). Definition and characterization of an extended multiple-demand network. *NeuroImage*, *165*, 138-147.

Cantlon, J. F., Brannon, E. M., Carter, E. J., & Pelphrey, K. A. (2006). Functional imaging of numerical processing in adults and 4-y-old children. *PLoS biology*, *4*(5), e125.

Cantlon, J. F., Platt, M. L., & Brannon, E. M. (2009). Beyond the number domain. *Trends in cognitive sciences*, *13*(2), 83-91.

Cisek P., & Kalaska J., F. (2010). Neural mechanisms for interacting with a world full of action choices. *Annual Review of Neuroscience, 33*, 269-298.

Chelazzi, L., Duncan, J., Miller, E. K., & Desimone, R. (1998). Responses of neurons in inferior temporal cortex during memory-guided visual search. *Journal of neurophysiology*, *80*(6), 2918-2940.

Christophel, T. B., Hebart, M. N., & Haynes, J. D. (2012). Decoding the contents of visual short-term memory from human visual and parietal cortex. *Journal of Neuroscience*, *32*(38), 12983-12989.

Christophel, T. B., Klink, P. C., Spitzer, B., Roelfsema, P. R., & Haynes, J. D. (2017). The distributed nature of working memory. *Trends in cognitive sciences*, *21*(2), 111-124.

Constantinidis, C., Funahashi, S., Lee, D., Murray, J. D., Qi, X. L., Wang, M., & Arnsten, A. F. (2018). Persistent spiking activity underlies working memory. *Journal of neuroscience*, *38*(32), 7020-7028.

Correia, J., Formisano, E., Valente, G., Hausfeld, L., Jansma, B., & Bonte, M. (2014). Brain-based translation: fMRI decoding of spoken words in bilinguals reveals language-independent semantic representations in anterior temporal lobe. *Journal of Neuroscience*, *34*(1), 332-338.

Cowan, N. (2001). The magical number 4 in short-term memory: A reconsideration of mental storage capacity. *Behavioral and brain sciences*, *24*(1), 87-114.

Dehaene, S. (1992). Varieties of numerical abilities. *Cognition*, *44*(1-2), 1-42.

Dehaene, S., Molko, N., Cohen, L., & Wilson, A. J. (2004). Arithmetic and the brain. *Current opinion in neurobiology*, *14*(2), 218-224.

Desimone, R., & Duncan, J. (1995). Neural mechanisms of selective visual attention. *Annual review of neuroscience*, *18*(1), 193-222.

D'Esposito, M. (2007). From cognitive to neural models of working memory. *Philosophical Transactions of the Royal Society B: Biological Sciences*, *362*(1481), 761-772.

D'Esposito, M., & Postle, B. R. (2015). The cognitive neuroscience of working memory. *Annual review of psychology*, *66*, 115-142.

D'Esposito, M., Postle, B. R., Ballard, D., & Lease, J. (1999). Maintenance versus manipulation of information held in working memory: an event-related fMRI study. *Brain and cognition*, *41*(1), 66-86.

Ding, L., & Gold, J. I. (2012). Neural correlates of perceptual decision making before, during, and after decision commitment in monkey frontal eye field. *Cerebral cortex, 22,* 1052-1067.

Duncan, J. (2001). An adaptive coding model of neural function in prefrontal cortex. *Nature reviews neuroscience*, *2*(11), 820-829.

Duncan, J., & Owen, A. M. (2000). Common regions of the human frontal lobe recruited by diverse cognitive demands. *Trends in neurosciences*, *23*(10), 475-483.

Filimon, F., Philiastides, M. G., Nelson, J. D., Kloosterman, N. A., & Heekeren, H. R. (2013). How embodied is perceptual decision making? Evidence for separate processing of perceptual and motor decisions. *Journal of Neuroscience*, *33*(5), 2121-2136.

Fitzgerald, J. K., Freedman, D. J., & Assad, J. A. (2011). Generalized associative representations in parietal cortex. *Nature neuroscience*, *14*(8), 1075-1079.

Fitzgerald, J. K., Swaminathan, S. K., & Freedman, D. J. (2012). Visual categorization and the parietal cortex. *Frontiers in Integrative Neuroscience*, *6*, 18.

Fox, M. D., Snyder, A. Z., Vincent, J. L., Corbetta, M., Van Essen, D. C., & Raichle, M. E. (2005). The human brain is intrinsically organized into dynamic, anticorrelated functional networks. *Proceedings of the National Academy of Sciences*, *102*(27), 9673-9678.

Freedman, D. J., & Assad, J. A. (2011). A proposed common neural mechanism for categorization and perceptual decisions. *Nature neuroscience*, *14*(2), 143-146.

Freedman, D. J., & Assad, J. A. (2016). Neuronal mechanisms of visual categorization: an abstract view on decision making. *Annual review of neuroscience*, *39*, 129-147.

Freedman, D. J., & Ibos, G. (2018). An integrative framework for sensory, motor, and cognitive functions of the posterior parietal cortex. *Neuron*, *97*(6), 1219-1234.

Freedman, D. J., Riesenhuber, M., Poggio, T., & Miller, E. K. (2001). Categorical representation of visual stimuli in the primate prefrontal cortex. *Science*, *291*(5502), 312-316.

Friston, K. J., Holmes, A. P., Poline, J. B., Grasby, P. J., Williams, S. C. R., Frackowiak, R. S., & Turner, R. (1995). Analysis of fMRI time-series revisited. *Neuroimage*, *2*(1), 45-53.

Fuster, J. M., & Alexander, G. E. (1971). Neuron activity related to short-term memory. *Science*, *173*(3997), 652-654.

Fuster, J. M., & Jervey, J. P. (1981). Inferotemporal neurons distinguish and retain behaviorally relevant features of visual stimuli. *Science*, *212*(4497), 952-955.

Glimcher, P. W. (2003). The neurobiology of visual-saccadic decision making. *Annual review of neuroscience*, *26*(1), 133-179.

Gold, J. I., & Shadlen, M. N. (2001). Neural computations that underlie decisions about sensory stimuli. *Trends in Cognitive Science, 5,* 10-16.

Gold, J. I., & Shadlen, M. N. (2007). The neural basis of decision making. *Annual review of neuroscience, 30,* 535-574.

Goldman-Rakic, P. S. (1995). Cellular basis of working memory. *Neuron*, *14*(3), 477-485.

Green D., & Swets, J. (1966). Signal detectability and psychophysics. *Wiley, New York.*

Grefkes, C., & Fink, G. R. (2005). The functional organization of the intraparietal sulcus in humans and monkeys. *Journal of anatomy*, *207*(1), 3-17.

Gruber, O., Indefrey, P., Steinmetz, H., & Kleinschmidt, A. (2001). Dissociating neural correlates of cognitive components in mental calculation. *Cerebral cortex*, *11*(4), 350-359.

Haller, M., Case, J., Crone, N. E., Chang, E. F., King-Stephens, D., Laxer, K. D., ... & Shestyuk, A. Y. (2018). Persistent neuronal activity in human prefrontal cortex links perception and action. *Nature human behaviour*, *2*(1), 80-91.

Haegens, S., Nácher, V., Hernández, A., Luna, R., Jensen, O., & Romo, R. (2011). Beta oscillations in the monkey sensorimotor network reflect somatosensory decision making. *Proceedings of the National Academy of Sciences*, *108*(26), 10708-10713.

Hanes, D. P., & Schall, J. D. (1996). Neural control of voluntary movement initiation. *Science,* 80(274), 427-430.

Hanks, T. D., & Summerfield, C. (2017). Perceptual decision making in rodents, monkeys, and humans. *Neuron, 93,* 15-31.

Harrison, S. A., & Tong, F. (2009). Decoding reveals the contents of visual working memory in early visual areas. *Nature*, *458*(7238), 632-635.

Haxby, J. V. (2012). Multivariate pattern analysis of fMRI: the early beginnings. *Neuroimage*, *62*(2), 852-855.

Haxby, J. V., Connolly, A. C., & Guntupalli, J. S. (2014). Decoding neural representational spaces using multivariate pattern analysis. *Annual review of neuroscience*, *37*, 435-456.

Haynes, J. D. (2015). A primer on pattern-based approaches to fMRI: principles, pitfalls, and perspectives. *Neuron*, *87*(2), 257-270.

Haynes, J. D., & Rees, G. (2006). Decoding mental states from brain activity in humans. *Nature reviews neuroscience*, *7*(7), 523-534.

Heekeren, H. R., Marrett, S., Bandettini, P. A., & Ungerleider, L. G. (2004). A general mechanism for perceptual decision-making in the human brain. *Nature*, *431*(7010), 859-862.

Heekeren, H. R., Marrett, S., Ruff, D. A., Bandettini, P. A., & Ungerleider, L. G. (2006). Involvement of human left dorsolateral prefrontal cortex in perceptual decision making is independent of response modality. *Proceedings of the National Academy of Sciences*, *103*(26), 10023-10028.

Hellström, Å. (1985). The time-order error and its relatives: Mirrors of cognitive processes in comparing. *Psychological Bulletin*, *97*(1), 35.

Herding, J., Ludwig, S., & Blankenburg, F. (2017). Response-modality-specific encoding of human choices in upper beta band oscillations during vibrotactile comparisons. *Frontiers in Human Neuroscience*, *11*, 118.

Herding, J., Spitzer, B., & Blankenburg, F. (2016). Upper beta band oscillations in human premotor cortex encode subjective choices in a vibrotactile comparison task. *Journal of cognitive neuroscience*, *28*(5), 668-679.

Hernández, A., Salinas, E., Garcıa, R., & Romo, R. (1997). Discrimination in the sense of flutter: new psychophysical measurements in monkeys. *Journal of Neuroscience*, *17*(16), 6391-6400.

Hernández, A., Nácher, V., Luna, R., Zainos, A., Lemus, L., Alvarez, M., ... & Romo, R. (2010). Decoding a perceptual decision process across cortex. *Neuron*, *66*(2), 300-314.

Hernández, A., Zainos, A., & Romo, R. (2000). Neuronal correlates of sensory discrimination in the somatosensory cortex. *Proceedings of the National Academy of Sciences*, *97*(11), 6191-6196.

Hernández, A., Zainos, A., & Romo, R. (2002). Temporal evolution of a decision-making process in medial premotor cortex. *Neuron*, *33*(6), 959-972.

Ho, T. C., Brown, S., & Serences, J. T. (2009). Domain general mechanisms of perceptual decision making in human cortex. *Journal of Neuroscience*, *29*(27), 8675-8687.

Horwitz, G. D., & Newsome, W. T. (1999). Separate signals for target selection and movement specification in the superior colliculus. *Science,* 80(284), 1158-1161.

Jackson, J. B., & Woolgar, A. (2018). Adaptive coding in the human brain: Distinct object features are encoded by overlapping voxels in frontoparietal cortex. *Cortex*, *108*, 25-34.

Jacob, S. N., Hähnke, D., & Nieder, A. (2018). Structuring of abstract working memory content by fronto-parietal synchrony in primate cortex. *Neuron*, *99*(3), 588-597.

Jacob, S. N., & Nieder, A. (2009). Tuning to non-symbolic proportions in the human frontoparietal cortex. *European Journal of Neuroscience*, *30*(7), 1432-1442.

Jacobsen, C. F. (1935). Functions of frontal association area in primates. *Archives of Neurology & Psychiatry*, *33*(3), 558-569.

Jacobsen, C. F., Elder, J. H., & Haslerud, G. M. (1936). Studies of cerebral function in primates.

Jonides, J., Lacey, S. C., & Nee, D. E. (2005). Processes of working memory in mind and brain. *Current Directions in Psychological Science*, *14*(1), 2-5.

Jun, J. K., Miller, P., Hernández, A., Zainos, A., Lemus, L., Brody, C. D., & Romo, R. (2010). Heterogenous population coding of a short-term memory and decision task. *Journal of Neuroscience*, *30*(3), 916-929.

Kantak, S. S., Stinear, J. W., Buch, E. R., & Cohen, L. G. (2012). Rewiring the brain: potential role of the premotor cortex in motor control, learning, and recovery of function following brain injury. *Neurorehabilitation and neural repair*, *26*(3), 282-292.

Kaufman, E. L., Lord, M. W., Reese, T. W., & Volkmann, J. (1949). The discrimination of visual number. *The American journal of psychology*, *62*(4), 498-525.

Kim, H., Daselaar, S. M., & Cabeza, R. (2010). Overlapping brain activity between episodic memory encoding and retrieval: roles of the task-positive and task-negative networks. *Neuroimage*, *49*(1), 1045-1054.

Kim, J-N., & Shadlen, M. N. (1999). Neural correlates of a decision in the dorsolateral prefrontal cortex of the macaque. *Nature Neuroscience, 2,* 176-185.

Knops, A., & Willmes, K. (2014). Numerical ordering and symbolic arithmetic share frontal and parietal circuits in the right hemisphere. *Neuroimage*, *84*, 786-795.

Koenigs, M., Barbey, A. K., Postle, B. R., & Grafman, J. (2009). Superior parietal cortex is critical for the manipulation of information in working memory. *Journal of Neuroscience*, *29*(47), 14980-14986.

Kriegeskorte, N., Mur, M., & Bandettini, P. A. (2008). Representational similarity analysis-connecting the branches of systems neuroscience. *Frontiers in systems neuroscience*, *4*.

Kubota, K., & Niki, H. (1971). Prefrontal cortical unit activity and delayed alternation performance in monkeys. *Journal of neurophysiology*, *34*(3), 337-347.

LaMotte, R. H., & Mountcastle, V. B. (1975). Capacities of humans and monkeys to discriminate vibratory stimuli of different frequency and amplitude: a correlation between neural events and psychological measurements. *Journal of Neurophysiology*, *38*(3), 539-559.

Leathers, M. L., & Olson, C. R. (2012). In monkeys making value-based decisions, LIP neurons encode cue salience and not action value. *Science*, *338*(6103), 132-135.

Lee, S. H., Kravitz, D. J., & Baker, C. I. (2013). Goal-dependent dissociation of visual and prefrontal cortices during working memory. *Nature neuroscience*, *16*(8), 997-999.

Lepsien, J., Griffin, I. C., Devlin, J. T., & Nobre, A. C. (2005). Directing spatial attention in mental representations: Interactions between attentional orienting and working-memory load. *Neuroimage*, *26*(3), 733-743.

Levy, R., & Goldman-Rakic, P. S. (2000). Segregation of working memory functions within the dorsolateral prefrontal cortex. *Executive control and the frontal lobe: Current issues*, 23-32.

Liu, T., & Hou, Y. (2013). A hierarchy of attentional priority signals in human frontoparietal cortex. *Journal of Neuroscience*, *33*(42), 16606-16616.

Liu, T., & Pleskac, T. J. (2011). Neural correlates of evidence accumulation in a perceptual decision task. *Journal of neurophysiology*, *106*(5), 2383-2398.

Machens, C. K., Romo, R., & Brody, C. D. (2005). Flexible control of mutual inhibition: a neural model of two-interval discrimination. *Science*, *307*(5712), 1121-1124.

Machens, C. K., Romo, R., & Brody, C. D. (2010). Functional, but not anatomical, separation of "what" and "when" in prefrontal cortex. *Journal of Neuroscience*, *30*(1), 350-360.

Macmillan, N.A., Creelman, C.D. (2004). Detection theory: A user's guide. *Psychology press*.

Marois, R. (2015). The brain mechanisms of working memory: An evolving story. In Jolicoeur, P., Lefebvre, C., Martinez-Trujillo, M. (Eds.), *Mechanisms of sensory working memory: Attention and performance XXV* (page 23 - 32). Academic Press.

Mazurek, M. E., Roitman, J. D., Ditterich, J., & Shadlen, M. N. (2003). A role for neural integrators in perceptual decision making. *Cerebral Cortex, 13,* 1257-1269.

Miller, G.A., Galanter, E., & Pribram, K.H. (1960). Plans and the structure of behavior. *Henry Holt and co.*

Mountcastle, V. B., LaMotte, R. H., & Carli, G. (1972). Detection thresholds for stimuli in humans and monkeys: comparison with threshold events in mechanoreceptive afferent nerve fibers innervating the monkey hand. *Journal of neurophysiology*, *35*(1), 122-136.

Mountcastle, V. B., Steinmetz, M. A., & Romo, R. (1990). Frequency discrimination in the sense of flutter: psychophysical measurements correlated with postcentral events in behaving monkeys. *Journal of Neuroscience*, *10*(9), 3032-3044.

Mulder, M. J., Van Maanen, L., & Forstmann, B. U. (2014). Perceptual decision neurosciences–a model-based review. *Neuroscience*, *277*, 872-884.

Myers, N. E., Stokes, M. G., & Nobre, A. C. (2017). Prioritizing information during working memory: beyond sustained internal attention. *Trends in cognitive sciences*, *21*(6), 449-461.

Nakayama, Y., Yamagata, T., Tanji, J., & Hoshi, E. (2008). Transformation of a virtual action plan into a motor plan in the premotor cortex. *Journal of Neuroscience*, *28*(41), 10287-10297.

Nieder, A. (2005). Counting on neurons: the neurobiology of numerical competence. *Nature Reviews Neuroscience*, *6*(3), 177-190.

Nieder, A. (2012). Supramodal numerosity selectivity of neurons in primate prefrontal and posterior parietal cortices. *Proceedings of the National Academy of Sciences*, *109*(29), 11860-11865.

Nieder, A. (2016). The neuronal code for number. *Nature Reviews Neuroscience*, *17*(6), 366-382.

Nieder, A., & Dehaene, S. (2009). Representation of number in the brain. *Annual review of neuroscience, 32*, 185-208.

Nieder, A., Diester, I., & Tudusciuc, O. (2006). Temporal and spatial enumeration processes in the primate parietal cortex. *Science*, *313*(5792), 1431-1435.

Nieder, A., Freedman, D. J., & Miller, E. K. (2002). Representation of the quantity of visual items in the primate prefrontal cortex. *Science*, *297*(5587), 1708-1711.

Nieder, A., & Miller, E. K. (2004). A parieto-frontal network for visual numerical information in the monkey. *Proceedings of the National Academy of Sciences*, *101*(19), 7457-7462.

Nierhaus, T., Wesolek, S., Pach, D., Witt, C. M., Blankenburg, F., & Schmidt, T. T. (2023). Content representation of tactile mental imagery in primary somatosensory cortex. *Eneuro*, *10*(6).

Nyberg, L., & Eriksson, J. (2016). Working memory: maintenance, updating, and the realization of intentions. *Cold Spring Harbor Perspectives in Biology*, *8*(2), a021816.

Oberauer, K., & Hein, L. (2012). Attention to information in working memory. *Current directions in psychological science*, *21*(3), 164-169.

Oberauer, K., & Kliegl, R. (2001). Beyond resources: Formal models of complexity effects and age differences in working memory. *European Journal of Cognitive Psychology*, *13*(1-2), 187-215.

O'Connell, R. G., Dockree, P. M., & Kelly, S. P. (2012). A supramodal accumulation-to-bound signal that determines perceptual decisions in humans. *Nature neuroscience*, *15*(12), 1729-1735.

O'Connell, R. G., Shadlen, M. N., Wong-Lin, K., & Kelly, S. P. (2018). Bridging neural and computational viewpoints on perceptual decision-making. *Trends in Neuroscience, 41*(11), 838-852.

Oristaglio, J., Schneider, D. M., Balan, P. F., & Gottlieb, J. (2006). Integration of visuospatial and effector information during symbolically cued limb movements in monkey lateral intraparietal area. *Journal of Neuroscience*, *26*(32), 8310-8319.

Owen, A. M., McMillan, K. M., Laird, A. R., & Bullmore, E. (2005). N-back working memory paradigm: A meta-analysis of normative functional neuroimaging studies. *Human brain mapping*, *25*(1), 46-59.

Park, I. M., Meister, M. L., Huk, A. C., & Pillow, J. W. (2014). Encoding and decoding in parietal cortex during sensorimotor decision-making. *Nature neuroscience*, *17*(10), 1395-1403.

Parker, A. J., & Newsome, W. T. (1998). Send and the single neuron: probing the physiology of perception. *Annual Reviews Neuroscience, 21,* 227-277.

Pasternak, T., & Greenlee, M. W. (2005). Working memory in primate sensory systems. *Nature Reviews Neuroscience*, *6*(2), 97-107.

Piazza, M., Izard, V., Pinel, P., Le Bihan, D., & Dehaene, S. (2004). Tuning curves for approximate numerosity in the human intraparietal sulcus. *Neuron*, *44*(3), 547-555.

Piazza, M., Pinel, P., Le Bihan, D., & Dehaene, S. (2007). A magnitude code common to numerosities and number symbols in human intraparietal cortex. *Neuron*, *53*(2), 293-305.

Pleger, B., Ruff, C. C., Blankenburg, F., Bestmann, S., Wiech, K., Stephan, K. E., ... & Dolan, R. J. (2006). Neural coding of tactile decisions in the human prefrontal cortex. *Journal of Neuroscience*, *26*(48), 12596-12601.

Pouget, A., Dayan, P., & Zemel, R. (2000). Information processing with population codes. *Nature Reviews Neuroscience*, *1*(2), 125-132.

Postle, B. R. (2006). Working memory as an emergent property of the mind and brain. *Neuroscience*, *139*(1), 23-38.

Preuschhof, C., Heekeren, H. R., Taskin, B., Schubert, T., & Villringer, A. (2006). Neural correlates of vibrotactile working memory in the human brain. *Journal of Neuroscience*, *26*(51), 13231-13239.

Ratcliff, R., Smith, P. L., Brown, S. D., & McKoon, G. (2016). Diffusion decision model: current issues and history. *Trends in Cognitive Sciences, 20,* 260-281.

Ratcliff, R., Cherian, A., & Segraves, M. (2003). A comparison of macaque behavior and superior colliculus neuronal activity to predictions from models of two-choice decisions. *Journal of Neurophysiology, 90*, 1392-1407.

Riggall, A. C., & Postle, B. R. (2012). The relationship between working memory storage and elevated activity as measured with functional magnetic resonance imaging. *Journal of Neuroscience*, *32*(38), 12990-12998.

Riley, M. R., & Constantinidis, C. (2016). Role of prefrontal persistent activity in working memory. *Frontiers in systems neuroscience*, *9*, 181.

Roitman, J. D., & Shadlen, M. N. (2002). Response of neurons in the lateral intraparietal area during a combined visual discrimination reaction time task. *Journal of Neuroscience, 22,* 9475-9489.

Romo, R., Brody, C. D., Hernández, A., & Lemus, L. (1999). Neuronal correlates of parametric working memory in the prefrontal cortex. *Nature*, *399*(6735), 470-473.

Romo, R., Hernández, A., Zainos, A., & Salinas, E. (1998). Somatosensory discrimination based on cortical microstimulation. *Nature*, *392*(6674), 387-390.

Romo, R., Hernández, A., Zainos, A., Brody, C. D., & Lemus, L. (2000). Sensing without touching: psychophysical performance based on cortical microstimulation. *Neuron*, *26*(1), 273-278.

Romo, R., Hernández, A., & Zainos, A. (2004). Neuronal correlates of a perceptual decision in ventral premotor cortex. *Neuron*, *41*(1), 165-173.

Romo, R., & de Lafuente, V. (2013). Conversion of sensory signals into perceptual decisions. *Progress in neurobiology*, *103*, 41-75.

Romo, R., Lemus, L., & de Lafuente, V. (2012). Sense, memory, and decision-making in the somatosensory cortical network. *Current opinion in neurobiology*, *22*(6), 914-919.

Romo, R., & Rossi-Pool, R. (2020). Turning touch into perception. *Neuron*, *105*(1), 16-33.

Romo, R., & Salinas, E. (2003). Flutter discrimination: neural codes, perception, memory and decision making. *Nature Reviews Neuroscience*, *4*(3), 203-218.

Rossi-Pool, R., Salinas, E., Zainos, A., Alvarez, M., Vergara, J., Parga, N., & Romo, R. (2016). Emergence of an abstract categorical code enabling the discrimination of temporally structured tactile stimuli. *Proceedings of the National Academy of Sciences*, *113*(49), E7966-E7975.

Rossi-Pool, R., Zainos, A., Alvarez, M., Zizumbo, J., Vergara, J., & Romo, R. (2017). Decoding a decision process in the neuronal population of dorsal premotor cortex. *Neuron*, *96*(6), 1432-1446.

Royall, D. R., Lauterbach, E. C., Cummings, J. L., Reeve, A., Rummans, T. A., Kaufer, D. I., ... & Coffey, C. E. (2002). Executive control function: a review of its promise and challenges for clinical research. A report from the Committee on Research of the American Neuropsychiatric Association. *The Journal of neuropsychiatry and clinical neurosciences*, *14*(4), 377-405.

Schmidt, T. T., Ostwald, D., & Blankenburg, F. (2014). Imaging tactile imagery: changes in brain connectivity support perceptual grounding of mental images in primary sensory cortices. *Neuroimage*, *98*, 216-224.

Schmidt, T. T., Wu, Y. H., & Blankenburg, F. (2017). Content-specific codes of parametric vibrotactile working memory in humans. *Journal of Neuroscience*, *37*(40), 9771-9777.

Schröder, P., Schmidt, T. T., & Blankenburg, F. (2019). Neural basis of somatosensory target detection independent of uncertainty, relevance, and reports. *elife*, *8*, e43410.

Scimeca, J. M., Kiyonaga, A., & D'Esposito, M. (2018). Reaffirming the sensory recruitment account of working memory. *Trends in cognitive sciences*, *22*(3), 190-192.

Seger, C. A., & Miller, E. K. (2010). Category learning in the brain. *Annual review of neuroscience*, *33*, 203-219.

Shadlen, M. N., Britten, K. H., Newsome, W. T., & Movshon, J. A. (1996). A computational analysis of the relationship between neuronal and behavioral responses to visual motion. *Journal of neuroscience, 16,* 1486-1510.

Shadlen, M., & Newsome, W. T. (1996). Motion perception: seeing and deciding. *Proceedings of the National Academy of Sciences, 93,* 628-633.

Shadlen, M. N., & Newsome, W. T. (1998). The variable discharge of cortical neurons: implications for connectivity, computation, and information coding. *Journal of neuroscience, 18,* 3870-3896.

Shadlen, M. N., & Newsome, W. T. (2001). Neural basis of a perceptual decision in the parietal cortex (area LIP) of the rhesus monkey. *Journal of neurophysiology, 86,* 1916-1936.

Shepard, R. N., & Metzler, J. (1971). Mental rotation of three-dimensional objects. *Science*, *171*(3972), 701-703.

Spitzer, B., Fleck, S., & Blankenburg, F. (2014). Parametric alpha-and beta-band signatures of supramodal numerosity information in human working memory. *Journal of Neuroscience*, *34*(12), 4293-4302.

Spitzer, B., Gloel, M., Schmidt, T. T., & Blankenburg, F. (2014). Working memory coding of analog stimulus properties in the human prefrontal cortex. *Cerebral Cortex*, *24*(8), 2229-2236.

Sreenivasan, K. K., Curtis, C. E., & D'Esposito, M. (2014). Revisiting the role of persistent neural activity during working memory. *Trends in cognitive sciences*, *18*(2), 82-89.

Stoet, G., & Snyder, L. H. (2004). Single neurons in posterior parietal cortex of monkeys encode cognitive set. *Neuron*, *42*(6), 1003-1012.

Stokes, M. G., Kusunoki, M., Sigala, N., Nili, H., Gaffan, D., & Duncan, J. (2013). Dynamic coding for cognitive control in prefrontal cortex. *Neuron, 78(2),* 364-375.

Swaminathan, S. K., & Freedman, D. J. (2012). Preferential encoding of visual categories in parietal cortex compared with prefrontal cortex. *Nature neuroscience*, *15*(2), 315-320.

Tong, F., & Pratte, M. S. (2012). Decoding patterns of human brain activity. *Annual review of psychology*, *63*, 483-509.

Uluç, I., Schmidt, T. T., Wu, Y. H., & Blankenburg, F. (2018). Content-specific codes of parametric auditory working memory in humans. *Neuroimage*, *183*, 254-262.

Uluç, I., Velenosi, L. A., Schmidt, T. T., & Blankenburg, F. (2020). Parametric representation of tactile numerosity in working memory. *Eneuro*, *7*(1).

van Ede, F., & Nobre, A. C. (2023). Turning attention inside out: How working memory serves behavior. *Annual Review of Psychology*, *74*, 137-165.

Velenosi, L. A., Wu, Y. H., Schmidt, T. T., & Blankenburg, F. (2020). Intraparietal sulcus maintains working memory representations of somatosensory categories in an adaptive, context-dependent manner. *NeuroImage*, *221*, 117146.

Veltman, D. J., Rombouts, S. A., & Dolan, R. J. (2003). Maintenance versus manipulation in verbal working memory revisited: an fMRI study. *Neuroimage*, *18*(2), 247-256.

Wager, T. D., & Smith, E. E. (2003). Neuroimaging studies of working memory. *Cognitive, Affective, & Behavioral Neuroscience*, *3*, 255-274.

Wolpert, D. M., Diedrichsen, J., & Flanagan, J. R. (2011). Principles of sensorimotor learning. *Nature reviews neuroscience*, *12*(12), 739-751.

Woolgar, A., Hampshire, A., Thompson, R., & Duncan, J. (2011). Adaptive coding of task-relevant information in human frontoparietal cortex. *Journal of Neuroscience*, *31*(41), 14592-14599.

Wu, Y. H., Uluç, I., Schmidt, T. T., Tertel, K., Kirilina, E., & Blankenburg, F. (2018). Overlapping frontoparietal networks for tactile and visual parametric working memory representations. *Neuroimage*, *166*, 325-334.

Wu, Y. H., Velenosi, L. A., & Blankenburg, F. (2021). Response modality-dependent categorical choice representations for vibrotactile comparisons. *NeuroImage*, *226*, 117592.

Wu, Y. H., Velenosi, L. A., Schröder, P., Ludwig, S., & Blankenburg, F. (2019). Decoding vibrotactile choice independent of stimulus order and saccade selection during sequential comparisons. *Human Brain Mapping*, *40*(6), 1898-1907.

Wurtz, R. H., Sommer, M. A., Paré, M., & Ferraina, S. (2001). Signal transformations from cerebral cortex to superior colliculus for the generation of saccades. *Vision research*, *41*(25-26), 3399-3412.

Xu, Y. (2017). Re-evaluating the sensory account of visual working memory storage. *Trends in Cognitive Sciences*, *21*(10), 794-815.

Xu, Y. (2018). Sensory cortex is nonessential in working memory storage. *Trends in cognitive sciences*, *22*(3), 192-193.

Yamagata, T., Nakayama, Y., Tanji, J., & Hoshi, E. (2009). Processing of visual signals for direct specification of motor targets and for conceptual representation of action targets in the dorsal and ventral premotor cortex. *Journal of neurophysiology*, *102*(6), 3280-3294.

Yamagata, T., Nakayama, Y., Tanji, J., & Hoshi, E. (2012). Distinct information representation and processing for goal-directed behaviour in the dorsolateral and ventrolateral prefrontal cortex and the dorsal premotor cortex. *Journal of Neuroscience*, *32*(37), 12934-12949.

Yan, C., Christophel, T. B., Allefeld, C., & Haynes, J. D. (2021). Decoding verbal working memory representations of Chinese characters from Broca's area. *NeuroImage*, *226*, 117595.

Yu, L., Hu, J., Shi, C., Zhou, L., Tian, M., Zhang, J., & Xu, J. (2021). The causal role of auditory cortex in auditory working memory. *Elife*, *10*, e64457.

Zhou, Y., & Freedman, D. J. (2019). Posterior parietal cortex plays a causal role in perceptual and categorical decisions. *Science*, *365*(6449), 180-185.

Original Research Articles

Publication 1 – Parametric representation of tactile numerosity in working memory

Uluç I, **Velenosi LA**, Schmidt TT, Blankenburg F (2020). Parametric representation of tactile numerosity in working memory. *Eneuro*, *7*(1).
DOI: https://doi.org/10.1523/ENEURO.0090-19.2019

This chapter includes the publisher's version (Version of Record).

Cognition and Behavior

Parametric Representation of Tactile Numerosity in Working Memory

Işıl Uluç,[1,2] Lisa Alexandria Velenosi,[1] Timo Torsten Schmidt,[1] and Felix Blankenburg[1,2]

https://doi.org/10.1523/ENEURO.0090-19.2019

[1]Neurocomputation and Neuroimaging Unit (NNU), Department of Education and Psychology, Freie Universität Berlin, 14195 Berlin, Germany and [2]Berlin School of Mind and Brain, Humboldt-Universität zu Berlin, 10099 Berlin, Germany

Abstract

Estimated numerosity perception is processed in an approximate number system (ANS) that resembles the perception of a continuous magnitude. The ANS consists of a right lateralized frontoparietal network comprising the lateral prefrontal cortex (LPFC) and the intraparietal sulcus. Although the ANS has been extensively investigated, only a few studies have focused on the mental representation of retained numerosity estimates. Specifically, the underlying mechanisms of estimated numerosity working memory (WM) is unclear. Besides numerosities, as another form of abstract quantity, vibrotactile WM studies provide initial evidence that the right LPFC takes a central role in maintaining magnitudes. In the present fMRI multivariate pattern analysis study, we designed a delayed match-to-numerosity paradigm to test what brain regions retain approximate numerosity memoranda. In line with parametric WM results, our study found numerosity-specific WM representations in the right LPFC as well as in the supplementary motor area and the left premotor cortex extending into the superior frontal gyrus, thus bridging the gap in abstract quantity WM literature.

Key words: Working memory; numerosity; tactile; fMRI; MVPA; abstract quantity

Significance Statement

While the perception of approximate numerosities has been extensively investigated, research into the mnemonic representation during working memory (WM) is relatively rare. Here, we present the first study to localize WM information for approximate numerosities using functional magnetic resonance imaging in combination with multivariate pattern analysis (MVPA). Extending beyond previous accounts that used either a priori brain regions or electrocorticography with poor spatial resolution and univariate analysis methods, we used an assumption-free, time-resolved, whole-brain searchlight MVPA approach to identify brain regions that code approximate numerosity WM content. Our findings in line with previous work, provide preliminary evidence for a modality- and format-independent, abstract quantitative WM system, which resides within the right lateral PFC.

Introduction

Humans can tell whether 100 people are a larger group than 50 people quite accurately without counting. This ability to quantify amount, size, length, or other analog stimulus properties can be performed nonsymbolically, independent of language (Dehaene, 1992; Spitzer et al., 2014b). Indeed, human infants and several animals are able to approximate a variety of quantities (Nieder, 2005; Piazza et al., 2007; Piazza and Izard, 2009; Nieder and Dehaene, 2009), suggesting a common elemental system which has been termed the approximate number system (ANS; Gallistel and Gelman, 1992; Dehaene, 2011).

While numerosity is a discrete stimulus property, the ANS allows an approximation of numerosity, resulting in

Received March 12, 2019; accepted August 2, 2019; First published January 9, 2020.

The authors declare no competing financial interests.

Author contributions: I.U., L.A.V., T.T.S., and F.B. designed research; I.U. and L.A.V. performed research; I.U., T.T.S., and F.B. analyzed data; I.U. wrote the paper; L.A.V., T.T.S., and F.B. commented on the paper.

an analog estimation. Thus, in contrast to the symbolic mental representation of numbers as classes or categories, it has been hypothesized that the ANS representation resembles that of continuous quantities or magnitudes such as intensities, lengths, or frequencies (Piazza et al., 2004; Nieder and Dehaene, 2009; Spitzer et al., 2014a). In support of this, neural representations underlying both the ANS and continuous quantities have been shown to be supramodal, implying a representation abstract in nature (Piazza et al., 2006; Spitzer and Blankenburg, 2012; Spitzer et al., 2014a; Vergara et al., 2016). Moreover, small numbers are rapidly and accurately identified without counting, known as subitizing (Kaufman et al., 1949). Thus, these numbers are represented as discrete values. If the number of items exceeds the subitizing threshold, counting is required to determine the exact amount. When there is insufficient time for counting, the ANS approximates the quantity in a fast and efficient manner.

The functional anatomy of the ANS has been extensively characterized in both human and nonhuman primates (NHPs). A frontoparietal network comprising the dorsolateral prefrontal cortex and the posterior parietal cortex (PPC), specifically the intraparietal sulcus (IPS), is involved in approximating quantities during perception (Dehaene et al., 2004; Piazza et al., 2004, 2007; Cantlon et al., 2006, 2009; Jacob and Nieder, 2009; Knops and Willmes, 2014). Moreover, the right hemisphere has been shown to be dominant with respect to quantity estimation (McGlone and Davidson, 1973; Young and Bion, 1979; Kosslyn et al., 1989); however, recent studies have found that both hemispheres respond to approximate visual numerosity (Piazza et al., 2004; Ansari et al., 2006). Particularly in nonsymbolic numerosity perception, the IPS has been shown to exhibit stronger numerosity-selective responses than the PFC (Tudusciuc and Nieder, 2009), and the PPC, especially the IPS, responds to the nonsymbolic numerosity processing (Piazza et al., 2004, 2007).

The ANS literature is primarily focused on perception with relatively few NHP studies extending to investigate working memory (WM) representations of approximate quantities (Nieder, 2016). As short-term maintenance of information is critical for higher-order cognitive functions such as decision-making and reasoning, it is crucial to investigate beyond perception to the maintenance of approximate quantities in WM. In line with results from perception studies of the ANS, neurons in the frontoparietal network were found, specifically in the PFC and IPS, to exhibit numerosity-selective activity during WM (Jacob et al., 2018). Furthermore, supramodal coding of numerosity memoranda in the frontoparietal cortex has been identified (Nieder, 2017). Interestingly, in contrast to perception, the proportion of numerosity-selective neurons in the PFC and their tuning strength to numerosity have been more prominent than the ones in the PPC during WM retention. Moreover, neurons in the PFC remained selective and discriminated numerosities better than neurons in the PPC during the WM delay (Nieder and Miller, 2004; Tudusciuc and Nieder, 2009; Nieder, 2016).

To the best of our knowledge, only a single study has focused on the WM representation of numerosity in humans (Spitzer et al., 2014a), although some approximate numerosity perception studies used fMRI multivariate pattern analysis (MVPA) method with WM-related paradigms focusing on the perceptual processes instead of the WM retention (Eger et al., 2009; Borghesani et al., 2019; Castaldi et al., 2019). Spitzer et al. (2014a) probed the oscillations underlying multimodal WM representations by training participants to estimate numerosity from sequential auditory, visual, and tactile stimuli. They identified strong and long-lasting alpha oscillations in the PPC reflecting WM load, whereas, in line with NHP results, beta-band activity in the right PFC showed numerosity-selective modulation.

Nevertheless, whole-brain research regarding the localization of numerosity memoranda in humans is lacking. To this end, we designed a tactile delayed match-to-numerosity (DMTN) task in combination with whole-brain, searchlight, MVPA of human fMRI data (Christophel et al., 2012; Schmidt et al., 2017; Uluç et al., 2018). Using this analysis approach, we localized brain regions maintaining approximate number content in WM. As per previous studies (Spitzer et al., 2014a; Nieder, 2016), we hypothesized that the content would be represented in frontal regions, specifically the right PFC.

Materials and Methods

Participants

Thirty-eight healthy volunteers participated in the study. The sample size was based on the successful use of similar sample sizes in earlier MVPA experiments with analog experimental designs and analyses (Schmidt et al., 2017; Christophel et al., 2018). In addition, it accords with recent theoretical work on power analysis for random field theory-based cluster-level statistical inference (Ostwald et al., 2019). The data of four participants were excluded due to low performance levels (≤60%), resulting in data from 34 participants (mean ± SD age, 25.53 ± 5.43 years; 19 females) being further analyzed. All were right handed according to the Edinburgh Handedness Inventory with a mean ± SD index of 0.82 ± 0.14 (Oldfield, 1971). The experimental procedure was approved by the local ethics committee and was conducted in accordance with the Human Subject Guidelines of the Declaration of Helsinki. All participants provided written informed consent before the experiment and were compensated for their participation.

I.U. was supported by Deutscher Akademischer Austauschdienst and the Berlin School of Mind and Brain. L.A.V. was supported by the Research Training Group GRK 1589/2 by the Deutsche Forschungsgemeinschaft.

Acknowledgments: We thank Yuan-hao Wu for assistance on data collection, and Alexander von Lautz for feedback on this manuscript.

Correspondence should be addressed to Işıl Uluç at isil.uluc@gmail.com.

https://doi.org/10.1523/ENEURO.0090-19.2019

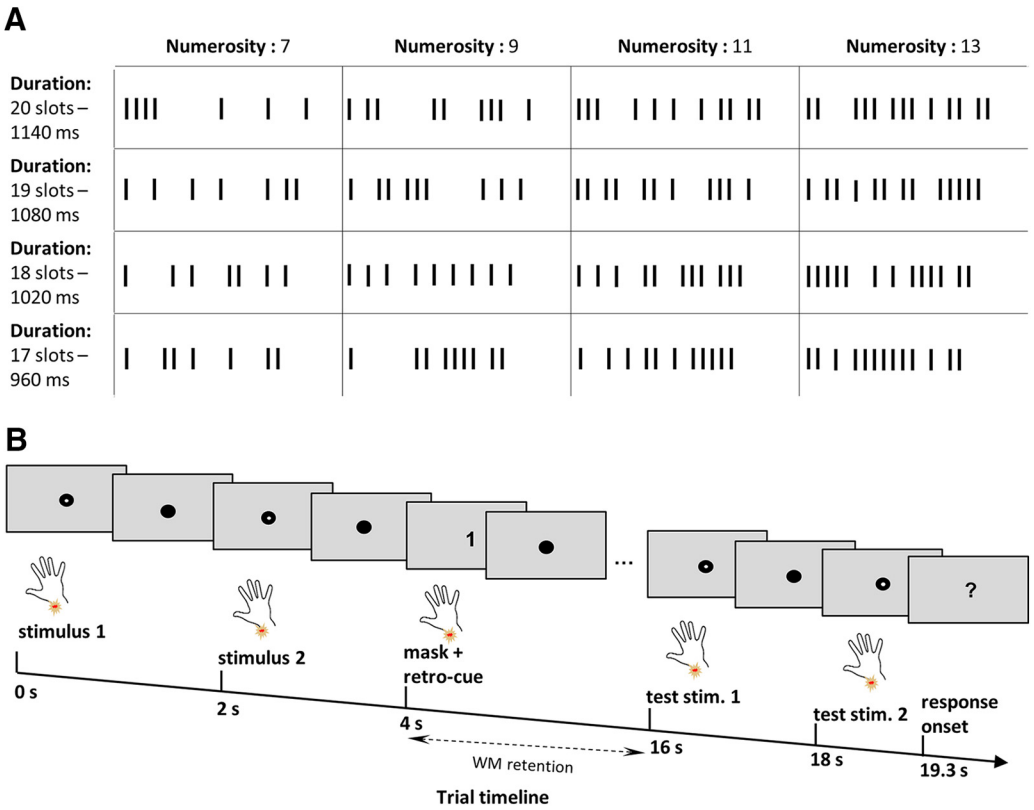

Figure 1. Sample pulse sequences and experimental paradigm. ***A***, Sample stimuli. Pulse sequences of 7, 9, 11, and 13 were used as experimental stimuli. For each numerosity, there were four different durations (960, 1020, 1080, and 1140 ms), where each duration was subdivided into 60 ms slots. The distribution of pulses to slots was randomized for each stimulus presentation. The first and the last slot of each stimulus always contained a pulse. The stimuli displayed are for illustrative purposes. ***B***, Experimental paradigm. A delayed match-to-numerosity task was used, where two sample stimuli and a mask were presented consecutively. A visual retro-cue that was presented simultaneously with the mask indicated which of the numerosities should be retained for the 12 s delay. After the delay, participants performed a two-alternative forced choice, indicating which of the two test stimuli had the same numerosity as the cued stimulus. The response period was 1.5 s. Please note that the stimulus duration and interstimulus interval changed depending on the stimulus duration, but the onset of each event was locked to coincide with the onset of an image acquisition.

Stimuli

Tactile stimuli consisted of trains of square-wave electric pulses (200 μs) delivered via a pair of surface-adhesive electrodes attached to the participant's left wrist. A constant current neurostimulator (model DS7A, Digitimer) was used to deliver the stimuli. Subjects reported tactile sensations radiating to the thumb, index, and middle finger, verifying stimulation of the median nerve. Individual sensory thresholds were determined for each participant. The stimulus intensity was then adjusted to a target value of ~200% of the sensory threshold (mean, 6.42 mA; SD, 1.20 mA).

A to-be-remembered stimulus sequence comprised 7, 9, 11, or 13 pulses. To dissociate stimulus length and perceived pulse frequency (spacing of tactile pulses) from the numerosity of pulses, the duration of the stimulus varied, and the interpulse intervals were randomized. To this end, we defined four stimulus durations (960, 1020, 1080, and 1140 ms). Each duration was subdivided into 60 ms slots, resulting in 17, 18, 19, and 20 slots, respectively. The temporal distribution of the pulses was then randomized across the slots (Fig. 1*A*, illustrative stimuli). Within each run, each numerosity was presented in a short (17 or 18) and a long (19 or 20) duration, resulting in 24 different numerosity–duration pairings (4 numerosities $\times$ 2 durations/run $\times$ 3 uncued numerosities). The different durations were balanced across runs. The alternatives for each cued numerosity were computed according to the respective sample ($\pm$3 pulses). Additionally, the target stimulus and the cued sample never had the same duration, ensuring that memorizing the duration or average frequency of the target does not help to perform the task. We also performed a Fourier transformation of the stimuli, which ensured that all stimuli were composed of similar combinations of frequencies. Therefore, this stimulus design ensured that participants had to memorize the stimulus numerosity since they could not use the temporal density of the pulses or the stimulus length as WM memoranda to solve the task.

Task

We used a DMTN paradigm in which participants remembered the estimated numerosity of a stimulus. Each trial began with the presentation of two pulse sequences with different numerosities. Next, a retro-cue ("1" or "2") indicated which of the two numerosities had to be remem-

bered. To suppress potential perceptual residues, in the sense of afterimages (Sperling, 1960; Christophel and Haynes, 2014; Christophel et al., 2015), a mask consisting of the longest duration (1140 ms) with a pulse in each of the 20 slots, was applied simultaneously with the onset of the retro-cue. Following a 12 s retention phase, two test stimuli were presented and a two-alternative forced choice was given. Neither of the test stimuli were identical to the encoded stimulus; however, one had the same numerosity, while the duration and the frequency were different. This ensured that participants used the approximated numerosity of the stimulus instead of some other stimulus feature to correctly match the test with the remembered stimulus. The numerosity of the alternative stimulus was three pulses plus or minus the target stimulus. To ensure that the number of pulses in a sequence could not be easily counted, the lower alternative stimulus for the lowest to-be-remembered numerosity (7), was set to 5 and thus above a previously established subitizing threshold of approximately 4 (for tactile modality, it was shown to be 3–4; Riggs et al., 2006; Plaisier et al., 2009, 2010; Plaisier and Smeets, 2011; Spitzer et al., 2014a; Tian and Chen, 2018). After the second target stimulus, participants had 1.5 s to indicate, via button press with their right middle or index finger, which of the two stimuli had the same numerosity as the encoded stimulus (Fig. 1*B*, experimental design). Furthermore, the response mapping was counterbalanced across participants. In total, a trial lasted 21 s and an experimental run, consisting of all possible stimulus pairings presented equally often (12 pairings $\times$ 4 presentations = 48 trials) in a randomized order, with intertrial intervals of 1.5 or 3.5 s, lasted 18.7 min. Four experimental runs were collected for each participant, resulting in a total recording time of 74.8 min.

Before the fMRI experiment, each participant was familiarized with the timing and structure of the task by performing up to two experimental runs outside the scanner.

Number naming test assessing countability

Subsequent to the fMRI session, we applied a number-naming task to ensure that participants were unable to count the number of pulses used in the stimulus set. Participants were asked to try to count the number of pulses. The stimuli ranged from 1 to 15 pulses with 5 different duration and temporal pulse distribution combinations of each numerosity were tested, resulting in 75 trials. The counting test was performed after fMRI data acquisition so as to prevent biasing the participants toward counting the pulses in the main experiment.

To ensure that the presented numerosities were above participants' subitizing thresholds, we calculated the mean performance for each numerosity across participants and calculated each average estimated numerosity. We then compared the slope of accuracy for estimating numerosities with earlier studies that calculated subitizing thresholds for tactile stimuli (Riggs et al., 2006; Plaisier et al., 2009, 2010; Plaisier and Smeets, 2011; Spitzer et al., 2014a; Tian and Chen, 2018). We performed a linear trend analysis using linear regression to determine whether the distance between the true and estimated numerosity scales with increasing true numerosity in a linear fashion.

fMRI data acquisition and preprocessing

fMRI data were acquired in four runs, with a Siemens 3 T Tim Trio MRI scanner (Siemens) equipped with a 32-channel head coil. In each run, 565 images were collected (T2$*$-weighted gradient echo EPI: 37 slices; ascending order; 20% gap; whole brain; TR = 2000 ms; TE = 30 ms; $3 \times 3 \times 3$ mm^3; flip angle = 70°; 64×64 matrix). After the last functional run, a high-resolution structural scan was recorded using a T1-weighted MPRAGE sequence ($1 \times 1 \times 1$ mm^3; TR = 1900 ms; TE = 2.52 ms; 176 sagittal slices). fMRI data preprocessing was performed using SPM12 (Wellcome Trust Center for Neuroimaging, Institute for Neurology, University College London, London, UK). Functional images were slice time corrected and spatially realigned to the mean image. To conserve the spatiotemporal structure of the fMRI data for the multivariate analyses, no smoothing or normalization was performed. For the univariate control analysis, functional images were normalized to MNI space and smoothed with an 8 mm FWHM kernel.

First-level finite impulse response models

A time-resolved, multivariate searchlight analysis (Kriegeskorte et al., 2006; Schmidt et al., 2017) was used to identify brain regions encoding memorized numerosity information. First, a general linear model (GLM) with a set of finite impulse response (FIR) regressors was fit to each participant's data to obtain runwise parameter estimates of each WM content (numerosity value of 7, 9, 11, or 13). A single FIR regressor was estimated for each fMRI image or 2 s time bin (1 TR); thus, the 20 s trial was divided into 10 time bins. We additionally included the first five principal components accounting for the most variance in the CSF and white matter signal time courses, respectively (Behzadi et al., 2007), and six head motion regressors, as regressors of no interest. Moreover, the data were filtered with a high-pass filter of 128 s. The resulting parameter estimates were used for the MVPA, performed with The Decoding Toolbox (TDT) version 3.52 (Hebart et al., 2015).

Multivariate pattern analysis

For the decoding of memorized numerosity information, a searchlight-based multivariate analysis using a support vector regression (SVR) approach was performed with the computational routines of LIBSVM (Chang and Lin, 2011), as implemented in TDT. SVR MVPA (for more discussion, see Kahnt et al., 2011; Schmidt et al., 2017) considers the variable of interest (memorized numerosity) as a continuous data vector with multiple independent variables (multivariate BOLD activities) as opposed to the commonly used support vector machine approach that treats the variable of interest as a categorical object. This means that the SVR MVPA approach seeks a linear continuum for the numerosities in which their distance is proportional to the distances of the rank order.

We analyzed each time bin independently by implementing a searchlight decoding analysis with a spherical

searchlight radius of 4 voxels. For a given voxel, *z*-scaled parameter estimates (across samples) corresponding to each WM condition were extracted from all voxels within the spherical searchlight for each run. This yielded 16 pattern vectors (4 WM contents × 4 runs), each corresponding to the BOLD activity pattern for a specific WM condition of a functional run. We then fitted a linear function to these pattern vectors such that the multivariate distribution for the different numerosities follows a linear mapping of numerosities. The *z*-scaled parameter estimates were entered into an SVR model with a fixed regularization parameter c that was set to 1.

We used a leave-one-run-out cross-validation scheme for the subject-level decoding analysis. The SVR classifier was trained on three runs (12 pattern vectors) and tested on the data of the independent fourth run (4 pattern vectors) for how well it predicted the values of the remaining run. The allocation of training and test runs was iterated so that each of the four functional runs was used as a test run once, resulting in four cross-validation folds. The prediction performance from each cross-validation fold was reported by a Fisher's *z*-transformed correlation coefficient between the predicted and the actual numerosity information estimate. The mean prediction accuracy across cross-validation folds was assigned to the center voxel of the searchlight, and the center of the searchlight was moved voxel by voxel through the brain, resulting in a whole-brain prediction accuracy map. Consequently, we obtained one prediction accuracy map for each time bin for each participant, where the prediction accuracy reflects how well a linear ordering according to the associated numerosities could be read out from the locally distributed BOLD activity pattern at a given voxel location and time.

Next, prediction accuracy maps were normalized to MNI space and smoothed with an 8 mm FWHM kernel. They were then entered into a second-level, repeated-measures ANOVA with subject and time (time bins) as factors. To assess which brain regions exhibit WM content-specific activation patterns during the delay period, we computed a *t*-contrast across the six time bins corresponding to the 12 s WM delay (time bins 3–8). The results are presented at $p < 0.05$ family-wise error (FWE) correction at the cluster level with a cluster-defining threshold of $p < 0.001$. Cytoarchitectonic references are based on the SPM anatomy toolbox where possible (Eickhoff et al., 2005). Presented images (e.g., surface projections with applied color scales) were created using MRIcron version9/9/2016 (McCausland Center for Brain Imaging, University of South Carolina, Columbia, SC).

Control analyses

In the first control analysis, we examined whether the decoded numerosity information during WM retention was specific to WM or could be assigned to perceptual residues. To this aim, we defined a second, first-level model with FIR regressors for the nonmemorized stimulus. We then implemented the identical searchlight decoding procedure as the main analysis. Thus, this control analysis tested for the presence of numerosity information of the nonmemorized stimulus.

Next, we conducted a parametric univariate analysis to ensure that the decoded information in the main analysis is not due to the modulation of mean activity level. To this end, we fitted a standard GLM with the following four HRF-convolved regressors: one regressor to capture WM processes, a parametrically modulated regressor for the numerosity content of the WM memoranda as well as eight [4 numerosities × 2 (sample, test)] additional parametrically modulated regressors for each sample and test stimulus. First-level baseline contrasts for the parametric effect of memorized numerosity were forwarded to a second-level one-sample *t* test.

Finally, to test the specificity of the SVR analysis to the parametric order of the four numerosities, we performed exhaustive whole-brain SVR searchlight analyses for all possible permutations of numerosity labels. To achieve this, we computed distance rank order as a sum of the absolute difference of adjacent ranks [e.g., 11, 13, 7, and 9 numerosity is distance 5 (|3–4|+|4–1|+|1–2|)] for all possible permutations of the numerosity order. Then, the permutations were grouped according to their distance from the original rank order. We used 12 instead of 24 permutations as the distances of rank order permutations are symmetric. Including the permutation with the correct linear order, the 12 permutations are aggregated into five classes depending on their distance from the correct linear order. Then, for each permutation analysis, we extracted the prediction accuracies of the group-peak voxels that are defined in the original analysis. For statistical assessment, we calculated the mean prediction accuracy across related time bins (WM time bins 3–8) for each peak voxel for each distance group (see Fig. 3*C*).

Results

Behavioral performance

Thirty-four participants performed with 65.36 ± 3.29% (mean ± SD) accuracy in the demanding DMTN task across the four experimental runs (Fig. 2*A*). To test whether the behavioral performance differed for the four numerosity values, we performed a one-way repeated-measures ANOVA with four levels, one for each numerosity. This test revealed a significant main effect ($F_{(3,135)} = 7.52$, $p < 0.001$). *Post hoc t* tests (Bonferroni corrected for multiple comparisons) between performances were significant for numerosity values 7 and 13 and 9 and 13 ($p < 0.05/6$; Fig. 2*A*). This is expected because we did not control for the Weber–Fechner effect except for the lowest numerosity (which we did due to subitizing concerns). As a result, as the numerosity increases, it becomes more difficult to differentiate between the sample and alternative stimuli, thus resulting in a lower performance for high numerosities (Fechner, 1966) but is unlikely to affect WM processing.

Behavioral performance on number naming test assessing countability

To test whether participants were able to count the numerosities used in the current study, participants per-

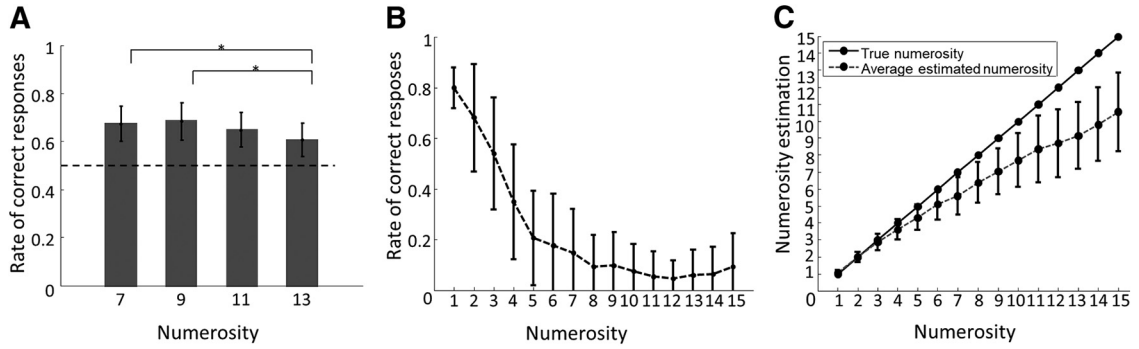

Figure 2. ***A***, Mean rate of correct responses across participants ($n = 34$) for different numerosities in the main WM DMTN task. The figure shows that the WM performance decreases with increasing numerosity. Error bars represent standard derivation (SD). Asterisks indicate statistical significance for pairwise *t* tests, Bonferroni corrected for multiple comparisons ($p < 0.05/6$). ***B***, Mean performance across subjects for estimated numerosity in number naming task (mean ± SD). ***C***, True numerosities versus mean numerosity estimations (error bars show SD).

formed an additional number-naming test. Previous research in tactile numerosity indicated the subitizing threshold for comparable stimuli to be four pulses (Riggs et al., 2006; Plaisier et al., 2009; 2010; Plaisier and Smeets, 2011; Spitzer et al., 2014a; Tian and Chen, 2018). The approximation of the subitizing threshold identified in the present study is in line with these reports (Fig. 2*B*). As expected, participants' perceptual accuracy decreased with increasing numerosity, and performance decreased to 50% when more than three pulses were presented. Similarly, the distance between the true and estimated numerosity increased with increasing numerosities ($p < 0.001$, linear trend analysis; Fig. 2*C*).

Multivariate mapping of regions that code numerosity as WM content

The time-resolved, searchlight-based multivariate regression analysis was performed to identify brain regions representing estimated numerosity memoranda. The SVR MVPA analysis for the WM retention period revealed numerosity-specific responses in the left premotor cortex (PMC) slightly extending to the primary motor area (MI), left middle frontal gyrus (MFG), left superior frontal gyrus (SFG) extending into bilateral supplementary motor areas (SMA), right SFG extending to the right frontal pole, and right MFG extending into the pars triangularis of the right inferior frontal gyrus (IFG). Results are reported at $p < 0.05$, FWE corrected at the cluster level with a cluster-defining threshold of $p < 0.001$ (Fig. 3, Table 1).

For the sake of completeness, we investigated whether numerosity information could be decoded from the IPS at an uncorrected statistical threshold of $p < 0.001$. We found a cluster in the right PPC extending to the IPS (peak at MNI: $x = 36$, $y = -52$, $z = 36$ mm; *z* score = 3.89; $k = 164$), which was identified as hIP1 with a 39.5% probability and hIP3 with a 5.9% probability using the SPM anatomy toolbox (Eickhoff et al., 2005) at $p_{uncorrected} < 0.001$.

Control analyses

To test whether the identified decoded information is indeed specific to the memorized numerosity representation, we applied the same searchlight procedure to the nonmemorized numerosity stimulus. This analysis did not reveal any clusters with above-chance prediction accuracy at $p_{FWE\text{-}Cluster} < 0.05$.

Additionally, we conducted a univariate parametric analysis to test whether the decoding results could be due to differences in activation strength between WM contents. A second level *t* test revealed no significant voxels at $p_{FWE\text{-}Cluster} < 0.05$, thus providing evidence for the multivariate nature of the numerosity representations identified in this study rather than the modulation of univariate mean activity.

Finally, we performed label-permutation tests to ensure the specificity of the linear ordering of stimuli in the SVR MVPA. Higher prediction accuracies were expected when the activation patterns in a given brain region represented the correct order of the four numerosity labels, and it was expected to decrease with the distance from the correct ordering. As expected, the prediction accuracy during WM was the highest for the true-labeled data and decreased with increasing distance from the correct ordering (Fig. 3*C*).

Discussion

The current study, to our knowledge, is the first to identify brain regions that code approximate numerosity WM content using human neuroimaging methods. Thus, this study extends the broad literature on ANS perception to the maintenance of mental representations, which can be used for higher-order cognitive functions. We used a well established, whole-brain, searchlight, DMTN paradigm to identify representations of tactile approximate numerosity memoranda. Specifically, we used an SVR technique, which, in contrast to support vector machines, treats the retained WM content as a continuous variable and thus predicts the ordering of content along the variable, rather than a singularly specific class label. Consequently, an above-chance prediction accuracy in a brain region means that the content-specific activation patterns follow a linear ordering according to the associated numerosity. Our searchlight analysis identified a distributed network spanning the left PMC, bilateral SFG, bilateral SMA, and right MFG extending into right IFG. Therefore,

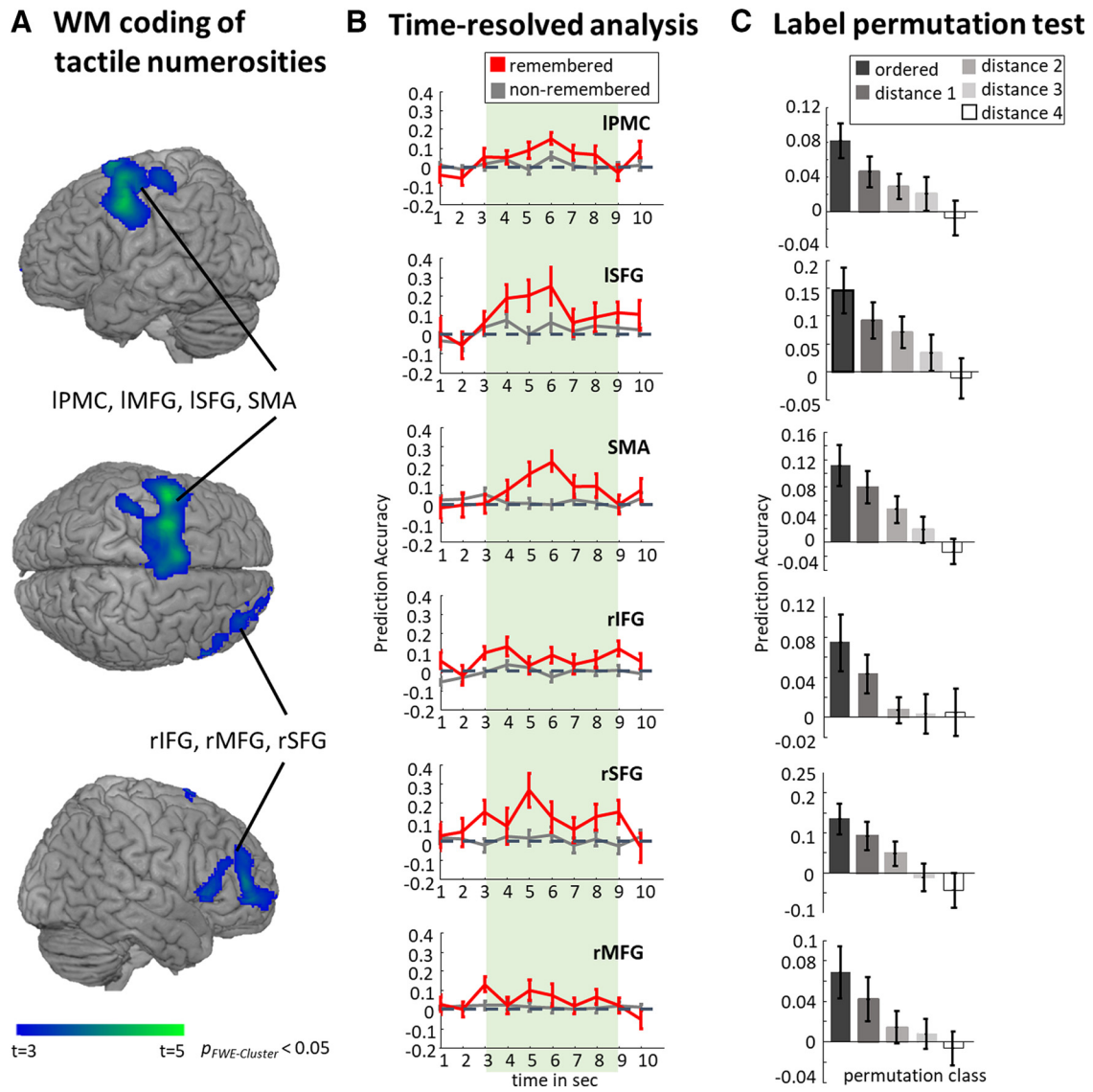

Figure 3. ***A***, Brain regions coding information for the memorized estimated numerosities. Group-level results of a *t*-contrast testing the 12 s WM delay for above-chance prediction accuracy. Brain regions carrying information about memorized scalar magnitudes are as follows: IFG, MFG, PMC, SMA, and SFG. ***B***, Time courses of decoding accuracies of remembered (red) and nonremembered (gray) stimuli for all identified brain regions in the main analysis (Fig. 3*A*). Error bars indicate standard error of the mean (SEM). The figure shows that, for all clusters depicted in the main analysis, there is more numerosity-specific WM information for the remembered than for the forgotten numerosity, and the information is present throughout the WM delay period. ***C***, Results of the label permutation tests. Five bars are shown for each brain region, respectively. Each bar displays the mean prediction accuracy estimated from the distance to correct order groups. The shade of the bar color, ranging from black to white, depicts the different distance to correct ordering. Black bars indicate the mean prediction performance of the group with the correct linear order, while white bars represent the mean prediction accuracy derived from the most linearly unordered data. Brain regions tested for label permutation are: IFG, MFG, PMC, SMA, and SFG. Error bars indicate SEM.

these regions contain linearly ordered, multivariate WM representations of the numerosities.

Our results are in line with previous numerosity WM studies in NHPs and human EEG, which have established the central role of the PFC. Indeed, previous unimodal and multimodal studies have identified content-specific representations in the PFC (Nieder and Miller, 2004; Tudusciuc and Nieder, 2009; Spitzer et al., 2014a; Nieder, 2016; Jacob et al., 2018). More specifically, in humans, parametric modulation of upper-β oscillations in the right lateral PFC has been shown to reflect analog numerosity estimation that has been derived from discrete sequences, both within and between stimulus modalities (Spitzer et al., 2014a). Thus, the numerosity representations in the PFC are likely to be supramodal in nature. However, those studies used either electrophysiological recordings from an a priori brain region or have used univariate data analysis methods. The present study extends the literature on numerosity WM in the following two ways: first, to whole-brain fMRI data; and second, to

Table 1: Anatomic label and MNI coordinates of brain areas depicting memorized numerosity information during WM

Cluster size	Anatomical region	Peak MNI coordinates			z-score	Prediction accuracy
		x	y	z		
4557	Left PMC/MI	−50	2	52	4.78	0.082
	Left SFG	−28	0	60	7.74	0.146
	SMA	−6	10	74	4.48	0.114
1342	Right SFG	32	50	10	4.17	0.135
	Right IFG (pars triangularis)	60	24	2	4.17	0.075
	Right MFG	40	50	30	3.69	0.069

All results are reported at $p_{FWE\text{-}Cluster} < 0.05$ with a cluster-defining threshold of $p < 0.001$. Mean prediction accuracy over the delay period is reported. Areas were, where possible, identified using the SPM anatomy toolbox (Eickhoff et al., 2005).

multivariate data analysis methods, specifically the SVR MVPA. The benefits of multivariate over univariate analysis methods have been well established (Haynes, 2015). Multivariate analysis techniques are sensitive to the combinatorial aspects of voxel activity, thereby enabling the identification of spatially distributed representations (Haynes, 2015; Hebart and Baker, 2018). Thus, our results agree with and extend the previous NHP and human EEG numerosity WM findings to whole-brain, spatially distributed activity patterns, suggesting that estimated numerosity WM content is maintained in the LPFC (Nieder et al., 2002; Nieder and Miller, 2003, 2004; Tudusciuc and Nieder, 2009; Spitzer et al., 2014a; Nieder, 2016).

It should be noted that we used temporally distributed tactile numerosity stimuli as the WM memoranda, namely the numerosity, was presented as a sequence of pulses. Evidence exists for potential differences in perceptual processing of spatially and temporally distributed numerosities, where spatially distributed stimuli appear to be processed in parietal regions while temporarily distributed stimuli do not (Cavdaroglu and Knops, 2019). In line with the finding of Cavdaroglu and Knops (2019), we used temporally distributed stimuli and did not find evidence of WM representations in posterior regions in our full brain FWE-corrected analysis. However, a small cluster ($k = 164$) extending to right IPS was observed to represent remembered numerosity content at an uncorrected threshold of $p < 0.001$. While our results agree with numerosity WM findings in NHPs that suggest frontal rather than parietal coding for spatial numerosity stimuli during WM retention (for review, see Nieder, 2016), further investigation is needed to conclusively decide for the role of the IPS. The role of the IPS could be interpreted as specific to perceptual processing, and therefore was only revealed at a lower threshold in our analysis, while the PFC contains WM instead. Alternatively, a potentially different nature of the neuronal code (e.g. spatial distribution of a multivariate code) in the IPS might lead to the observed findings (Hebart and Baker, 2018). That is, it might be the temporarily distributed nature of the applied stimuli that drives the effects in the PFC, and the IPS would be more specialized for spatially distributed presentations as used by most previous studies. A future direct comparison of our results with spatial numerosity stimuli is necessary to test for differences determined by the stimulus types.

Moreover, while the literature relating to numerosity WM is limited, there is extensive work exploring the WM representation of abstract quantities more generally. Specifically, the frequency discrimination task has been systematically explored in a multitude of modalities with a wide range of methods (Romo et al., 1999; Lemus et al., 2009; Spitzer et al., 2010; Spitzer and Blankenburg, 2011; 2012; Fassihi et al., 2014; Vergara et al., 2016; Schmidt et al., 2017; von Lautz et al., 2017; Uluç et al., 2018; Wu et al., 2018). Numerosity and frequency share several traits, particularly that they are both abstract magnitudes that may be represented in a supramodal fashion (Nieder and Miller, 2003; Spitzer and Blankenburg, 2012; Nieder, 2016; Vergara et al., 2016). However, whether their underlying WM representations are maintained by a shared network has yet to be explored. The present study provides an initial step toward resolving this question by providing the first evidence that frequency and numerosity WM representations are maintained in overlapping brain regions. We identified numerosity-specific WM content in the right IFG, SMA, and left PMC, which is in agreement with results from frequency studies also using an fMRI MVPA approach in humans (Schmidt et al., 2017; Wu et al., 2018; Uluç et al., 2018). Unimodal and multimodal research in both NHPs and humans has identified frequency-specific content in the right LPFC and SMA, thereby suggesting that the WM representations are modality independent in nature (Romo et al., 1999; Hernández et al., 2002, 2010; Barak et al., 2010; Spitzer et al., 2010; Spitzer and Blankenburg, 2011, 2012; Vergara et al., 2016; Schmidt et al., 2017; Wu et al., 2018). However, the explicit relationship between frequency and numerosity still needs to be explored, particularly with respect to the underlying neural codes of numerosity and frequency representations (Nieder, 2017).

Additionally, we identified numerosity-specific content in the left PMC. Previous findings from frequency WM fMRI MVPA studies identified abstract quantity information in the PMC (Schmidt et al., 2017; Uluç et al., 2018; Wu et al., 2018) . Moreover, the dorsal PMC has been shown to represent abstract numerical rules, such as comparison and calculation (Gruber et al., 2001; Eger et al., 2003; Nieder, 2005). This is in line with the present task, which required the comparison of numerical quantities, suggesting representation of task-relevant, numerosity-specific information to be used in numerical comparison.

In summary, the data at hand is in line with the suggestion of a domain general, abstract magnitude processing system. This abstract processing system can be identified by multivariate WM representations of tactile numerosity stimuli within the right PFC. Together with previous findings that found WM representations of tactile frequency (Spitzer et al., 2010, 2014a; Spitzer and Blankenburg, 2012; Schmidt et al., 2017; Wu et al., 2018), visual flicker frequency (Spitzer and Blankenburg, 2012; Spitzer et al., 2014a; Wu et al., 2018), auditory frequency (Spitzer and Blankenburg, 2012, Uluç et al., 2018), and the reports of number coding (Nieder et al., 2002; Nieder and Miller, 2003, 2004; Tudusciuc and Nieder, 2009; Nieder, 2016) in the PFC, the present study provides additional evidence suggesting that the PFC is capable of representing both analog quantities as well as parametric stimulus properties as frequencies. Thus, we provide preliminary evidence for a higher-level, modality- and format-independent, abstract quantitative WM system that resides within the PFC.

References

Ansari D, Dhital B, Siong SC (2006) Parametric effects of numerical distance on the intraparietal sulcus during passive viewing of rapid numerosity changes. Brain Res 1067:181–188.

Barak O, Tsodyks M, Romo R (2010) Neuronal population coding of parametric working memory. J Neurosci30:9424–30.

Behzadi Y, Restom K, Liau J, Liu TT (2007) A component based noise correction method (CompCor) for BOLD and perfusion based fMRI. Neuroimage 37:90–101.

Borghesani V, Dolores de Hevia M, Viarouge A, Chagas PP, Eger E, Piazza M (2019) Processing number and length in the parietal cortex: sharing resources, not a common code. Cortex 114:17–27.

Cantlon JF, Brannon EM, Carter EJ, Pelphrey KA (2006) Functional imaging of numerical processing in adults and 4-y-old children. PLoS Biol 4:e125.

Cantlon JF, Platt ML, Brannon EM (2009) Beyond the number domain. Trends Cogn Sci 13:83–91.

Castaldi E, Piazza M, Dehaene S, Vignaud A, Eger E (2019) Attentional amplification of neural codes for number independent of other quantities along the dorsal visual stream. bioRxiv. Advance online publication. Retrieved January 9, 2020. doi:10.7554/eLife.45160.

Cavdaroglu S, Knops A (2019) Evidence for a posterior parietal cortex contribution to spatial but not temporal numerosity perception. Cereb Cortex 29:2965–2977.

Chang C-C, Lin C-J (2011) LIBSVM: a library for support vector machines. ACM Trans Intell Syst Technol 2:1–27.

Christophel TB, Haynes J-D (2014) Decoding complex flow-field patterns in visual working memory. Neuroimage 91:43–51.

Christophel TB, Hebart MN, Haynes J-D (2012) Decoding the contents of visual short-term memory from human visual and parietal cortex. J Neurosci 32:12983–12989.

Christophel TB, Cichy RM, Hebart MN, Haynes J-D (2015) Parietal and early visual cortices encode working memory content across mental transformations. Neuroimage 106:198–206.

Christophel TB, Allefeld C, Endisch C, Haynes J-D (2018) View-independent working memory representations of artificial shapes in prefrontal and posterior regions of the human brain. Cereb Cortex 28:2146–2161.

Dehaene S (1992) Varieties of numerical abilities. Cognition 44:1–42.

Dehaene S (2011) The number sense: how the mind creates mathematics. New York: Oxford UP.

Dehaene S, Molko N, Cohen L, Wilson AJ (2004) Arithmetic and the brain. Curr Opin Neurobiol 14:218–224.

Eger E, Sterzer P, Russ MO, Giraud A-L, Kleinschmidt A (2003) A supramodal number representation in human intraparietal cortex. Neuron 37:719–726.

Eger E, Michel V, Thirion B, Amadon A, Dehaene S, Kleinschmidt A (2009) Deciphering cortical number coding from human brain activity patterns. Curr Biol 19:1608–1615.

Eickhoff SB, Stephan KE, Mohlberg H, Grefkes C, Fink GR, Amunts K, Zilles K (2005) A new SPM toolbox for combining probabilistic cytoarchitectonic maps and functional imaging data. Neuroimage 25:1325–1335.

Fassihi A, Akrami A, Esmaeili V, Diamond ME (2014) Tactile perception and working memory in rats and humans. Proc Natl Acad Sci U S A 111:2331–2336.

Fechner G (1966) Elements of psychophysics. New York: Holt Rinehart & Winston.

Gallistel CR, Gelman R (1992) Preverbal and verbal counting and computation. Cognition 44:43–74.

Gruber O, Indefrey P, Steinmetz H, Kleinschmidt A (2001) Dissociating neural correlates of cognitive components in mental calculation. Cereb Cortex 11:350–359.

Haynes J-D (2015) A primer on pattern-based approaches to fMRI: principles, pitfalls, and perspectives. Neuron 87:257–270.

Hebart MN, Baker CI (2018) Deconstructing multivariate decoding for the study of brain function. Neuroimage 180:4–18.

Hebart MN, Görgen K, Haynes J-D (2015) The Decoding Toolbox (TDT): a versatile software package for multivariate analyses of functional imaging data. Front Neuroinform 8:88.

Hernández A, Zainos A, Romo R (2002) Temporal Evolution of a Decision-Making Process in Medial Premotor Cortex. Neuron 33: 959–972.

Hernández A, Nácher V, Luna R, Zainos A, Lemus L, Alvarez M, Vázquez Y, Camarillo L, Romo R (2010) Decoding a perceptual decision process across cortex. Neuron 66:300–314.

Jacob SN, Nieder A (2009) Tuning to non-symbolic proportions in the human frontoparietal cortex. Eur J Neurosci 30:1432–1442.

Jacob SN, Hähnke D, Nieder A (2018) Structuring of abstract working memory content by fronto-parietal synchrony in primate cortex. Neuron 99:588–597.e5.

Kahnt T, Heinzle J, Park SQ, Haynes J-D (2011) Decoding different roles for vmPFC and dlPFC in multi-attribute decision making. Neuroimage 56:709–715.

Kaufman EL, Lord MW, Reese TW, Volkmann J (1949) The discrimination of visual number. Am J Psychol 62:498.

Knops A, Willmes K (2014) Numerical ordering and symbolic arithmetic share frontal and parietal circuits in the right hemisphere. Neuroimage 84:786–795.

Kosslyn SM, Koenig O, Barrett A, Cave CB, Tang J, Gabrieli JD (1989) Evidence for two types of spatial representations: hemispheric specialization for categorical and coordinate relations. J Exp Psychol Hum Percept Perform 15:723–735.

Kriegeskorte N, Goebel R, Bandettini P (2006) Information-based functional brain mapping. Proc Natl Acad Sci U S A 103:3863–8.

Lemus L, Hernández A, Romo R (2009) Neural encoding of auditory discrimination in ventral premotor cortex. Proc Natl Acad Sci U S A 106:14640–14645.

McGlone J, Davidson W (1973) The relation between cerebral speech laterality and spatial ability with special reference to sex and hand preference. Neuropsychologia 11:105–113.

Nieder A (2005) Counting on neurons: the neurobiology of numerical competence. Nat Rev Neurosci 6:177–190.

Nieder A (2016) The neuronal code for number. Nat Rev Neurosci 17:366–382.

Nieder A (2017) Magnitude codes for cross-modal working memory in the primate frontal association cortex. Front Neurosci 11:202.

Nieder A, Dehaene S (2009) Representation of number in the brain. Annu Rev Neurosci 32:185–208.

Nieder A, Miller EK (2003) Coding of cognitive magnitude: compressed scaling of numerical information in the primate prefrontal cortex. Neuron 37:149–157.

Nieder A, Miller EK (2004) A parieto-frontal network for visual numerical information in the monkey. Proc Natl Acad Sci U S A 101: 7457–7462.
Nieder A, Freedman DJ, Miller EK (2002) Representation of the quantity of visual items in the primate prefrontal cortex. Science 297:1708–1711.
Oldfield RC (1971) The assessment and analysis of handedness: the Edinburgh inventory. Neuropsychologia 9:97–113.
Ostwald D, Schneider S, Bruckner R, Horvath L (2019) Power, positive predictive value, and sample size calculations for random field theory-based fMRI inference. bioRxiv. Advance online publication. Retrieved January 9, 2020. doi:10.1101/613331.
Piazza M, Izard V (2009) How humans count: numerosity and the parietal cortex. Neuroscientist 15:261–273.
Piazza M, Izard V, Pinel P, Le Bihan D, Dehaene S (2004) Tuning curves for approximate numerosity in the human intraparietal sulcus. Neuron 44:547–555.
Piazza M, Mechelli A, Price CJ, Butterworth B (2006) Exact and approximate judgements of visual and auditory numerosity: an fMRI study. Brain Res 1106:177–188.
Piazza M, Pinel P, Le Bihan D, Dehaene S (2007) A magnitude code common to numerosities and number symbols in human intraparietal cortex. Neuron 53:293–305.
Plaisier MA, Smeets JBJ (2011) Haptic subitizing across the fingers. Atten Percept Psychophys 73:1579–1585.
Plaisier MA, Bergmann Tiest WM, Kappers AML (2009) One, two, three, many - subitizing in active touch. Acta Psychol (Amst) 131:163–170.
Plaisier MA, Bergmann Tiest WM, Kappers AML (2010) Range dependent processing of visual numerosity: similarities across vision and haptics. Exp Brain Res 204:525–537.
Riggs KJ, Ferrand L, Lancelin D, Fryziel L, Dumur G, Simpson A (2006) Subitizing in tactile perception. Psychol Sci 17:271–272.
Romo R, Brody CD, Hernández A, Lemus L (1999) Neuronal correlates of parametric working memory in the prefrontal cortex. Nature 399:470–473.
Schmidt TT, Wu YH, Blankenburg F (2017) Content-specific codes of parametric vibrotactile working memory in humans. J Neurosci 37:9771–9777.
Sperling G (1960) The information available in brief visual presentations. Washington, DC: American Psychological Association.
Spitzer B, Blankenburg F (2011) Stimulus-dependent EEG activity reflects internal updating of tactile working memory in humans. Proc Natl Acad Sci U S A 108:8444–8449.
Spitzer B, Blankenburg F (2012) Supramodal parametric working memory processing in humans. J Neurosci32:3287–95.
Spitzer B, Wacker E, Blankenburg F (2010) Oscillatory correlates of vibrotactile frequency processing in human working memory. J Neurosci 30:4496–502.
Spitzer B, Fleck S, Blankenburg F (2014a) Parametric alpha- and beta-band signatures of supramodal numerosity information in human working memory. J Neurosci 34:4293–4302.
Spitzer B, Gloel M, Schmidt TT, Blankenburg F (2014b) Working memory coding of analog stimulus properties in the human prefrontal cortex. Cereb Cortex 24:2229–2236.
Tian Y, Chen L (2018) Cross-modal attention modulates tactile subitizing but not tactile numerosity estimation. Atten Percept Psychophys 80:1229.
Tudusciuc O, Nieder A (2009) Contributions of primate prefrontal and posterior parietal cortices to length and numerosity representation. J Neurophysiol 101:2984–2994.
Uluç I, Schmidt TT, Wu Y-H, Blankenburg F (2018) Content-specific codes of parametric auditory working memory in humans. Neuroimage 183:254–262.
Vergara J, Rivera N, Rossi-Pool R, Romo R (2016) A neural parametric code for storing information of more than one sensory modality in working memory. Neuron 89:54–62.
von Lautz AH, Herding J, Ludwig S, Nierhaus T, Maess B, Villringer A, Blankenburg F (2017) Gamma and beta oscillations in human MEG encode the contents of vibrotactile working memory. Front Hum Neurosci 11:576.
Wu Y, Uluç I, Schmidt TT, Tertel K, Kirilina E, Blankenburg F (2018) Overlapping frontoparietal networks for tactile and visual parametric working memory representations. Neuroimage 166:325–334.
Young AW, Bion PJ (1979) Hemispheric laterality effects in the enumeration of visually presented collections of dots by children. Neuropsychologia 17:99–102.

Study 2 - Intraparietal sulcus maintains working memory representations of somatosensory categories in an adaptive, context-dependent manner

Velenosi LA, Wu YH, Schmidt TT, Blankenburg F (2020). Intraparietal sulcus maintains working memory representations of somatosensory categories in an adaptive, context-dependent manner. *NeuroImage*, *221*, 117146.
DOI: https://doi.org/10.1016/j.neuroimage.2020.117146

NeuroImage 221 (2020) 117146

Contents lists available at ScienceDirect

NeuroImage

journal homepage: www.elsevier.com/locate/neuroimage

Intraparietal sulcus maintains working memory representations of somatosensory categories in an adaptive, context-dependent manner

Lisa Alexandria Velenosi [a,*], Yuan-Hao Wu [a,b,c], Timo Torsten Schmidt [a], Felix Blankenburg [a,b]

[a] Neurocomputation and Neuroimaging Unit, Freie Universität Berlin, Habelschwerdter Allee 45, Berlin, 14195, Germany
[b] Berlin School of Mind and Brain, Humboldt-Universität zu Berlin, Luisenstraße 56, Berlin, 10117, Germany
[c] NYU Grossman School of Medicine, New York University, 550 First Avenue, New York, 10016, USA

ARTICLE INFO

Keywords:
Working memory
Somatosensory
Adaptive coding
Categorization
Multivariate
fMRI

ABSTRACT

Working memory (WM) representations are generally known to be influenced by task demands, but it is not clear whether this extends to the somatosensory domain. One way to investigate the influence of task demands is with categorization paradigms, wherein either a single stimulus or an associated category is maintained in WM. In the somatosensory modality, category representations have been identified in the premotor cortex (PMC) and the intraparietal sulcus (IPS). In this study we used multivariate-pattern-analysis with human fMRI data to investigate whether the WM representations in the PMC, IPS or other regions are influenced by changing task demands. We ensured the task-dependent, categorical WM information was decorrelated from stimulus features by (1) teaching participants arbitrary, non-rule based stimulus groupings and (2) contrasting identical pairs of stimuli across experimental conditions, where either a single stimulus or the associated group was maintained in WM. Importantly, we also decoupled the decision and motor output from the WM representations. With these experimental manipulations, we were able to pinpoint stimulus-specific WM information to the left frontal and parietal cortices and context-dependent, group-specific WM information to the left IPS. By showing that grouped stimuli are represented more similarly in the Group condition than in the Stimulus condition, free from stimulus and motor output confounds, we provide novel evidence for the adaptive nature of somatosensory WM representations in the IPS with changing task-demands.

1. Introduction

Working memory (WM) is the ability to maintain and manipulate representations of stimuli which are no longer being perceived (Baddeley and Hitch, 1974) and underlies fundamental human behaviours and abilities (Logie and Cowan, 2015). As a result, identifying the neural correlates of WM is a major focus of scientific interest. Presently, a large body of evidence suggests that the localization of WM content depends on the to-be-maintained stimulus feature (Postle, 2006) as well as the goals of the experimental condition (Lee et al., 2013). However, while the topography of brain regions that retain specific stimulus features has been thoroughly investigated (for a review see Christophel et al., 2017), the influence of top-down task-demands on the localization of WM representations is less well understood.

One means by which to investigate the influence of task-demands is by employing categories or groups of stimuli. The act of categorizing a stimulus abstracts the WM representation away from the stimulus' physical features to a label or exemplar (Seger and Miller, 2010). Previous work, wherein non-human primates (NHPs) were trained to categorize images of gradual transitions between cats and dogs found that neurons in the lateral intraparietal cortex (LIP), analogous to the human intraparietal sulcus (IPS, Grefkes and Fink, 2005), represented the categorical decision instead of a continuous change with the stimulus feature (Freedman et al., 2001). Moreover, LIP neurons have also been shown to change their categorical firing pattern with changing category definitions (Freedman and Assad, 2006), known as adaptive coding (Duncan, 2001). Recently, an optogenetic study in mice went a step further and showed that parietal neurons are necessary for learning new olfactory category boundaries and generalizing from category exemplars to novel stimuli (Zhong et al., 2019).

While extensive work has been done exploring visual categorization in NHPs (Fitzgerald et al., 2011; Fitzgerald et al., 2012; Freedman and

* Corresponding author.
E-mail addresses: lisa.velenosi@fu-berlin.de (L.A. Velenosi), yuanhao.wu@nyulangone.org (Y.-H. Wu), titoschmi@zedat.fu-berlin.de (T.T. Schmidt), felix.blankenburg@fu-berlin.de (F. Blankenburg).

https://doi.org/10.1016/j.neuroimage.2020.117146
Received 6 August 2019; Received in revised form 3 July 2020; Accepted 4 July 2020
Available online 11 July 2020

Assad, 2016; Freedman et al., 2001; Sarma et al., 2016; Swaminathan and Freedman, 2012), the generalizability of the findings to other modalities is poorly understood. Rossi-Pool et al. (2016) adapted the classic delayed-match-to-sample (DMTS) comparison paradigm to explore the neuronal response of somatosensory categorical-match decisions in NHPs. The researchers recorded from primary somatosensory (SI) and premotor cortices (PMC) and found distinct neuronal firing patterns for the respective WM categories in the PMC. Moreover, a recent study using whole-brain multivariate pattern analysis (MVPA) of human fMRI data identified perceptual categories of vibrotactile stimulation in the PMC (Malone et al., 2019). Interestingly, also using MVPA with fMRI data, supramodal auditory and somatosensory category representations were identified in the IPS (Levine and Schwarzbach, 2017). Thus, somatosensory categorical-information has been consistently identified in the IPS and PMC. The present study was designed to extend this finding by identifying brain regions which maintain somatosensory WM representations in a context-dependent manner.

To this end, we defined four stimuli, composed of different pulse sequences similar to those employed by Rossi-Pool et al. (2016), which participants were pseudorandomly trained to pair together into two groups of two stimuli. We used a DMTS paradigm with two conditions: a Stimulus condition where participants were instructed to maintain only the temporal nature of the cued stimulus, and a Group condition where participants maintained the cued stimulus' group. Using a multivariate ANOVA approach (MANOVA, Allefeld and Haynes, 2014) with human fMRI data, we first identified regions maintaining condition-general stimulus-specific WM information and, in a second step, identified context-dependent group-specific WM information. We hypothesized that our experimental manipulation, maintaining individual stimuli in the Stimulus condition as opposed to groups of stimuli in the Group condition, would result in the condition-dependent modification of the multivariate WM representations, such that, in the Group condition, the group members' representations would be more similar to one another than in the Stimulus condition.

2. Materials & methods

2.1. Participants

In total, data from 38 participants was collected and two were excluded from the analysis due to low task performance, which was defined as a mean performance on either condition, Stimulus or Group, two standard deviations below the group mean. The final data set consisted of 36 participants between the ages of 20 and 39 (mean 26.92 ± 4.66 (SD) years, 19 male and 17 female). All participants provided written informed consent to take part in the study which was approved by the Ethics Committee of the Freie Universität Berlin and corresponded to the Human Subject Guidelines of the Declaration of Helsinki.

2.2. Procedure

The experiment took place across two sessions: training and fMRI data collection. The training session was used to determine the participant's sensory threshold and to adjust the subjective amplitude as well as familiarize participants with the stimuli (detailed in 2.3) and the experimental procedure (detailed in 2.4).

The training session lasted between 40 min to an hour. First, the participant-specific stimulation intensity was determined by estimating the participant's subjective detection threshold (mean: 2.33 mA ± .75 (SD)). The chosen amplitude, about double the detection threshold, was always below the participant's motor and pain thresholds resulting in a mean factor increase of 2.13 (± .50). Next, the four experimental stimuli were presented to the participant. The participant was able to freely replay each of the stimuli until they felt confident that they could differentiate the stimuli. The participant was then taught their assigned grouping. The groupings were introduced by playing the group members one after another and then participants were able to freely replay the grouped stimuli. To ensure participants had learned their assigned grouping, two stimuli were chosen at random and the participant indicated whether they belonged to the same group. This was repeated ten times. Next, the participant completed one block of each experimental condition (see 2.4). Performance above 80% on all of the behavioural tests was used to determine whether participants could perform the task. The training session thus served to familiarize participants with the stimuli, groupings and trial structure, including their assigned response and cue-mappings.

2.3. Stimuli & groupings

Stimuli were presented to the participant's left median nerve using a Digitimer DS7A constant current neurostimulator (Digitimer Ltd, Hertfordshire, UK) with MR-compatible adhesive electrodes (GVB-geliMED GmbH, Bad Segeberg, Germany). Four stimuli, each consisting of a different pulse sequence lasting 0.75 s, were created and used for all participants (Fig. 1A). The stimuli were composed of four 50 μs pulses with two of the pulses marking the on- and offset of each stimulus. The timing of the two remaining pulses was chosen to create a stimulus set with similar differentiability and performance rates across the stimuli, as assessed using behavioural pilot data. Stimuli were presented using custom MATLAB code (R2013b, The MathWorks, Inc., Natick, Massachusetts, United States) and the Psychophysics Toolbox extension (Brainard, 1997).

Each participant was pseudorandomly assigned a grouping. For four stimuli, three permutations of two groups of two stimuli exist (1) group A: s1 + s2 vs group B: s3 + s4, 2) A: s1 + s3 vs B: s2 + s4, and (3) A: s1 + s4 vs B: s2 + s3). To protect against potential naming confounds, three additional groups were included with the group A vs group B label exchanged (4) group A: s3 + s4 vs group B: s1 + s2, etc.). Therefore, six stimulus groupings were used in total, and each was pseudorandomly assigned to six participants. Arbitrary groupings were implemented because, while neurophysiological recordings can dissociate categorical from stimulus feature-specific neuronal activity, the distinction is more nuanced with fMRI data. Rule-based categorization, wherein categories are formed by applying a rule to stimulus features, is inherently coupled with the neuronal response to the underlying features. This is in contrast to arbitrary categorization, which we refer to as grouping, which classifies stimuli without the use of a stimulus-based rule (Seger and Miller, 2010). Consequently, a group can consist of physically unrelated members whereas category members share common features. Therefore, the use of arbitrary groups of stimuli, where groups are not defined according to physical attributes, provides a means of exploring the effect of task-demands on WM stimulus representations while maintaining the ability to dissociate condition-effects from stimulus features with neuroimaging data, a technique that has previously been employed in visual (Li et al., 2007; Fitzgerald et al., 2011; Senoussi et al., 2016) and audiotactile (Levine and Schwarzbach, 2018) studies.

2.4. Experimental conditions and design

The experiment comprised two independent blocks of WM conditions: Stimulus and Group. The trial timing and structure was identical in the two conditions and each experimental run consisted of one Stimulus and one Group block of trials (Fig. 1B). Each trial began with the sequential presentation of two different 0.75 s stimuli with a 0.5 s inter-stimulus-interval. Stimuli from the same group were never presented together in a trial. Additionally, during stimulus presentation, the fixation cross increased in brightness to help participants attend to the stimulus as well as ensure that the on- and offset of each stimulus was well defined. A 0.5 s visual retro-cue, square or diamond, presented after the second stimulus, indicated which of the two stimuli should be maintained in WM for the following 7.5 s delay period. In the Stimulus trials, participants were instructed to maintain only the cued stimulus. A

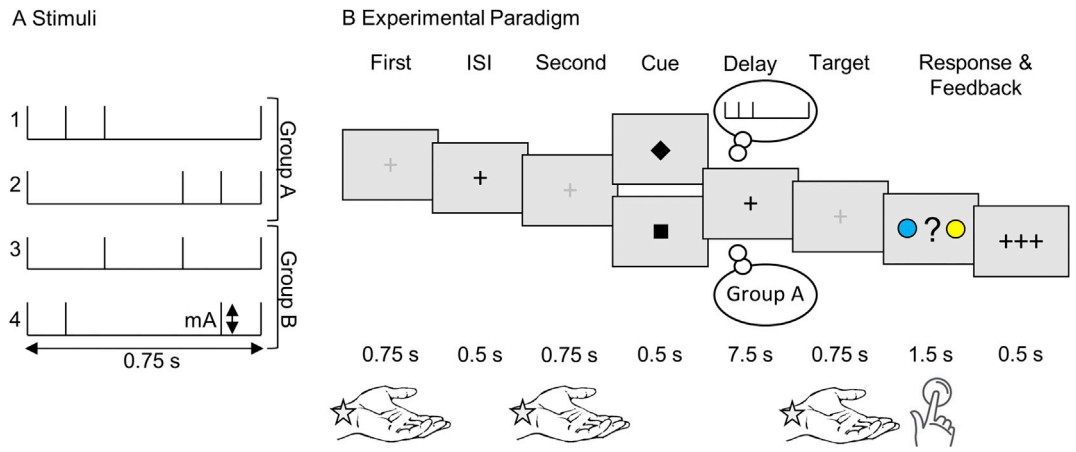

Fig. 1. Experimental Design. A. Visual depiction of the tactile stimuli used in the study. Four 0.75 s duration stimuli, each composed of four 50 μs electrical pulses and participant-specific amplitude (mA), with different stimulation pulse timings were used. The stimuli were pseudorandomly grouped into two groups of two stimuli, with group assignment balanced across participants. Six different groupings were used, for example: group A = stimulus 1 + 2 vs group B = stimulus 3 + 4. **B.** The design consisted of two blocks of conditions: Stimulus and Group. For both conditions, each trial began with the sequential presentation of two different stimuli. A visual retro-cue indicated which stimulus should be maintained in WM during the delay period. In the Stimulus trials, participants maintained only the cued stimulus, whereas in the Group trials they were instructed to maintain the group which the cued stimulus belonged to. An example of the WM content is shown for the Stimulus trials in the thought bubble above the experimental paradigm, and below for the Group trials. After the delay, participants indicated with a button response whether a target stimulus matched the maintained stimulus (Stimulus trials) or was a member of the same group (Group trials). Visual feedback was provided after each trial.

target stimulus, one of the four experimental stimuli, was presented after the delay. In the Stimulus condition, participants decided whether the target stimulus was identical to the maintained stimulus. In contrast, in the Group condition, participants were instructed to maintain the group to which the cued stimulus belonged in WM and indicated whether the target was either the cued stimulus or it's group member. Thus, the target-specific decision and response differed between the two conditions.

For both conditions, the correct target, meaning the target matching the cued stimulus, or the cued-stimulus' group member in the Group condition, was presented in 50% of trials. After the target was presented, a question mark replaced the fixation cross and a yellow and blue circle appeared on either side. Participants indicated whether the target was a match to the cued stimulus by selecting, via button press using the right index or middle finger, either the blue or yellow circle according to a pseudorandomly-defined response mapping. The response period was limited to 1.5 s. The quick response encouraged participants to actively keep the maintained stimulus or group in WM, thereby allowing a fast comparison to the target stimulus. Feedback was provided after each trial. Importantly, we implemented retro-cues (shapes) to dissociate perceptual processes from WM content as well as unpredictable response colour-map locations (left, right) to prevent a direct mapping between WM content and the decision. Furthermore, we counter-balanced the retro-cues and response choices across participants.

For each participant, four fMRI runs of experimental data were collected. Each run consisted of one Stimulus and one Group condition block, the order of which was counter-balanced across runs for each participant and was verbally communicated to the participant at the beginning of each run. The transition between blocks was indicated by the visual presentation of the mean performance on the first block, followed by the fixation cross for 12 s before beginning the second block. Moreover, we ensured that participants performed the correct task by monitoring their performance and asking after each run. The conditions consisted of identical trials, meaning that we presented the same stimulus pairings in each condition, and the trial order was randomized separately. In each condition, participants remembered each stimulus eight times, resulting in a total of 32 trials/condition (8 repetitions x 4 stimuli) and 64 trials/run (32 trials x 2 conditions). A trial lasted 12 s and inter-trial intervals (2 or 4 s) were equally distributed across trials. A run lasted 15 min. Finally, after data collection was completed, participants underwent a debriefing session wherein they drew a portrayal of the stimuli and explained the approach they used to represent the stimuli and groups.

2.5. Data acquisition

Functional imaging was performed on a 3T Siemens Tim Trio system (Siemens Medical Solutions, Erlangen, Germany) equipped with a 32-channel head coil at the Centre for Cognitive Neuroscience Berlin. 475 volumes were acquired in each of the four experimental runs using a gradient-echo echoplanar T2*-weighted imaging sequence (TR = 2000 ms, TE = 30 ms, 37 contiguous slices, ascending order, gap = 20%, matrix size = 64 × 64, 3 × 3 × 3 mm^3, flip angle = 70°, FOV = 192 mm). Additionally, a T1-weighted, whole-brain structural scan was obtained using a Magnetization Prepared Rapid Gradient Echo sequence (TR = 1900 ms, TE = 2.52 ms, 176 slices, matrix size = 256 × 256, 1 × 1 × 1 mm^3, flip angle = 9°, FOV = 256 mm). Furthermore, we implemented 'delay-locked' acquisition timing, wherein the onset of the retro-cue coincided with the onset of a volume acquisition. Delay-locking ensures that a given slice is always measured at the same time relative to the experimental paradigm (Christophel et al., 2012; Schmidt et al., 2017).

2.6. fMRI data analysis

All data analyses were performed using SPM12 (Wellcome Trust Centre for Neuroimaging, Institute for Neurology, University College London, London, UK) in combination with the cvMANOVA Toolbox (Allefeld and Haynes, 2014) and custom MATLAB code (R2013b, The MathWorks, Inc., Natick, Massachusetts, United States; code available upon request). We hypothesized that our experimental manipulation, maintaining individual or groups of stimuli in WM, would result in the context-dependent modification of WM information such that the multivariate representations of grouped stimuli should be more similar to one another in the Group condition than in the Stimulus condition. To identify differences between WM representations across conditions, we took advantage of the cvMANOVA's ability to perform interaction analyses in multivariate space. All reported coordinates correspond to MNI space and, where possible, the SPM anatomy toolbox was used to establish cytoarchitectonic references (Eickhoff, 2007). The brain figures were made using MRIcron (www.nitrc.org).

2.6.1. Data pre-processing

A 1/192 Hz high pass filter was used to remove slow varying trends in the data. To preserve the spatiotemporal structure of the data for the cvMANOVA, pre-processing was limited to slice-time correction and motion-correction, wherein images are initially realigned to the first image and then to the mean using six parameter rigid body transformation, to reduce slice order and movement-related artefacts. Functional images were normalized to standard MNI space using SPM's unified segmentation. Structural images were coregistered to the mean functional image.

2.6.2. First-level models

General Linear Models (GLMs) were defined for each participant to yield run-wise beta estimates of voxel-wise activation for the regressors of interest. First, we defined a regressor for each cued stimulus for each condition separately (4 stimuli x 2 conditions = 8 regressors). The regressor onsets coincided with the retro-cue offset and spanned the WM delay period. We refer to the Stimulus condition regressors as S1, S2, S3, and S4 and the associated Group condition regressors as A1, A2, B3, and B4. The regressor label indicates the stimulus number (1:4) as well as the associated group (A, B). Importantly, the regressors for both conditions, Stimulus and Group, were defined according to the participant-specific grouping. Thus, the regressors S1 and A1 refer to the same physical stimulus in the Stimulus and Group condition respectively. Nine impulse regressors of no interest were included with the onsets defined according to the respective trial timing: stimulus perception collapsed over first and second presentation (4 stimuli), visual retro-cues (2 cues), target presentation (1) and response (2 options). Thus, each run was modelled with 17 regressors and the first level models included 72 regressors ((17 regressors x 4 runs) + 4 run constants) which were convolved with the hemodynamic response function.

2.6.3. Searchlight cvMANOVA

The resulting run-wise beta parameter estimates were used in a whole-brain searchlight, cross-validated, multivariate analysis of variance (cvMANOVA, Allefeld and Haynes, 2014) which allowed the identification of WM information in a spatially-unbiased manner (Kriegeskorte et al., 2006). Analogous to well-established multivariate decoding methods such as support vector machines, the cvMANOVA identifies brain regions which show a difference between the multivariate BOLD activation patterns for contrasted stimuli. In the present study, the cvMANOVA was chosen instead of other multivariate decoding methods for a number of reasons. First, the cvMANOVA provides a parameter-free analysis built on a data-specific probabilistic model. Second, the resulting pattern distinctness value (Ds) directly estimates the amount of multivariate variance accounted for by the contrast. Thus, the pattern distinctness value indicates the dissimilarity of, in the present case, the contrasted WM representations. Third, and most importantly, the cvMANOVA enables interaction analyses to be performed in multivariate space which is not possible using classifiers (for a more in-depth description, see Allefeld and Haynes, 2014).

Using the cvMANOVA toolbox (https://github.com/allefeld/cvmanova), a 4-voxel radius searchlight was defined (~257 voxels) which delineated which voxels would be included in the analysis. The run-wise beta estimates for voxels contained within the searchlight were then fit with a multivariate normal distribution for each contrasted condition separately (e.g. S1 – S2). The pattern distinctness is defined as the magnitude of the covariance between contrasted conditions normalized with respect to the error covariance. Thus, the pattern distinctness estimates the amount of variance which can be explained by the contrast, measured in error variance units (Allefeld and Haynes, 2014). In other words, the larger the pattern distinctness, the more variance is accounted for by the contrast, the more distinctive the WM representations. Moreover, we employed a cross-validation approach wherein data from three of the four runs were used to fit the multivariate normal distributions and the remaining data were used to test the generalizability of the fit. This cross-validated, pattern distinctness estimate (Ds) was recorded as the value at the centre of the searchlight. The searchlight then progressed, voxel by voxel, through the brain producing a participant-specific, whole-brain pattern distinctness image for the contrast of interest. A whole-brain searchlight analysis was performed because, while we had a strong a priori hypothesis regarding the cortical regions (IPS, PMd), mainly from NHPs, the relevant subregions were unknown.

2.6.4. Stimulus-specific WM information

First, for each participant, we performed pair-wise stimulus contrasts to identify brain regions maintaining stimulus-specific WM information in both, Stimulus and Group, experimental conditions. To ensure that the cvMANOVA identified stimulus-specific information and not information relating to the different experimental conditions, stimuli in each condition were first contrasted separately and a second level conjunction analysis (Nichols et al., 2005) was used to identify stimulus-specific WM information across both conditions (explained in detail below). Moreover, to ensure that the identified information related to the cued and not the uncued stimulus on each trial, pair-wise contrasts were performed on a specific set of stimulus comparisons. The experimental design comprised trials where stimuli from the same participant-specific group were never presented together (i.e., A1 and A2 or B1 and B2). Thus, on trials when A1 was cued to be maintained in WM, B3 or B4 was the uncued stimulus. The same is true for trials where A2 was cued: B3 or B4 was uncued. Thus, regressors for A1 and A2 (and B3 and B4) were defined using trials where the cued stimulus differed (A1 or A2) but the uncued stimuli are the same within a regressor (B3, B4). We refer to these regressors as matched with respect to the uncued stimuli. Consequently, regressors for A1 and B3 were not matched with respect to the uncued stimuli. The same was true for the Stimulus condition: S1 and S2, S3 and S4 are matched for the uncued stimuli. To ensure that the WM information was specific to the cued stimuli and not confounded by activation relating to the uncued stimuli, only regressors matched for the uncued stimuli were contrasted (condition-specific contrast matrices: Ds(Stimulus condition) = mean([(S1 – S2), (S3 – S4)]), Ds(Group condition) = mean([(A1 – A2), (B3 – B4)]). Thus, the stimulus-specific WM analysis identified brain regions with pattern distinctness estimates greater than zero ($Ds > 0$). Thereby identifying regions with multivariate representations for contrasted stimuli in the Stimulus and Group conditions respectively. The complete contrast matrices are provided in the Supplemental Table 1a.

The resulting whole-brain, participant-specific pattern distinctness (Ds) images for both the Stimulus and Group condition contrasts were normalized to MNI space, smoothed with an 8 mm FWHM kernel and entered into a second-level repeated-measures ANOVA. A conjunction across the two experimental conditions identified brain regions maintaining condition-general stimulus-specific WM information ($Ds > 0$) regardless of the experimental task demands (Ds(Stimulus-specific) = mean([(S1 – S2), (S3 – S4)]) ∩ mean([(A1 – A2), (B3 – B4)]).

All statistical maps were thresholded at $p < 0.05$ family-wise error (FWE) corrected at the cluster level with a cluster-defining threshold of $p < 0.001$. In SPM, FWE correction relies on random field theory assuming smooth spatial maps of activation (for a description see Ostwald et al., 2019).

2.6.5. Context-dependent WM information

Next, as the core test of group-specific WM, we identified brain regions maintaining context-dependent WM information. We hypothesized that our experimental manipulation, forming groups of stimuli in the Group condition, would result in the modification of the multivariate representation of stimuli from the same group such that the stimuli share a more similar WM representation in the Group condition than in the Stimulus condition. Thus, the experimental manipulation should result in an interaction across conditions such that the pattern distinctness estimates between group members should differ in the two conditions (Ds(Group condition) < Ds(Stimulus condition)). Note, it is insufficient

to identify group-specific WM information by contrasting the groups against one another ([A1, A2] - [B3, B4]) because the groups were composed of physically distinct stimuli. Thus, contrasting group A against group B would identify a mixture of stimulus- and group-specific WM information. Instead, to isolate context-dependent, group-specific information, we performed an interaction analysis across the Stimulus and Group conditions (interaction contrast matrix Ds(interaction) = mean([(A1 – A2) – (S1 – S2)], [(B3 – B4) – (S3 – S4)]). Importantly, analogous to the stimulus-specific WM analysis, this interaction only contrasts regressors which were matched for the respective uncued stimuli. The complete contrast matrix is provided in the Supplemental Material Table 1b. Analogous to the stimulus-specific WM information, the resulting whole-brain, interaction pattern distinctness contrast images were normalized to MNI space and smoothed with an 8 mm FWHM kernel. Participant-specific images were forwarded to a second level one-sample *t*-test against zero to identify brain regions containing context-dependent group-specific WM representations.

As an additional step to visualize the interaction results, we plotted the mean participant-specific, context-dependent pattern distinctness values obtained for each condition (Ds(Stimulus condition) = mean([S1 – S2, S3 – S4]); Ds(Group condition) = mean([A1 - A2, B3 – B4]) from the whole-brain searchlight group-level interaction result peaks.

2.7. Control analyses

2.7.1. Group representation control analysis

While the interaction analysis indicates a differential representation of the stimuli across the two experimental conditions, it does not warrant the presence of a group representation in the Group condition. It is possible that, instead of being represented according to group membership, all stimuli are represented more similarly in the Group condition than in the Stimulus condition. Contrasting different-group members against same-group members is the most direct method for determining whether group representations were formed in the Group condition, because grouped stimuli should share a more similar WM representation than stimuli from different groups (Ds(different-group) > Ds(same-group)). Unfortunately, this analysis is confounded. Contrasts of stimuli from different groups (i.e., A1 - B3) are unbalanced with respect to the uncued stimulus (see **2.6.4** for an explanation) resulting in an overestimation of the pattern distinctness for contrasts of stimuli from different groups.

However, with this confound in mind, we performed an additional searchlight cvMANOVA analysis to determine whether, in the Group condition, stimuli from different groups were represented more differently than stimuli from the same group. We defined four different-group contrasts (A1 - B3, A1 - B4, A2 - B3, A2 - B4) and two same-group contrast (A1 - A2, B3 - B4). Next, we extracted the pattern distinctness values for the peak voxels identified by the context-dependent WM analysis (**2.6.5**) and performed a paired *t*-test to determine whether the mean participant-specific different-group pattern distinctness values were significantly different from the same-group values.

2.7.2. Behavioural control analysis

In a second control analysis, we aimed to identify whether the neuroimaging results were driven by the observed behavioural differences across stimuli and conditions. To this end, we median-split the participants according to the participant-specific difference in performance between stimulus 3 and 4 in the Stimulus condition. We chose this definition because this was the major cause of the observed behavioural effects. The two sub-samples (n = 18) were composed of participants who either performed similarly across all four stimuli and those who performed differently. We then re-ran the stimulus-specific (**2.6.4**) and context-dependent WM analyses **(2.6.5)** for each sub-sample independently. We expected that we would be able to replicate our main findings in both sub-samples, thereby demonstrating that the observed neuroimaging results are independent of the differences in behaviour. However, if only the differently-performing sub-sample was able to reproduce the results, then the neuroimaging results were indeed driven by the difference in behavioural factors.

2.7.3. Response time control analysis

Next, we performed a control analysis to determine whether the neuroimaging results were influenced by the observed difference in response times. To this end, we defined new first level models and included an HRF-convolved parametric response time regressor of no-interest. We then repeated both the stimulus-specific **(2.6.4)** and the context-dependent WM **(2.6.5)** main analyses. We expected that we would be able to replicate our main findings, thereby demonstrating that our neuroimaging findings are independent of the observed differences in response times.

2.7.4. WM-specificity control analysis

Next, we performed a control analysis to ensure that the identified regions were specific to the stimulus in WM and not corrupted by ongoing perceptual processes. To this end, we repeated both the stimulus-specific **(2.6.4)** and the context-dependent **(2.6.5)** WM analyses with new first level models with regressors modelling the uncued stimuli. This control analysis enabled the detection of information relating to the uncued stimulus and provided a method for testing the specificity of our results.

2.7.5. Multivariate control analysis

In a final control analysis, we aimed to determine whether the identified WM information was indeed multivariate in nature, or if the neuroimaging results could be explained by mass-univariate differences between the conditions. We repeated both the stimulus-specific **(2.6.4)** and the context-dependent **(2.6.5)** analyses using a searchlight comprising only one voxel. This analysis collapsed the multivariate cvMANOVA to a single dimension and tested whether the identified WM information comprised a univariate representation.

3. Results

3.1. Behavioural results

Overall, participants performed with a mean accuracy of 81.87% (±7.59% (SD) range: 68.36–97.27%). To test for potential performance differences between experimental conditions or stimuli, we performed a 4 × 2 repeated-measures ANOVA with the stimuli (1:4) and conditions (Stimulus, Group) as within-subject factors. The ANOVA identified a significant main effect of stimulus ($F(3, 105) = 10.9367$, $p = 2.6098e\text{-}06$, $\eta^2 = 0.1207$) and condition ($F(1, 35) = 5.0929$, $p = 0.0304$, $\eta^2 = 0.0234$) and no interaction between the factors ($F(3, 105) = 2.2282$, $p = 0.0892$). Post-hoc, Bonferroni-corrected, paired t-tests of the stimulus effect revealed it to be driven by differences in performance between stimulus 1 and 3, and stimulus 4 and all other stimuli (mean performance stimulus 1: 81.38 ± 1.52% (SE), S2: 82.55 ± 1.56%, S3: 86.15 ± 1.59%, S4: 77.39% ± 1.65%; S1 vs S3: $T(35) = 3.0014$, $p = 0.0049$, Cohen's $d = 0.5116$, S1 vs S4: $T(35) = 2.9083$, $p = 0.0063$, $d = 0.4195$, S2 vs S4: $T(35) = 3.8237$, $p = 0.0005$, $d = 0.5366$, S3 vs S4: $T(35) = 4.9355$, $p < 0.0001$, $d = 0.9019$). The mean performance results across participants are shown in Fig. 2A with the stimulus labelling referring to the physical, and not participant-specific labelling. The significant differences between stimuli ($p < 0.05$, Bonferroni-corrected) are indicated by grey lines.

Participants responded with a mean of 735.1 ms ± 105.5 ms (SD), well-within the allotted 1.5 s response window. We performed a second 4 × 2 repeated-measures ANOVA using response time as the dependent variable and found a main effect of condition, with Stimulus condition response times significantly shorter than the Group condition (Stimulus mean: 663.5 ± 17.5 ms (SE), Group mean: 807.1 ± 19.4 ms, $F(1, 35) = 162.3934$, $p = 1.0436e\text{-}14$, $\eta^2 = 0.6313$), and no main effect of stimulus

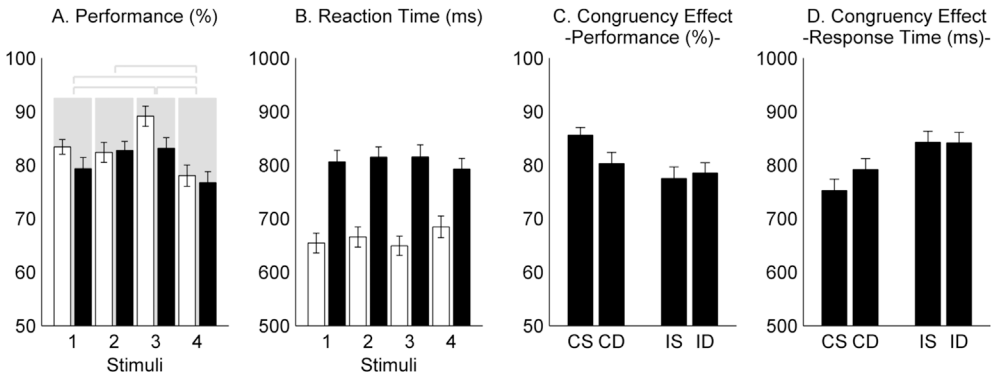

Fig. 2. Behavioural Results A. The mean behavioural performance across participants for the four stimuli, in both conditions: Stimulus (white) and Group (black). The grey brackets indicate significant differences ($p < 0.05$, Bonferroni-corrected) in performance between stimuli across conditions. **B.** The mean response time across participants for the four stimuli, in both conditions. **C.** The mean performance across participants in the Group condition with trials sorted according to the relationship between the cued and target stimulus. CS: same group – same stimulus, CD: same group – different stimulus, IS: different group – 'same' stimulus, ID: different group – 'different' stimulus. **D.** Shows the same as C with response time data. In both C. and D., the CD trials are intermediate to the CS and incongruent trials suggesting that a group was maintained in the Group condition. Error bars for all plots indicate standard error of the means.

($F(3, 105) = 0.5766$, $p = 0.6316$). However, an interaction between the factors was present ($F(3, 105) = 5.9177$, $p = 9.0422e\text{-}04$, $\eta^2 = 0.0142$, Fig. 2B). The main effect of condition is expected given the Group condition required two stimuli, the two maintained group members, to be compared with the target stimulus, thereby requiring more time than the single comparison in the Stimulus condition. The influence of the observed behavioural effects on the neuroimaging results is explored in subsequent control analyses (2.7.2, 2.7.3).

Finally, we investigated whether participants performed according to the experimental manipulation and represented groups in the Group condition. We theorised that grouping the stimuli would influence the congruency effect by creating an intermediate level between congruent trials (target is identical to cued stimulus) and incongruent trials (target is not the cued stimulus). To test this, we defined two independent 2×2 repeated measure ANOVAs for the performance and response time data with factors congruency (target stimulus from the same group as cued stimulus or different group) and stimulus identity (same or different stimulus from cued). Thus, the ANOVAs were composed of four cells: congruent-same stimulus (CS: e.g. cued A1 – target A1), congruent-different stimulus (CD: cued A1 – target A2), incongruent-'same' (IS), incongruent-'different' (ID). For the IS and ID cells, the trials (cued A1 - target B3 or B4) were equally divided between the two levels. Each trial type (B3 or B4 as target) was repeated twice in each experimental run. Thus, the IS cell comprised the first trial-instance and the ID cell the second. The performance data ANOVA identified a main effect of congruency ($F(1, 35) = 13.9126$, $p = 6.7655e\text{-}04$, $\eta^2 = 0.1169$), no effect of group-member identity ($F(1, 35) = 3.3718$, $p = 0.0748$), and an interaction between the factors ($F(1, 35) = 5.8944$, $p = 0.0205$, $\eta^2 = 0.0488$; Fig. 2C). The response time data replicated the performance data results with the addition of a main effect of stimulus identity which, as seen in Fig. 2D, is the result of the near-identical response times on incongruent trials (congruency: $F(1, 35) = 52.6285$, $p = 1.7985e\text{-}08$, $\eta^2 = 0.4343$; group-member identity: $F(1, 35) = 9.1019$, $p = 0.0047$, $\eta^2 = 0.0315$; interaction: $F(1, 35) = 14.2528$, $p = 5.9488e\text{-}04$, $\eta^2 = 0.0359$). Thus, trials when the target stimulus was a group-member of the cued stimulus were intermediate in performance and response time to congruent and incongruent trials, thereby providing evidence for participants having likely maintained groups in the Group condition.

3.2. Neuroimaging results

3.2.1. Stimulus-specific WM information

Using the whole-brain, searchlight cvMANOVA, we identified regions maintaining stimulus-specific WM information in the Stimulus and Group experimental conditions respectively (condition-specific results are shown in Supplemental Figure 1). Moreover, to ensure that the results are independent from the uncued stimuli, we contrasted pairs of regressors which were matched for the uncued but differed with respect to the maintained (cued) stimulus. Because we were interested in regions which maintain stimulus-specific WM information across experimental conditions, we performed a second-level conjunction analysis (logical AND, Friston et al., 2005) across the two experimental conditions to identify regions which maintain context-general, stimulus-specific WM (Fig. 3A (blue), Table 1a). This analysis identified a cluster in the left inferior frontal gyrus (IFG) extending to the middle frontal gyrus (MFG) as well as a cluster in the left superior parietal lobule (SPL) as maintaining stimulus-specific WM information independent of experimental context.

3.2.2. Context-dependent WM information

We hypothesized that our experimental manipulation, grouping stimuli in the Group condition and treating them as individuals in the Stimulus condition, would result in the context-dependent modification of the group members' pattern distinctness estimates. We expected a smaller difference between the multivariate WM representations of the grouped stimuli in the Group as compared to the Stimulus condition ($Ds(\text{Group condition}) < Ds(\text{Stimulus condition})$). Therefore, regions which maintain context-dependent group-specific WM information should display different pattern distinctness estimates between group members across the two conditions, which is accessible with an interaction analysis (see **2.6.5**). Moreover, because the implemented interaction only contrasts physically identical pairs of stimuli while also controlling for the uncued stimuli (see **2.6.4**), the contrast is not confounded by stimulus feature information. The interaction contrast identified the left IPS (Fig. 3A (yellow), Table 1b). Thus, the WM representations of the grouped stimuli in the left IPS are represented differently in the two conditions, or put another way, the left IPS adaptively modifies its WM information with respect to the experimental condition. Additionally, due to strong a priori expectations regarding the presence of group-specific somatosensory information in the PMC (Malone et al., 2019; Rossi-Pool et al., 2016, 2017, 2019), we further explored the interaction contrast result and identified context-dependent WM representations in the left PMd at an uncorrected threshold ($p < 0.001$). Other regions with effects detectable at this threshold included the right middle frontal gyrus, left inferior frontal gyrus, left premotor cortex and the cluster in the left intraparietal sulcus extending from the superior parietal lobule to the angular gyrus (see the unthresholded statistical maps at Neurovault: https://identifiers.org/neurovault.collec

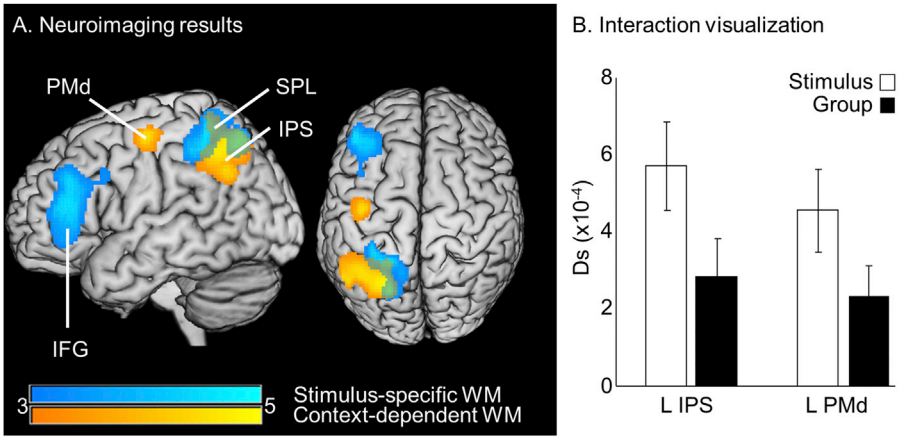

Fig. 3. Neuroimaging cvMANOVA results A. We identified brain regions which maintain condition-general stimulus-specific (blue) and context-dependent group-specific (yellow) WM information with overlapping regions shown in green. Using a conjunction analysis across the Stimulus and Group condition results, we identified condition-general stimulus-specific WM information in the left IFG and SPL whereas context-dependent WM information was identified in the left IPS. Results are reported at $p < 0.05_{FWE}$ with $p < 0.001_{cluster}$. The left PMd cluster was significant at, and shown at, an uncorrected threshold ($p < 0.001$). Coloured bars indicate the respective voxel-wise T-statistic values. PMd: dorsal premotor cortex, SPL: superior parietal lobule, IPS: intraparietal sulcus, IFG: inferior frontal gyrus. **B.** To visualize the interaction, we extracted the mean pattern distinctness values across participants at the context-dependent WM analysis peaks (L IPS, L PMd) for the two experimental conditions (Stimulus, Group). The error bars indicate the standard error of the means. Unthresholded group contrast images for the Stimulus and Group condition stimulus-specific and context-dependent WM results are available on Neurovault (https://identifiers.org/neurovault.collection:5623).

Table 1
Neuroimaging results overview. **1a**. Regions maintaining stimulus-specific WM information independent of experimental context as revealed by a conjunction analysis. **1b**. Regions maintaining context-dependent WM information as revealed by an interaction analysis. For both Table 1a and b, the Anatomy Toolbox (Eickhoff, 2007) was used, where possible, to establish the label and the x, y, z coordinates refer to MNI space. The T-stat value refers to the peak voxel in the cluster with size k. Ds is the cross-validated pattern distinctness estimate with 1a referring to the mean Ds across the two conditions and 1b referring to the interaction contrast value.

Table 1a: Stimulus-specific WM information						
Label	X	Y	Z	T-stat	k	Ds x 10^{-4}
L IFG	−42	36	14	4.76	1373	8.0137
L SPL	−22	−48	60	4.74	1071	6.7954
Table 1b: Context-dependent group-specific WM information						
L IPS	−26	−66	54	5.09	1441	7.6486
L PMd	−42	−12	58	4.39	207	6.4042

tion:5623).

We additionally visualized the two halves of the interaction analysis, the Stimulus and Group condition, for the peaks identified by the whole-brain, context-dependent searchlight analysis (L IPS, L PMd, Fig. 3B). As expected, the pattern distinctness estimates for grouped stimuli are smaller in the Group condition than in the Stimulus condition, indicating that the IPS represented grouped stimuli more similarly in the Group condition than in the Stimulus condition.

3.3. Control analyses results

3.3.1. Group representation control analysis results

To ensure that the context-dependent WM analysis identified groups in the Group condition and not condition-general changes in pattern distinctness, we performed a control analysis to test whether grouped stimuli were represented more similarly in the Group condition than stimuli from different groups. In the IPS, the grouped stimuli were more similarly represented than stimuli from different groups (same-group mean: 2.8334e-04 ± 0.9532e-04 (SE); different-groups mean: 5.6038e-04 ± 1.1092e-04; T(35) = 2.6518, p = 0.0119, Cohen's d = 0.4465). Whereas there was no evidence of stimulus grouping in the PMd (same-group mean: 2.3017e-04 ± 0.8008e-04, different-groups mean: 3.4602e-04 ± 0.8626e-04; T(35) = 1.6302, p = .1120). Thus the IPS and not the PMd represented the grouped stimuli significantly more similarly than stimuli from different groups in the Group condition.

3.3.2. Behavioural control analysis results

In a second control analysis, we aimed to identify the influence of the behavioural effects on the neuroimaging results. To this end, we median-split the participant sample according to the performance difference between stimuli resulting in two sub-samples: similarly- (SIM) and differently-performing participants (DIF). For the SIM sub-sample, the 4 × 2 ANOVA on performance data identified no main effect of stimulus ($F(3,51) = 0.7833$, $p = 0.5088$), no effect of condition ($F(1,17) = 3.6479$, $p = 0.0732$) and no interaction between the factors ($F(3,51) = 0.8678$, $p = 0.4639$). Moreover, the 4 × 2 ANOVA on response time data identified a large condition effect ($F(1,17) = 82.8068$, $p = 6.0569e-08$, $\eta^2 = 0.6579$) and no stimulus effect ($F(3,51) = 0.3274$, $p = 0.8055$) or interaction between the factors ($F(3,51) = 1.6130$, $p = 0.1978$). Thus we were able to remove all but the condition difference in response times (addressed in **2.7.3**). The neuroimaging results for the SIM sub-sample identified a cluster overlapping with the left SPL cluster in the stimulus-specific WM analysis (peak: −22, −50, 62, T-statistic = 2.65) and in the left IPS in the context-dependent WM analysis (peak: −26, −64, 54, T-statistic = 2.40).

Next, we performed the same analysis with the differently-performing sub-sample. In contrast to the SIM sub-sample, the 4 × 2 ANOVA on the performance data identified a main effect of stimulus ($F(3,51) = 22.4457$, $p = 2.1093e-09$, $\eta^2 = 0.3191$), no effect of condition ($F(1,17) = 1.8571$, $p = 0.1907$) but an interaction between the factors was present ($F(3,51) = 6.3505$, $p = 9.6535e-04$, $\eta^2 = 0.0722$). Moreover, the 4 × 2 ANOVA on response time data identified a large condition effect ($F(1,17) = 76.2258$, $p = 1.0885e-07$, $\eta^2 = 0.6047$), no stimulus effect ($F(3,51) = 2.2522$, $p = 0.0934$) and an interaction between the factors ($F(3,51) = 6.8480$, $p = 5.7756e-04$, $\eta^2 = 0.0315$). Once again, we identified clusters overlapping with those identified in the main analyses. The left SPL contained stimulus-specific WM information (peak: −22, −50, 56, T-statistic = 5.09) whereas the left IPS contained context-dependent WM information (peak: −24, −62, 50, T-statistic = 5.22). The greater T-statistics observed with the differently-performing sub-sample, combined with our ability to replicate our findings with both sub-samples, suggests that the effect identified in the IPS might result from the combination of context-dependent WM amplified by task-difficulty.

3.3.3. Response time control analysis results

Thirdly, to identify whether the observed condition-difference in response times influenced the neuroimaging results, we reproduced the main analyses results with new first level models including an additional parametric response time nuisance regressor. We identified stimulus-specific WM information in the left SPL (peak −22, −48, 60, T-statistic = 4.69) and IFG (peak −40, 36, 14, T-statistic = 4.69) and context-dependent WM in the left IPS (peak −24, −66, 54, T-statistic = 5.06). Thus suggesting that the neuroimaging results are independent from the observed differences in response times.

3.3.4. WM-specificity control analysis results

To ensure that the results are specific to WM information, we performed a control analysis wherein we repeated the two main analyses, stimulus-specific (**2.6.4**) and context-dependent WM (**2.6.5**), with regressors defined for the uncued stimuli. The analyses did not identify any region with uncued stimulus-specific WM information even at an uncorrected threshold of $p < 0.001$ and did not identify any region showing an interaction across conditions at the corrected significance threshold. Therefore, both the stimulus-specific regions as well as the context-dependent group-specific regions are indeed maintaining information which is specific to WM.

3.3.5. Multivariate control analysis results

Finally, we tested whether the identified WM representations are multivariate in nature. To this end, we repeated the stimulus-specific (**2.6.4**) and context-dependent WM analyses (**2.6.5**) using a single voxel instead of the 4-voxel radius searchlight. Neither the stimulus-specific nor the interaction analysis identified any significant clusters of univariate WM content at the corrected statistical threshold, thereby demonstrating that the WM representations are multivariate in nature.

4. Discussion

Using whole-brain fMRI in humans in combination with the cross-validated, searchlight, multivariate ANOVA, we explored which brain regions maintain WM representations of individual and groups of somatosensory pulse sequences. In a first step, we identified the left IFG and SPL as maintaining stimulus-specific information in WM, across experimental conditions. Next, by comparing the differences in pattern distinctness across conditions, where participants were asked to maintain either an individual stimulus or group-information in WM, we identified an interaction between conditions in the left IPS (and in the left PMd at an uncorrected threshold). Moreover, in the left IPS, group members shared a more similar multivariate WM representation in the Group than in the Stimulus condition. Thus, our results suggest that the left IPS contains context-modulated WM information such that the stimuli from the same group are more similarly represented in the Group condition than in the Stimulus condition. Accordingly, our results provide additional insight into the adaptive coding ability of the parietal cortex, where task-demands influence WM representations.

4.1. Stimulus-specific WM representations

The present study identified condition-general stimulus-specific WM content within the left IFG and SPL. Moreover, we revealed that the WM representations maintained in the IFG and SPL are both specific to the cued WM content and employ a multivariate code. The identified stimulus-specific WM regions are well in line with previous findings which suggest that the IFG and SPL are capable of maintaining a wide-range of features in WM (Christophel et al., 2017; Sreenivasan & D'Esposito, 2019). Using the well-established vibrotactile WM paradigm, frequency-specific WM information has been identified in human (Schmidt et al., 2017; Spitzer et al., 2010) as well as NHP IFG (Romo et al., 1999). Moreover, experiments employing trains or sequences of stimuli, similar to those used in the present study, have shown that the IFG is involved in the perception of visual sequences (Cavdaroglu and Knops, 2018) and the maintenance of auditory sequences in WM (Uluç et al., 2018). Notably, a majority of participants (83.3%) reported in the debriefing session having remembered the stimuli by mentally verbalizing or internally singing the stimuli, thus it is not surprising that the left IFG, which is known to be involved in language production (Binder et al., 1997) and has been shown to maintain roman characteristic-specific WM content (letters) in WM (Polanía et al., 2011), maintained stimulus-specific WM information in the present study. In agreement with our results, Polanía and colleagues also found evidence for WM letter representations in the left posterior parietal cortex. The posterior parietal cortex, or SPL more specifically, has previously been shown to maintain a wide variety of WM information including locations (Jerde et al., 2012; Sprague et al., 2014, 2016), shapes (Christophel and Haynes, 2014a) and patterns composed of colour (Christophel et al., 2015; Christophel et al., 2012) and motion (Christophel and Haynes, 2014b). In line with this, we identified stimulus-specific WM information in the SPL using stimuli comprising temporal patterns of somatosensory pulses. Thus, it's possible that the SPL also maintains temporal patterns in addition to colour and motion patterns. However, previous studies have shown a divergence where frontal areas represent temporally-distributed stimuli and parietal regions represent spatially-distributed stimuli (Cavdaroglu and Knops, 2018). Therefore, participants likely transformed the stimulus features into a different representational code which was subsequently maintained in the SPL. Future studies which probe the nature of the WM representation are required to further explore the nature of the code maintained in the SPL. Consequently, we provide evidence for the maintenance of WM representations of somatosensory pulse sequences, independent of experimental context, in higher-order, frontoparietal regions.

4.2. Context-dependent WM representations

Next, we identified the left IPS and (found preliminary evidence for) the left dPMC as regions that modify their WM representations in response to changing task-demands. We expected that, by training participants on pseudorandom groupings, the resulting WM representations would be modulated such that representations of grouped stimuli would be more similar to each other when the task required the maintenance of the group, than when an individual stimulus was maintained in WM. Thus, using an interaction contrast, we localized WM representations which adapted to the changing task-demands in the left IPS. Moreover, because we compared the same physical pairs of stimuli across experimental conditions while controlling for the uncued stimuli, the identified adaptive WM information is independent of stimulus features and specific to the cued stimulus. This is significant because, due to the sluggish and indirect nature of the BOLD response, distinguishing between group- and stimulus-specific information is more nuanced with neuroimaging than with neurophysiological data. Thus, by contrasting identical pairs of stimuli across the two experimental conditions, we can be certain that the resulting WM information is specific to the group and not contaminated by stimulus feature-specific BOLD responses.

Additionally, to visualize the interaction, we plotted the group members' multivariate pattern distinctness estimates for the two experimental conditions separately (Fig. 3B). Due to a strong a priori hypothesis regarding the presence of group-specific WM information in the PMC (Malone et al., 2019; Rossi-Pool et al., 2016, 2017, 2019), we included a cluster in the left PMd which did not survive multiple comparison correction for completeness. This visualization illustrates that, for the left IPS and PMd, the group members were more similarly represented in the Group than in the Stimulus condition. In a control analysis, we additionally found evidence for the grouped stimuli to be represented more similarly than non-grouped stimuli in the Group condition in the left IPS but not the PMd. While this control analysis may be confounded (see **2.7.1**), these analyses provide additional evidence for the maintenance of context-dependent temporal patterns of vibrotactile

stimuli in WM in the left IPS. Of note, in the present study we employed cluster-based correction thresholding which may result in larger brain regions (e.g. the PPC) crossing the statistical threshold more easily than smaller regions (e.g. the PMd). This is however unlikely to have biased the reported results as post-hoc analyses with different searchlight radii (2 to 5 voxels) did not change the location of the identified clusters.

The finding of task-modulated WM information in the IPS is in line with previous work which has shown that representations of task-relevant features in the IPS change with task demands and difficulty (Jackson and Woolgar, 2018; Liu and Hou, 2013; Woolgar et al., 2011). Moreover, the IPS has been suggested to be an integral member of the multiple-demand or task-positive network, a network which processes and maintains features essential for the successful performance of a task, across changing task demands, and is influenced by rule complexity, memory load, attentional switching among other factors (Fedorenko et al., 2013; Wen et al., 2018). This is especially relevant for the present study. According to these studies, the effect of task-difficulty is to increase the resolution or strength of a task-relevant representation. Our results show the opposite effect. In the more difficult task, the Group condition, the representations of grouped-stimuli become more similar to one another instead of more distinct. Thus, it is evidence in favour of a group representation. To further explore the influence of task-difficulty in our data, we median-split the participant sample according to the consistency of the performance across stimuli. While we were able to replicate our findings with both sub-samples, the sub-sample with larger behavioural effects demonstrated larger neuroimaging effects. Thus, it is conceivable that the effect identified in the IPS is the result of a combination of context-dependent WM modification amplified by task-difficulty.

The central role of the IPS in grouping and categorizing stimuli across sensory domains and species has been well established (Freedman and Assad, 2016). A large body of research has been accumulated demonstrating the maintenance of categorical and group-specific WM information across stimulus modalities in the LIP, the IPS homologue in NHPs (Fitzgerald et al., 2011, 2013, 2012; Freedman and Assad, 2006, 2016; Freedman et al., 2001; Sarma et al., 2016; Swaminathan and Freedman, 2012). Furthermore, a new study has shown that the NHP IPS is necessary for the transformation of a stimulus representation into a more-abstract category label which is then passed to motor-selective neurons in the NHP IPS (Zhou and Freedman, 2019). More generally, Nieder (2012) has shown that both the LIP as well as NHP prefrontal regions represent auditory and visual percepts of number sets, tantamount to abstract numerical categories, in a supramodal fashion. Indeed, the PPC has been shown to be involved in a wide variety of abstract cognitive functions including the representation of cognitive sets (Oristaglio et al., 2006; Stoet and Snyder, 2004), numerosity (Nieder et al., 2006; Nieder and Miller, 2004; Tudusciuc and Nieder, 2007) and salience (Leathers and Olson, 2012), all of which can be considered various forms of categorization (Freedman and Assad, 2016). Recently, using optogenetics in combination with calcium imaging, the mouse PPC was shown to be central for the categorization of auditory frequencies (Zhong et al., 2019). The authors provide evidence for the stable representation of category exemplars in the PPC over several days and show that the PPC is necessary for the generalization from category exemplars to novel stimuli as well as for the updating of category boundaries. Furthermore, a recent study exploring cross-modal categorization employed an auditory and tactile delayed-match-to-category paradigm in humans, in combination with multivariate pattern analysis, and found overlapping tactile and auditory category information in the IPS (Levine and Schwarzbach, 2017). Taken together, the evidence across species provides a strong argument for the involvement of the IPS, and PPC more generally, in the categorization and grouping of stimuli. Indeed, a recent article merged the various LIP functions into a single role: the identification of behaviourally relevant stimuli (Freedman and Ibos, 2018). The authors suggest that the nonlinear nature of responses observed in LIP neurons in DMTS tasks points to the integration and comparison of incoming bottom-up signals with the specific top-down task-goals. Thus, taken across species, the IPS likely maintains WM representations indicating the current task goal, for example, the stimulus or group which is to be compared with the target at the end of the trial.

The PPC, prefrontal cortex, and PMC have been suggested to act together in a network which implements abstract cognitive computations, including categorization and grouping of stimuli (Freedman and Assad, 2016). Indeed, previous work investigating the representation of somatosensory categories also identified category-specific information in ventral human (Malone et al., 2019) and NHP PMd (Rossi-Pool et al., 2016, 2017, 2019). Importantly, both studies used explicit categorical rules on stimulus feature properties to define their categories (high vs low frequencies; same vs different stimulus) whereas, with the present study, we wanted to explore how abstract group representations, unrelated to the stimulus features and dissociated from an explicit rule, would affect the WM representations. In line with the NHP findings, we identified a trend towards a pattern distinctness difference for the group members in the two experimental conditions in the PMd. Of note, we identified smaller pattern distinctness values for the PMd than for the SPL and IPS across all analyses. Because the pattern distinctness value is an estimate of the amount of variance explained by a contrast, normalized by the error covariance, it is interpretable. However, it is difficult and ill-advised to compare across brain regions. Different regions are known to have different neural vasculature (Gardner, 2010), connectivity (Zalesky et al., 2012), and morphology (Bianchi et al., 2013), all of which may influence the hemodynamic response and recorded fMRI signal (Handwerker, Ollinger, & D'Esposito, 2004) making it difficult to compare the results across regions (for more information see Haynes, 2015).

A potentially important distinction between the present study and that of Malone et al. (2019) and Rossi-Pool et al. (2016) concerns the ability to prepare a motor decision. Traditionally, the PMC has been deemed responsible for the organization and planning of movements (Wise, 1985). Thus, one hypothesized role of the PMC in categorization suggests that the PMC maintains information relating to 'motor ideas' which may provide the basis for cognitive functions (Fadiga et al., 2000). In support of this hypothesis, the PMC has been shown to represent rules in a behaviourally relevant manner (Muhammad et al., 2006; Vallentin et al., 2012; Wallis and Miller, 2003). In the present study, participants maintained WM information and were not able to prepare a prospective motor plan as they did not know whether the target would match the maintained stimulus. Moreover, we included an additional precaution and pseudorandomly alternated the locations of the motor targets, thereby ensuring that participants could neither select a decision nor a motor plan. In contrast, Malone et al. (2019) did not require participants to respond to a target and therefore participants were able to select a motor response at the onset of the stimulus presentation. Similarly, Rossi-Pool et al. (2016) identified categorical representations in the PMd during the delay between the presentation of the target and the motor output, a timepoint when the NHPs had already made but not yet communicated their decision. Thus, the inability of participants in the present study to select a decision and prepare a motor output may have prevented the transformation of group-specific WM information in the IPS into a motor plan in the PMC. In line with this, the PMC has been implicated in the preparation of so-called virtual motor plans which can be transformed into a motor plan (Nakayama et al., 2008; Yamagata et al., 2012, Yamagata et al., 2009). Indeed, Rossi-Pool et al. (2019) recently re-analysed their data and found that, while there was category information in the PMd, the majority of neuronal variance could be explained by experimental timing. Thus, it is possible that the PMC is mainly responsible for determining the specific timing of events and coordinating the associated network regions, such as the stimulus-specific WM information in the IFG and SPL and the context-dependent, group-specific WM information in the IPS.

4.3. WM representations

Finally, by considering both the context-dependent and the stimulus-specific results together, we can speculate on the probable nature of the WM representational codes in the various regions. Regions identified by the stimulus-specific conjunction analysis, area 5A of the SPL and area 45 of the IFG, likely maintain stimulus feature information in WM independent of experimental conditions. Moreover, regions identified by the interaction analysis, the IPS and PMd, may maintain stimulus feature information only in the stimulus condition and an abstracted categorical or group label in the group condition (e.g. stimulus A1 and A2 maintained as A). This would also result in the difference in pattern distinctness estimates observed in the interaction analysis. Finally, the region identified by the overlap of the two analyses, area 7A of the SPL, likely maintains a combination of stimulus features as well as abstracted WM information in the group condition. Future studies are required to further probe the representational nature of the WM codes implemented by the different regions under various task-demands.

5. Conclusion

In conclusion, we present evidence for the maintenance of WM information in frontoparietal regions across experimental conditions wherein participants were instructed to maintain either individual or groups of somatosensory sequences. Additionally, we identified the maintenance of context-dependent, group-specific WM representations in the left IPS independent of stimulus properties in a paradigm that disentangled the WM representation from the categorical decision and the motor response. We show that the WM representations in the IPS adaptively change with task-demands such that, in the Group condition, group members are represented more similarly than in the Stimulus condition. Thus, we provide novel evidence for the adaptive nature of somatosensory WM representations in the IPS and suggest that somatosensory WM representations are maintained in the IPS in an adaptive, context-dependent manner.

Declaration of competing interest

The authors declare that the research was conducted in the absence of any commercial or financial relationship that could be construed as a potential conflict of interest.

CRediT authorship contribution statement

Lisa Alexandria Velenosi: Conceptualization, Data curation, Formal analysis, Funding acquisition, Investigation, Visualization, Writing - original draft. **Yuan-Hao Wu:** Conceptualization, Formal analysis, Investigation, Writing - review & editing. **Timo Torsten Schmidt:** Conceptualization, Writing - review & editing. **Felix Blankenburg:** Conceptualization, Formal analysis, Supervision, Writing - review & editing.

Acknowledgements

The authors would like to thank Pia Schröder for helpful discussions and Carsten Allefeld for comments on the methods and Alexander von Horst for help with the manuscript. Finally, the authors would like to extend their sincere gratitude to Reviewer 1 for significantly improving the quality of the manuscript.

Appendix A. Supplementary data

Supplementary data to this article can be found online at https://doi.org/10.1016/j.neuroimage.2020.117146.

Funding

LAV was supported by the Research Training Group GRK 1589/2 "Sensory Computation in Neural Systems" by the German Research Foundation (DFG).

Data code and availability statement

In accordance with the EU's General Data Protection Regulation we are unable to share raw fMRI data. However, unthresholded group contrast images for each result can be directly inspected on Neurovault (https://identifiers.org/neurovault.collection:5623). Analysis code is available upon request.

References

Allefeld, C., Haynes, J.D., 2014. Searchlight-based multi-voxel pattern analysis of fMRI by cross-validated MANOVA. Neuroimage 89, 345–357. https://doi.org/10.1016/j.neuroimage.2013.11.043.

Baddeley, A.D., Hitch, G., 1974. Working memory. Psychol. Learn. Motiv. 8, 47–89.

Bianchi, S., Stimpson, C.D., Bauernfeind, A.L., Schapiro, S.J., Baze, W.B., McArthur, M.J., et al., 2013. Dendritic morphology of pyramidal neurons in the chimpanzee neocortex: regional specializations and comparison to humans. Cerebr. Cortex 23 (10), 2429–2436.

Binder, J.R., Frost, J.A., Hammeke, T.A., Cox, R.W., Rao, S.M., Prieto, T., 1997. Human brain language areas identified by functional magnetic resonance imaging. J. Neurosci.: Off. J. Soc. Neurosci. 17 (1), 353–362.

Brainard, D.H., 1997. The Psychophysics toolbox. Spatial Vis. 10 (4), 433–436. https://doi.org/10.1163/156856897X00357.

Cavdaroglu, S., Knops, A., 2018. Evidence for a posterior parietal cortex contribution to spatial but not temporal numerosity perception. Cerebr. Cortex 2965–2977. https://doi.org/10.1093/cercor/bhy163. July 2018.

Christophel, Thomas B., Cichy, R.M., Hebart, M.N., Haynes, J.-D., 2015. Parietal and early visual cortices encode working memory content across mental transformations. Neuroimage 106, 198–206. https://doi.org/10.1016/j.neuroimage.2014.11.018.

Christophel, Thomas B., Haynes, J.D., 2014. Decoding complex flow-field patterns in visual working memory. Neuroimage 91, 43–51. https://doi.org/10.1016/j.neuroimage.2014.01.025.

Christophel, Thomas B., Hebart, M.N., Haynes, J.-D., 2012. Decoding the contents of visual short-term memory from human visual and parietal cortex. J. Neurosci.: Off. J. Soc. Neurosci. 32 (38), 12983–12989. https://doi.org/10.1523/JNEUROSCI.0184-12.2012.

Christophel, Thomas B., Klink, P.C., Spitzer, B., Roelfsema, P.R., Haynes, J.-D., 2017. The distributed nature of working memory. Trends Cognit. Sci. 21 (2), 111–124. https://doi.org/10.1016/j.tics.2016.12.007.

Duncan, J., 2001. An adaptive coding model of neural function in prefrontal cortex. Nat. Rev. Neurosci. 2 (November), 820–829. Retrieved from. http://www.cnbc.cmu.edu/~tai/readings/nature/duncan_code_prefrontal.pdf.

Eickhoff, S., 2007. SPM Anatomy toolbox. Neuroimage 91 (14), 1–21.

Fadiga, L., Fogassi, L., Gallese, V., Rizzolatti, G., 2000. Visuomotor neurons: ambiguity of the discharge or "motor" perception? Int. J. Psychophysiol. 35 (2–3), 165–177. https://doi.org/10.1016/S0167-8760(99)00051-3.

Fedorenko, E., Duncan, J., Kanwisher, N., 2013. Broad domain generality in focal regions of frontal and parietal cortex. Proc. Natl. Acad. Sci. Unit. States Am. 110 (41), 16616–16621. https://doi.org/10.1073/pnas.1315235110.

Fitzgerald, J.K., Freedman, D.J., Assad, J.a., 2011. Generalized associative representations in parietal cortex. Nat. Neurosci. 14 (8) https://doi.org/10.1038/nn.2878, 1075-U179.

Fitzgerald, Jamie K., Freedman, D.J., Fanini, A., Bennur, S., Gold, J.I., Assad, J.A., 2013. Biased associative representations in parietal cortex. Neuron 77 (1), 180–191. https://doi.org/10.1016/j.neuron.2012.11.014.

Fitzgerald, Jamie K., Swaminathan, S.K., Freedman, D.J., 2012. Visual categorization and the parietal cortex. Front. Integr. Neurosci. 6 (May), 1–6. https://doi.org/10.3389/fnint.2012.00018.

Freedman, D.J., Assad, J.A., 2006. Experience-dependent representation of visual categories in parietal cortex. Nature 443 (7107), 85–88. https://doi.org/10.1038/nature05078.

Freedman, David J., Assad, J.A., 2016. Neuronal mechanisms of visual categorization: an abstract view on decision making. Annu. Rev. Neurosci. 39 (1), 129–147. https://doi.org/10.1146/annurev-neuro-071714-033919.

Freedman, David J., Ibos, G., 2018. An integrative framework for sensory, motor, and cognitive functions of the posterior parietal cortex. Neuron 97 (6), 1219–1234. https://doi.org/10.1016/j.neuron.2018.01.044.

Freedman, David J., Riesenhuber, M., Poggio, T., Miller, E.K., 2001. Categorical representation of visual stimuli in the primate prefrontal cortex. Science (New York, N.Y.) 291 (5502), 312–316. https://doi.org/10.1126/science.291.5502.312.

Friston, K.J., Penny, W.D., Glaser, D.E., 2005. Conjunction revisited. Neuroimage 25 (3), 661–667.

Gardner, J.L., 2010. Is cortical vasculature functionally organized? Neuroimage 49 (3), 1953–1956.

Grefkes, C., Fink, G.R., 2005. The functional organization of the intraparietal sulcus in the macaque monkey. J. Anat. 207, 3–17. https://doi.org/10.1167/16.12.1302.
Handwerker, D.A., Ollinger, J.M., D'Esposito, M., 2004. Variation of BOLD hemodynamic responses across subjects and brain regions and their effects on statistical analyses. Neuroimage 21 (4), 1639–1651.
Haynes, JD, 2015. A primer on pattern-based approaches to fMRI: principles, pitfalls, and perspectives. Neuron. https://doi.org/10.1016/j.neuron.2015.05.025.
Jackson, J.B., Woolgar, A., 2018. Adaptive coding in the human brain: distinct object features are encoded by overlapping voxels in frontoparietal cortex. Cortex 108, 25–34. https://doi.org/10.1016/j.cortex.2018.07.006.
Jerde, T.A., Merriam, E.P., Riggall, A.C., Hedges, J.H., Curtis, C.E., 2012. Prioritized maps of space in human frontoparietal cortex. J. Neurosci. 32 (48), 17382–17390. https://doi.org/10.1523/jneurosci.3810-12.2012.
Kriegeskorte, N., Goebel, R., Bandettini, P., 2006. Information-based functional brain mapping. Proc. Natl. Acad. Sci. 103 (10), 3863–3868. https://doi.org/10.1073/pnas.0600244103.
Leathers, M.L., Olson, C.R., 2012. In monkeys making value-based decisions, LIP neurons encode cue salience and not action value. Science 338 (October), 132–135. https://doi.org/10.1126/science.1226405.
Lee, S.-H., Kravitz, D.J., Baker, C.I., 2013. Goal-dependent dissociation of visual and prefrontal cortices during working memory. Nat. Neurosci. 16 (8), 997–999. https://doi.org/10.1038/nn.3452.
Levine, S.M., Schwarzbach, J., 2017. Decoding of auditory and tactile perceptual decisions in parietal cortex. Neuroimage 162 (August), 297–305. https://doi.org/10.1016/j.neuroimage.2017.08.060.
Levine, S.M., Schwarzbach, J.V., 2018. Cross-decoding supramodal information in the human brain. Brain Struct. Funct. 223 (9), 4087–4098. https://doi.org/10.1007/s00429-018-1740-z.
Li, S., Ostwald, D., Giese, M., Kourtzi, Z., 2007. Flexible coding for categorical decisions in the human brain. J. Neurosci. 27 (45), 12321–12330. https://www.jneurosci.org/content/jneuro/27/45/12321.full.pdf.
Liu, T., Hou, Y., 2013. A hierarchy of attentional priority signals in human frontoparietal cortex. J. Neurosci. 33 (42), 16606–16616. https://doi.org/10.1523/jneurosci.1780-13.2013.
Logie, R.H., Cowan, N., 2015. Perspectives on Working Memory: Introduction to the Special Issue. Memory & Cognition. https://doi.org/10.3758/s13421-015-0510-x (March), 315–324.
Malone, P.S., Eberhardt, S.P., Wimmer, K., Sprouse, C., Klein, R., Glomb, K., et al., 2019. Neural mechanisms of vibrotactile categorization. Hum. Brain Mapp. 40 (10), 3078–3090. https://doi.org/10.1002/hbm.24581.
Muhammad, R., Wallis, J.D., Miller, E.K., 2006. A comparison of abstract rules in the prefrontal cortex, premotor cortex, inferior temporal cortex, and striatum. J. Cognit. Neurosci. 18 (6), 974–989. https://doi.org/10.1162/jocn.2006.18.6.974.
Nakayama, Y., Yamagata, T., Tanji, J., Hoshi, E., 2008. Transformation of a virtual action plan into a motor plan in the premotor cortex. J. Neurosci. 28 (41), 10287–10297. https://doi.org/10.1523/jneurosci.2372-08.2008.
Nichols, T., Brett, M., Andersson, J., Wager, T., Poline, J.B., 2005. Valid conjunction inference with the minimum statistic. Neuroimage 25 (3), 653–660.
Nieder, A., 2012. Supramodal numerosity selectivity of neurons in primate prefrontal and posterior parietal cortices. Proc. Natl. Acad. Sci. Unit. States Am. 109 (29), 11860–11865. https://doi.org/10.1073/pnas.1204580109.
Nieder, A., Diester, I., Tudusciuc, O., 2006. Temporal and spatial enumeration processes in the primate parietal cortex. Science 313 (September), 1431.
Nieder, Andreas, Miller, E.K., 2004. A parietol-frontal network for visual numerical information in the monkey. Proc. Natl. Acad. Sci. Unit. States Am. 101 (19), 7457–7462.
Oristaglio, J., Schneider, D.M., Balan, P.F., Gottlieb, J., 2006. Integration of visuospatial and effector information during symbolically cued limb movements in monkey lateral intraparietal area. J. Neurosci. 26 (32), 8310–8319. https://doi.org/10.1523/jneurosci.1779-06.2006.
Ostwald, D., Schneider, S., Bruckner, R., Horvath, L., 2019. Power, positive predictive value, and sample size calculations for random field theory-based fMRI inference. BioRxiv 613331. https://doi.org/10.1101/613331.
Polanía, R., Paulus, W., Nitsche, M.A., 2011. Noninvasively decoding the contents of visual working memory in the human prefrontal cortex with high-gamma oscillatory patterns. J. Cognit. Neurosci. 24, 304–314.
Postle, B.R., 2006. Working memory as an emergent property of the mind and brain. Neuroscience 139 (1), 23–38. https://doi.org/10.1016/j.neuroscience.2005.06.005.
Romo, R., Brody, C.D., Hernández, a, Lemus, L., 1999. Neuronal correlates of parametric working memory in the prefrontal cortex. Nature 399 (6735), 470–473. https://doi.org/10.1038/20939.
Rossi-Pool, R., Salinas, E., Zainos, A., Alvarez, M., Vergara, J., Parga, N., Romo, R., 2016. Emergence of an abstract categorical code enabling the discrimination of temporally structured tactile stimuli. Proc. Natl. Acad. Sci. Unit. States Am. https://doi.org/10.1073/pnas.1618196113, 201618196.
Rossi-Pool, R., Zainos, A., Alvarez, M., Zizumbo, J., Vergara, J., Romo, R., 2017. Decoding a decision process in the neuronal population of dorsal premotor cortex. Neuron 96 (6), 1432–1446. https://doi.org/10.1016/j.neuron.2017.11.023 e7.
Rossi-Pool, R., Zizumbo, J., Alvarez, M., Vergara, J., Zainos, A., Romo, R., 2019. Temporal signals underlying a cognitive process in the dorsal premotor cortex. Proc. Natl. Acad. Sci. Unit. States Am. 116 (15), 7523–7532. https://doi.org/10.1073/pnas.1820474116.
Sarma, A., Masse, N.Y., Wang, X.-J., Freedman, D.J., 2016. Task-specific versus generalized mnemonic representations in parietal and prefrontal cortices. Nat. Neurosci. 19 (1), 143–149. https://doi.org/10.1038/nn.4168.
Schmidt, T.T., Wu, Y., Blankenburg, F., 2017. Content-specific codes of parametric vibrotactile working memory in humans. J. Neurosci. 37 (40), 9771–9777. https://doi.org/10.1523/jneurosci.1167-17.2017.
Seger, C.A., Miller, E.K., 2010. Category learning in the brain. Annu. Rev. Neurosci. 33 (1), 203–219. https://doi.org/10.1146/annurev.neuro.051508.135546.
Senoussi, M., Berry, I., VanRullen, R., Reddy, L., 2016. Multivoxel object representations in adult human visual cortex are flexible: an associative learning study. J. Cognit. Neurosci. 28 (6), 852–868. https://doi.org/10.1162/jocn_a_00933.
Spitzer, B., Wacker, E., Blankenburg, F., 2010. Oscillatory correlates of vibrotactile frequency processing in human working memory. J. Neurosci. 30 (12), 4496–4502. https://doi.org/10.1523/JNEUROSCI.6041-09.2010.
Sprague, T.C., Ester, E.F., Serences, J.T., 2014. Reconstructions of information in visual spatial working memory degrade with memory load. Curr. Biol. 24 (18), 2174–2180. https://doi.org/10.1016/j.cub.2014.07.066.
Sprague, T.C., Ester, E.F., Serences, J.T., 2016. Restoring latent visual working memory representations in human cortex. Neuron 91 (3), 694–707. https://doi.org/10.1016/j.neuron.2016.07.006.
Sreenivasan, K.K., D'Esposito, M., 2019. The what, where and how of delay activity. Nat. Rev. Neurosci. 10–14. https://doi.org/10.1038/s41583-019-0176-7.
Stoet, G., Snyder, L.H., 2004. Single neurons in posterior parietal cortex of monkeys encode cognitive set. Neuron 42 (6), 1003–1012. https://doi.org/10.1016/j.neuron.2004.06.003.
Swaminathan, S.K., Freedman, D.J., 2012. Preferential encoding of visual categories in parietal cortex compared with prefrontal cortex. Nat. Neurosci. 15 (2), 315–320. https://doi.org/10.1038/nn.3016.
Tudusciuc, O., Nieder, A., 2007. Neuronal population coding of continuous and discrete quantity in the primate posterior parietal cortex. Proc. Natl. Acad. Sci. Unit. States Am. 104 (36), 14513–14518. https://doi.org/10.1073/pnas.0705495104.
Uluç, I., Schmidt, T.T., Wu, Y. Hao, Blankenburg, F., 2018. Content-specific codes of parametric auditory working memory in humans. Neuroimage 183, 254–262. https://doi.org/10.1016/j.neuroimage.2018.08.024.
Vallentin, D., Bongard, S., Nieder, A., 2012. Numerical rule coding in the prefrontal, premotor, and posterior parietal cortices of macaques. J. Neurosci. 32 (19), 6621–6630. https://doi.org/10.1523/jneurosci.5071-11.2012.
Wallis, J.D., Miller, E.K., 2003. From rule to response: neuronal processes in the premotor and prefrontal cortex. J. Neurophysiol. 90 (3), 1790–1806. https://doi.org/10.1152/jn.00086.2003.
Wen, T., Mitchell, D.J., Duncan, J., 2018. Response of the multiple-demand network during simple stimulus discriminations. Neuroimage 177 (March), 79–87. https://doi.org/10.1016/j.neuroimage.2018.05.019.
Wise, S.P., 1985. The primate premotor cortex: past, present, and preparatory. Annu. Rev. Neurosci. 8, 1–19.
Woolgar, A., Hampshire, A., Thompson, R., Duncan, J., 2011. Adaptive coding of task-relevant information in human frontoparietal cortex. J. Neurosci. 31 (41), 14592–14599. https://doi.org/10.1523/jneurosci.2616-11.2011.
Yamagata, T., Nakayama, Y., Tanji, J., Hoshi, E., 2012. Distinct information representation and processing for goal-directed behavior in the dorsolateral and ventrolateral prefrontal cortex and the dorsal premotor cortex. J. Neurosci. 32 (37), 12934–12949. https://doi.org/10.1523/jneurosci.2398-12.2012.
Yamagata, Tomoko, Nakayama, Y., Tanji, J., Hoshi, E., 2009. Processing of visual signals for direct specification of motor targets and for conceptual representation of action targets in the dorsal and ventral premotor cortex. J. Neurophysiol. 102 (6), 3280–3294. https://doi.org/10.1152/jn.00452.2009.
Zalesky, A., Cocchi, L., Fornito, A., Murray, M.M., Bullmore, E.D., 2012. Connectivity differences in brain networks. Neuroimage 60 (2), 1055–1062.
Zhong, L., Zhang, Y., Duan, C.A., Deng, J., Pan, J., Xu, N. Long, 2019. Causal contributions of parietal cortex to perceptual decision-making during stimulus categorization. Nat. Neurosci. 22 (6), 963–973. https://doi.org/10.1038/s41593-019-0383-6.
Zhou, Y., Freedman, D.J., 2019. Posterior parietal cortex plays a causal role in perceptual and categorical decisions. Science 2 (July), 1–5. https://doi.org/10.1007/978-1-4614-7320-6_310-1.

Study 3 - Decoding vibrotactile choice independent of stimulus order and saccade selection during sequential comparisons

Wu, YH, **Velenosi LA**, Schröder P, Ludwig, S, Blankenburg, F (2019). Decoding vibrotactile choice independent of stimulus order and saccade selection during sequential comparisons. *Human brain mapping*, *40(6)*, 1898 - 1907.
DOI: https://doi.org/10.1002/hbm.24499

This chapter includes the publisher's version (Version of Record).

Study 4 - Response modality-dependent categorical choice representations for vibrotactile comparisons

Wu, YH, **Velenosi, LA**, Blankenburg F (2021). Response modality-dependent categorical choice representations for vibrotactile comparisons. *NeuroImage*, *226*, 117592.
DOI: https://doi.org/10.1016/j.neuroimage.2020.117592

NeuroImage 226 (2021) 117592

Contents lists available at ScienceDirect

NeuroImage

journal homepage: www.elsevier.com/locate/neuroimage

Response modality-dependent categorical choice representations for vibrotactile comparisons

Yuan-hao Wu*, Lisa A. Velenosi, Felix Blankenburg

Neurocomputation and Neuroimaging Unit (NNU), Department of Education and Psychology, Freie Universität Berlin, Habelschwerdter Allee 45, 14195 Berlin, Germany

ARTICLE INFO

Keywords:
Vibrotactile comparison
Perceptual decision making
Categorical choice
FMRI
Multivariate pattern analysis

ABSTRACT

Previous electrophysiological studies in monkeys and humans suggest that premotor regions are the primary loci for the encoding of perceptual choices during vibrotactile comparisons. However, these studies employed paradigms wherein choices were inextricably linked with the stimulus order and selection of manual movements. It remains largely unknown how vibrotactile choices are represented when they are decoupled from these sensorimotor components of the task. To address this question, we used fMRI-MVPA and a variant of the vibrotactile frequency discrimination task which enabled the isolation of choice-related signals from those related to stimulus order and selection of the manual decision reports. We identified the left contralateral dorsal premotor cortex (PMd) and intraparietal sulcus (IPS) as carrying information about vibrotactile choices. Our finding provides empirical evidence for an involvement of the PMd and IPS in vibrotactile decisions that goes above and beyond the coding of stimulus order and specific action selection. Considering findings from recent studies in animals, we speculate that the premotor region likely serves as a temporary storage site for information necessary for the specification of concrete manual movements, while the IPS might be more directly involved in the computation of choice. Moreover, this finding replicates results from our previous work using an oculomotor variant of the task, with the important difference that the informative premotor cluster identified in the previous work was centered in the bilateral frontal eye fields rather than in the PMd. Evidence from these two studies indicates that categorical choices in human vibrotactile comparisons are represented in a response modality-dependent manner.

1. Introduction

In everyday life, we are continuously encountering situations wherein we need to make decisions based on comparisons between stimuli occurring at different times. Imagine choosing an avocado at a grocery store: one squeezes two or more avocados sequentially and decides for one based on their firmness. Neural processes underlying this type of decision have been extensively studied in the somatosensory domain using the vibrotactile frequency discrimination task (reviewed in Romo and de Lafuente, 2013). In their seminal work, Romo and colleagues trained monkeys to compare frequencies of two sequentially presented vibrotactile stimuli and report with a manual response whether the second frequency (f2) was higher or lower than the first (f1). Crucially, firing rates in premotor regions implicated in the planning and execution of manual movements, such as the supplementary motor area (SMA), ventral (PMv), and dorsal premotor cortices (PMd), have been consistently found to reflect vibrotactile choices (i.e., the categorical outcomes of the vibrotactile decision process; Hernández et al., 2002, 2010; Romo et al., 2004).

The involvement of motor-related regions during vibrotactile comparisons agrees well with findings from an influential line of decision-making research in the visual domain. Monkey neurophysiological experiments employing random motion dot tasks with saccade responses consistently reported decision-related signals in regions implicated in saccadic movement (reviewed in Gold and Shadlen, 2007), such as the lateral intraparietal area (LIP, Shadlen and Newsome, 2001; Roitman and Shadlen, 2002), the frontal eye fields (FEF, Kim and Shadlen, 1999; Ding and Gold, 2012), and the superior colliculus (Horwitz and Newsome, 1999; Ratcliff et al., 2003). Findings from these two lines of work have converged to the view that decisions are directly implemented in regions involved in the planning and execution of the resultant action (Gold and Shadlen, 2007; Cisek and Kalaska, 2010). In other words, decisions are implemented in a response modality-dependent manner. Moreover, the posited response modality-specific implementation appears to translate to human vibrotactile comparisons. Herding and colleagues (2016, 2017) reported premotor regions as the most likely source of choice-selective beta oscillatory activity in the EEG signal. The choice-related modulation was localized in the medial part of the premotor cortex when human observers used button presses to indicate their choices (Herding et al., 2016). However, when they reported

* Corresponding author.
E-mail address: yuanhao.wu@nyulangone.org (Y.-h. Wu).

https://doi.org/10.1016/j.neuroimage.2020.117592
Received 11 October 2019; Received in revised form 15 November 2020; Accepted 18 November 2020
Available online 26 November 2020

their choices with saccades, the source of the choice-related modulation shifted to the FEF (Herding et al., 2017).

Importantly, most findings in the context of vibrotactile comparisons were yielded from experimental settings wherein categorical choices were inextricably linked to various sensory and motor components of the task. For instance, f1 typically served as the reference stimulus against which f2 (the comparison stimulus) was compared. Thus, observers would mostly decide for the percept "higher" if frequencies were presented in an increasing order (f1 < f2), and "lower" if presented in a decreasing order (f1 < f2). Contents of the choices were directly bound with the physical properties of the stimulus order. Moreover, vibrotactile choices in these studies were linked with specific motor requirements at different levels. That is, observers had explicit foreknowledge of the required response effector for decision reports; and in addition, decisions were typically implemented as choices between two alternative actions within the required response modality (e.g., specific saccade directions, button presses) so that choosing a particular percept was the same as choosing a specific action with the required effector. Due to these dependencies, the reported choice-related signals in the above-mentioned studies may reflect a multiplicity of choice and task-specific sensorimotor components rather than the choice per se (Park et al., 2014; see also Huk et al., 2016 for a review). Indeed, human neuroimaging studies in the visual domain showed that decision-related signals are reflected by different or additional regions than the motor-related regions when choices were decoupled from specific motor requirements (Liu and Pleskac, 2011; Hebart et al., 2012; Filimon et al., 2013). These findings lead to the question of how categorical choices during vibrotactile comparisons in humans are represented when they are disentangled from one or another of the above-mentioned sensorimotor aspects.

Our previous work (Wu et al., 2019) was the first to address this question. We investigated brain regions representing vibrotactile choices independent of stimulus order and specific saccade direction by using human fMRI and a novel variant of the vibrotactile frequency discrimination task. Intriguingly, although participants' choices were decoupled from the preceding stimulus orders and ensuing saccade movements used for reporting the decisions, regions implicated in saccade planning and selection such as the FEF and intraparietal sulci (IPS) were identified as representing vibrotactile choices. The finding suggests that choice-related activities in these motor-related regions do not merely reflect specific action selection but might be involved in the computation of categorical choices in perceptual decision-making tasks. Moreover, it hints at the possibility that such categorical choices may also be represented in an effector-specific manner.

In the present fMRI study, we sought to further explore the interplay between the topographic organization of categorical choice representations and response modality during vibrotactile comparisons. We asked participants to perform an analogous version of the vibrotactile frequency discrimination task as in our previous work, with saccadic responses replaced by manual button presses. Further, the same whole-brain searchlight multivariate analysis routines (Kriegeskorte et al., 2006) as implemented in the previous work was employed to identify brain regions that carry information about vibrotactile choices. Following the interpretation drawn from our previous study, we expected vibrotactile choice representations in premotor regions implicated in the selection of manual responses such as the PMd, PMv, or SMA.

2. Materials and methods

2.1. Participants

Thirty-one volunteers participated in the fMRI experiment. They were right-handed, had no history of neurological or psychiatric impairment, and normal or corrected-to-normal vision. Data of four participants were excluded due to poor behavioral performance (accuracy rate < 0.5 in at least one stimulus pair), leaving the data of 27 participants in the analyses (18 females and 9 males; mean age: 25, range: 18 – 34). All participants provided written informed consent as approved by the ethics committee of the Freie Universität Berlin and received monetary compensation for their time.

2.2. Task design and stimuli

We asked participants to complete a variant of the vibrotactile frequency discrimination task (Fig. 1). Similar to standard versions of the task, participants compared two sequentially presented vibrotactile frequencies and decided whether the frequency of the comparison stimulus was higher or lower than that of the reference stimulus. It differed from standard versions in two important aspects: First, we introduced task rules that alternately designate f1 or f2 as the comparison/reference stimulus across trials so that the perceptual choices were independent of the physical properties of the stimulus order. Second, instead of using a direct choice-motor response mapping, participants reported a match or mismatch between their percept and the proposition of a visual matching cue. After the decision phase, participants selected a color-coded target, from which their perceptual choice was inferred. Hence, participants were not able to plan a specific manual movement or anticipate a target color during the decision phase. As a consequence of these measures, if there were detectable choice-related signals during the decision phase, it would be unlikely to result from the physical properties of the stimulus order or selection of specific button presses.

Each trial was preceded by a variable fixation period (3 – 6 s), during which participants were asked to fixate on a white cross presented centrally on the screen. The trial started with a switch from the fixation cross to either a square or a diamond for 500 ms, instructing participants which task rule applied. In half of the trials, participants used f1 as the comparison stimulus and evaluated whether it was higher or lower than the reference stimulus f2. In the other half, participants made comparisons in the reversed direction. That is, they evaluated f2 relative to f1. The rule cue was followed by two sequentially presented vibrotactile stimuli with different frequencies administered to participants' left index finger (each of 500 ms separated by a 1 s retention). After a decision phase of 2 s, a visual matching cue in the form of either an upward-pointing or a downward-pointing equilateral triangle appeared centrally on the screen for 500 ms, indicating a comparison stimulus of higher or lower frequency, respectively. Following the offset of the visual matching cue, a target screen with a central fixation cross and two color-coded targets (blue and yellow disks) in the periphery along the horizontal meridian was displayed for 1.5 s. During this period, participants reported a match or mismatch between their perceptual choice ('higher' vs. 'lower') and the visual matching cue by selecting one of the color-coded targets corresponding to their report. Depending on the spatial location of the corresponding target, participants pressed the left or right button of a response box held in their right hand with their index or middle finger.

Visual stimuli were generated using MATLAB version 8.2 (The MathWorks, Inc, Natick, MA) and the Psychophysics toolbox version 3 (Brainard, 1997). Except for the two peripheral, color-coded discs on target screens, all other visual symbols were presented centrally in white on a black background. During the fMRI session, visual stimuli were projected with an LCD projector (800 × 600, 60 Hz frame rate) onto a screen on the MR scanner's bore opening. Participants observed the visual stimuli via a mirror attached to the MR head coil from a distance of 110 ± 2 cm. Suprathreshold vibrotactile stimuli with a consistent peak amplitude were applied to participants' distal phalanx of the left index finger using a 16-dot piezoelectric Braille-like display (4 × 4 quadratic matrix, 2.5 mm spacing), controlled by a programmable stimulator (QuaeroSys Medical Devices, Schotten, Germany). Frequencies of the first vibratory stimuli (f1) varied between 16 and 28 Hz in steps of 4 Hz. The second stimulus was either 4 Hz higher or lower than the preceding f1, yielding a total of eight possible stimulus pairings.

Participants performed six experimental runs of the vibrotactile frequency discrimination task, each lasting ~12.5 min. During each run,

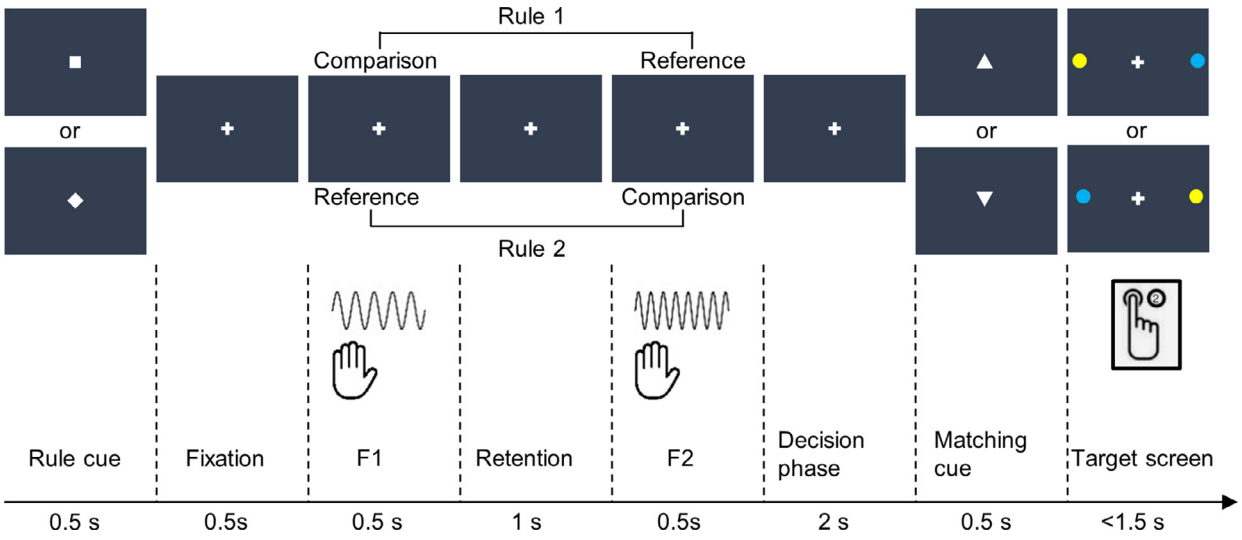

Fig. 1. Trial schematic. A rule cue (square or diamond) indicated whether f1 or f2 served as the comparison stimulus. The stimuli presentation was followed by a decision phase. Thereafter, a matching cue (equilateral triangle) was presented. An upward-pointing triangle represented a comparison stimulus of higher frequency, while a downward-pointing triangle represented a lower comparison frequency. Participants compared their perceptual choice with the matching cue. A match or mismatch was indicated by choosing one of the color-coded disks presented in the periphery via a button press. See Wu et al. (2019) for an oculomotor variant of the task.

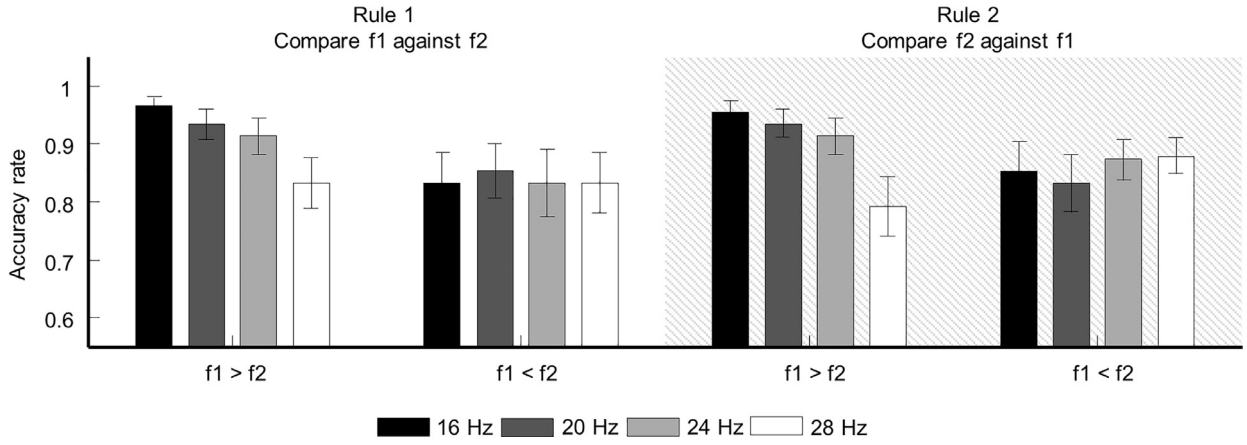

Fig. 2. Behavioral performance. The bar plots show the mean accuracy rates across participants over all runs for different stimulus orders, rules, and f1 magnitudes. Error bars represent 95% confidence intervals (CIs) of the means.

each stimulus pair was presented eight times, each time with a unique combination between rule cues (diamond vs. square), matching cues (upward-pointing vs. downward-pointing triangles), and target screens (blue-left, yellow-right vs. yellow-left, blue-right). This yielded a total of 64 trials per run, which were presented in a randomized order. Furthermore, the association between visual symbols and task rules as well as between target colors and match reports was counterbalanced across participants.

2.3. FMRI data acquisition

The fMRI data were obtained with a 3 T Tim Trio MRI scanner (Siemens, Erlangen, Germany) equipped with a 12-channel head coil at the Center for Cognitive Neuroscience Berlin. Functional volumes sensitive to the BOLD signal were acquired using a T2* weighted echo planar imaging sequence (TR = 2000 ms, TE = 30 ms, field of view = 192 mm, flip angle = 70°). Each volume consisted of 37 axial slices and was acquired in an ascending order (64 × 64 in-plane, 3 mm isotropic with 0.6 mm gaps between slices). 378 functional volumes were obtained in each experimental run. In addition to the six experimental runs, a T1 weighted structural volume was acquired for co-registration and spatial normalization purposes using a 3D MPRAGE sequence (TR = 1900 ms, TE = 2.52 ms, 256 × 256 in-plane, 1 mm isotropic).

2.4. Data preprocessing and analyses

FMRI data preprocessing and general linear model estimation (GLM) were performed with SPM12 version 6685 (www.fil.ion.ucl.ac.uk/spm) and custom MATLAB scripts (https://github.com/yuanhaowu/DecodingAbstractChoices) while multivariate decoding analyses were performed using The Decoding Toolbox version 3.991 (Hebart, Goergen and Haynes, 2015; https://sites.google.com/site/tdtdecodingtoolbox/). During the preprocessing, functional volumes were corrected for slice acquisition time differences and spatially realigned to the mean functional volume.

2.4.1. Decoding choices

The focus of the present study was to identify brain regions that carry information about choice-related information independent of stimulus order and selection of specific manual response. To this end, we used MVPA combined with a whole-brain searchlight routine to pinpoint

brain regions that show distinguishable local activity patterns between different choices during the decision phase.

We first obtained run-wise beta estimates for choice-related activity during the decision phase for each voxel. We fitted a GLM (192 s high-pass filter) to each participant's data. Separate impulse regressors were defined to model the two choices ('higher' vs. 'lower'), convolved with the canonical hemodynamic response function at the onset of the decision phases. To minimize the number of potential indecisions during decision phases, only correctly answered trials were modelled. Incorrectly answered and missed trials were modelled with a separate regressor of non-interest and not included in the subsequent MVPA. In addition, six movement parameters, the first five principal components explaining variance in the white matter and cerebrospinal fluid signals respectively (Behzadi et al., 2007), and a run constant were added as nuisance regressors, culminating in a total of 120 parameter estimates per participant (20 × 6 runs).

To identify brain regions that exhibit choice-selective activity patterns, a searchlight MVPA was performed on each participant's data using linear support vector machine classifiers (SVM) in the implementation of LIBSVM 2.86 (Chang and Lin, 2011) with a fixed cost parameter of $c = 1$. We generated a 4-voxel radius spherical searchlight and moved it voxel-by-voxel through the entire measured volume. The searchlight was centered on each voxel in turn and comprised a maximum of 251 voxels (note that searchlights with 3 and 5 voxel radii yielded similar results). At each brain location, run-wise beta estimates for each of the two choice regressors extracted from voxels within the searchlight formed the 12 response patterns (2 conditions x 6 runs) for the decoding analysis. To avoid overfitting, we estimated the classifier's decoding accuracy using a leave-one-run-out cross-validation routine. That is, we iteratively trained the classifier to distinguish between response patterns corresponding to participant's choices with data from five runs and tested how well the classifier predicted participant's choices based on response patterns in the remaining run. This procedure was repeated until all runs were used as the test set. The decoding accuracy of the classifier was estimated as the number of correct predictions divided by the total number of predictions. Decoding accuracy resulting from the searchlight analysis around a given voxel was stored at the corresponding location of a whole-brain volume before the searchlight moved to the next voxel. The searchlight analysis was applied to all voxels in the measured volume so that a continuous whole-brain accuracy map could be obtained. For each voxel in the measured volume, the resulting accuracy map displayed the extent to which the multivariate signal in the local spherical neighborhood was selective for choices. Notably, due to the use of a balanced design, different perceptual choices were expected to have approximately the same number of trials associated with each stimulus order and motor response. That is, each choice regressor contained roughly the same amount of information about stimulus order and button press. Thus, choice-selective activity detected during the decision phase would be unlikely to result from the physical properties of stimulus order or planning of button press responses.

For the group inference, each participant's accuracy map was transformed to MNI space, resampled to 2 × 2 × 2 mm^3 voxel size, and smoothed with a 3 mm full width at half maximum Gaussian filter. The transformed maps were submitted to a group, one-tailed, one-sample *t*-test to assess whether the decoding accuracy at any voxel was significantly higher than chance level (50%). Thus, a voxel with significant above-chance decoding accuracy would indicate that the local activity pattern around that voxel carries information about choices.

2.4.2. Behavioral control analyses

By virtue of the balanced experimental design, the implemented variant of the vibrotactile frequency discrimination task has proven to be capable of disentangling choice-related activity from that related to stimulus order and selection of a specific action (Wu et al., 2019). However, it remains possible that the classifier could exploit the subtle difference in the distributions of the two stimulus orders (f1 > f2 vs. f1 < f1) or motor responses (left vs. right button press) between choice conditions to achieve above-chance decoding accuracy (Görgen et al., 2018; Hebart and Baker, 2018). This is of particular relevance for the present study as the balanced number of trials across conditions might not hold after the exclusion of incorrectly answered trials and have a biasing effect on MVPA on fMRI data. To address this concern, we applied the same decoding analysis pipeline for neuroimaging data to behavioral data, which enabled us to directly test whether choices can be predicted based on the number of trials associated with different stimulus orders and motor responses within each choice.

For each of the variables of interest, we performed an independent analysis with the following procedure: For each choice in each run, we generated a two-dimensional vector using the number of trials associated with different variable levels. For instance, if a participant responded 15 times with a left and 17 times with a right button press to indicate a comparison stimulus of higher frequency, it was coded as [15 17]. The remainder of the analysis proceeded in a manner analogous to the fMRI data analysis pipeline. Twelve data vectors (2 choices x 6 runs) were used to predict participant's choices in a decoding analysis with a leave-one-run-out cross-validation routine. For the group inference, we used one-tailed Wilcoxon sign rank tests to probe the statistical significance against chance accuracy (50%). Significant results would imply potential confounds due to the biased distributions of stimulus orders or/and motor responses.

2.4.3. Neuroimaging control analysis

As informative clusters identified in the main fMRI analysis include brain regions typically implicated in the planning and execution of manual movements (see result), we did an additional analysis on the fMRI data to test whether the result might be driven by specific action selection. We repeated the searchlight choice decoding analysis 100 times for each participant. In each repetition, we randomly sampled a subset of trials so that the number of trials associated with the left and right button presses was fully balanced across choices and runs. We then performed the same GLM and searchlight analysis as described above on a subset of data to obtain a decoding accuracy map per repetition, yielding a total of 100 accuracy maps per participant. The within-participant averaged accuracy maps were then forwarded to a group level *t*-test to identify brain regions that carry choice-related information. Importantly, by keeping the number of left and right button presses balanced across choices and runs, this analysis eliminated potential confounds related to motor planning. If informative clusters reported in the main result were mainly driven by motor planning rather than by choices, we would not expect choice-related information in the reported regions. Reversely, a similar pattern of informative clusters would strengthen the result of the main analysis.

3. Results

3.1. Behavior

The overall behavioral performance of participants during the scanning session was highly accurate (Fig. 2). The average accuracy rate was 0.881 (SD: 0.057; range: 0.778 – 0.99), while the average reaction time (latencies between the onsets of the target screens and button presses) was 0.554 s (SD: 0.104, range: 0.359 – 0.77).

We further examined participants' behavioral accuracies and reaction times with three-way repeated measure ANOVAs with task rule (compare f1 against f2 vs. f2 against f1), stimulus order (f1 > f2 vs. f1 < f2), and f1 frequency (16 Hz, 20 Hz, 24 Hz, and 28 Hz) as within-subject factors, respectively. For the behavioral accuracy, there was no task rule effect observable ($F(1,26) = 1.663$, $p = 0.209$). The performance remained stable regardless of which particular rule was applied, suggesting that the cognitive demands were equivalent across rules. In addition, we observed a significant effect of stimulus order ($F(1, 26) = 7.749$, $p = 0.001$), with a slightly better performance in f1 > f2 trials than in

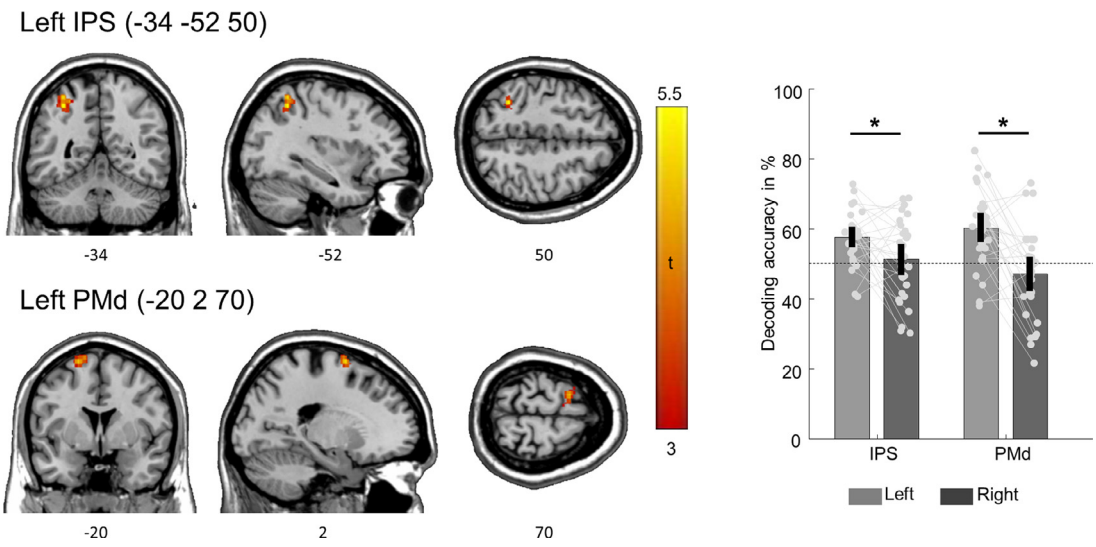

Fig. 3. FMRI decoding results. The left IPS and the PMd were found to carry choice-related information independent of stimulus order and ensuing button press, contralateral to the response effector (pFDR < 0.05, cluster corrected for multiple comparisons). Coordinates refer to MNI space and indicate the peak voxel of each region respectively. The unthresholded statistical map can be inspected at https://www.neurovault.org/images/256,861/.The bar plot shows decoding accuracies at the reported peak voxels and at the equivalent positions in the right hemisphere, ipsilateral to the response effector. Error bars represent 95% CIs of the means, while dots indicate individual participants' decoding accuracies in each brain region. Asterisks indicate statistically significant differences between hemispheres at $p < 0.05$, Holm corrected for multiple comparisons. Participant-specific decoding accuracy maps are available at https://doi.org/10.6084/m9.figshare.9920111.v2.

f1 < f2 trials ($mean_{f1>f2} = 0.911$, $mean_{f1<f2} = 0.851$, $CI_{95} = [0.0166\ 0.1035]$). Moreover, there was a significant interaction between stimulus order and f1 frequency ($F(3, 78) = 11.239$, $p < 0.001$). As indicated by linear trend analyses, participants' performance decreased slightly with an increasing f1 in f1>f2 trials (slope = −0.0113, $p < 0.001$), while the performance was unaffected by f1 frequency in f1 < f2 trials (slope = 0.003, $p = 0.233$). Contrary to the behavioral accuracy, we did not reveal any difference in reaction times between conditions (all $p > 0.05$).

Considering the possibility that response biases and the exclusion of incorrect trials from fMRI analysis may cause differences in stimulus order and motor response distributions between choices and thereby distort the outcome of the fMRI analysis, we performed Pearson chi-square tests on data included in the fMRI analysis, for each participant respectively. The tests did not reveal significant differences in the distribution of stimulus orders and motor responses between choices in any of the participants (all $p > 0.1$, uncorrected), suggesting that participants' choice behavior included in the fMRI analysis was not biased by the stimulus order or motor response.

In addition, the same decoding analysis routine as used for the fMRI data was performed to test whether the numbers of trials associated with different stimulus orders and motor responses were predictive of choices. As the results of one-sided, one-tailed Wilcoxon sign rank tests show, neither stimulus order nor motor response was predictive of choices (all $p > 0.05$, Holm corrected).

Collectively, there is no evidence from our behavioral analyses indicating that the fMRI results reported below were confounded by the physical properties of the stimulus order and selection of the ensuing motor responses.

3.2. Neuroimaging results

The main objective of the present study was to identify brain regions that carry information about categorical choice independent of the physical properties of stimulus orders and selection of the ensuing manual responses during vibrotactile comparisons. Using whole-brain searchlight MVPA, we tested for brain regions exhibiting distinguishable local activity patterns between choices during the 2 s decision phase. The result of the whole-brain searchlight analysis is shown in Fig. 3 (displayed at $p < 0.05$, FDR corrected for multiple comparisons at the cluster level with a cluster-defining voxel-wise threshold of $p < 0.001$). We were able to decode perceptual choices from the intraparietal sulcus (IPS, mainly in area hIP3; cluster size = 130, peak voxel: [−34 −52 50], t26 = 5.115, mean decoding accuracy at the peak = 57.737%, CI95 = [54.628% 60.847%]) and the dorsal premotor cortex (PMd, BA 6) in the left hemisphere, contralateral hemisphere to the response effector (cluster size = 109, peak voxel: [−20 2 70], t26 = 4.864, mean decoding accuracy = 60.504%, CI95 = [56.066% 64.943%). To test whether choices are indeed represented in a lateralized manner, we conducted two-sided paired t-tests between decoding accuracies extracted from the identified peak voxels and those extracted from the corresponding locations in the right hemisphere (right panel in Fig. 3). These tests show that decoding accuracies extracted from the identified peak voxels were significantly higher than those in the right hemisphere, ipsilateral to the response effector (IPS: t26 = 2.413, $p = 0.002$, CI95 = [0.928% 11.619%]; PMd: t26 = 4.43, $p < 0.001$, CI95 = [7.137% 19.467%]), corroborating the lateralized representation of choice-related information.

We were further interested in whether decoding accuracies in the reported regions predicted behavioral performance. To this end, we estimated the Pearson correlation between the decoding accuracy and behavioral performance. We were not able to find statistical evidence for such a linkage between them in any of the reported regions (IPS: rho = 0.089, $p = 0.659$; PMd: rho = −0.016, $p = 0.938$).

Importantly, the pattern of informative clusters at the group level remains similar across different searchlight radii. We performed the same MVPA with searchlight radii of 3 – 5 voxels and found that locations of significant informative clusters remain centered in the left IPS and PMd (Fig. 4). Moreover, results of two-sided paired t-tests between all possible pairs showed that decoding accuracies do not differ across searchlight radii (all $p > 0.05$, Holm corrected).

We performed an additional decoding analysis to explore whether the identified brain regions with significant above-chance decoding accuracies may result from a bias toward a particular choice-response association. We repeated the searchlight choice decoding analysis and eliminated the potential motor-related confound by keeping the left and right button presses balanced across choices and runs. This analysis yielded a highly similar pattern of brain regions carrying choice-related information as in the main analysis. As shown in Fig. 5 (reported at

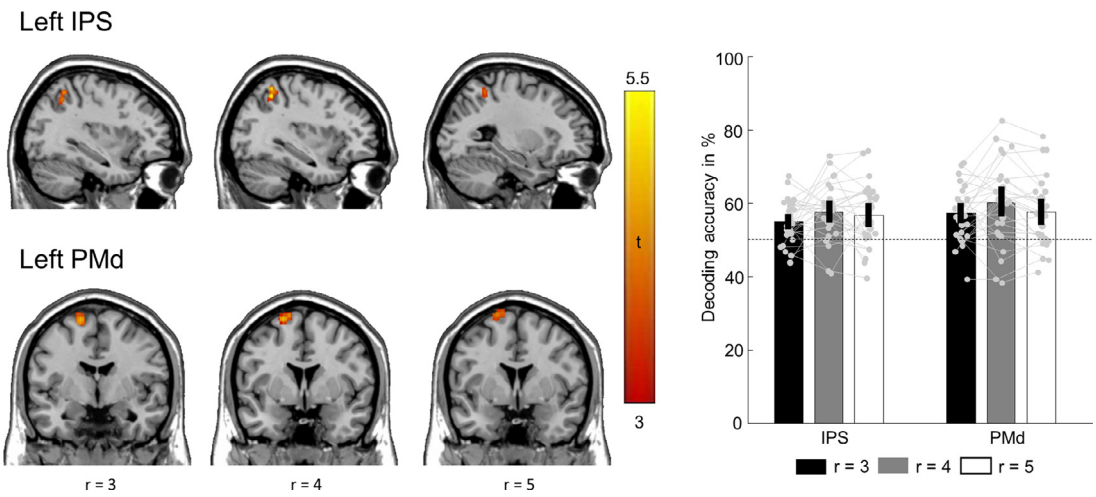

Fig. 4. FMRI decoding results using three different searchlight radii. The left panel depicts the informative clusters (one column for each radius, indicated by r). Bar plot in the right panel displays decoding accuracies at peak voxels of the IPS and PMd clusters for each radius respectively. The unthresholded statistical maps are available at https://www.neurovault.org/collections/5936/. Error bars indicate 95% CIs of the means. Gray dots and lines represent individual participants' decoding accuracies.

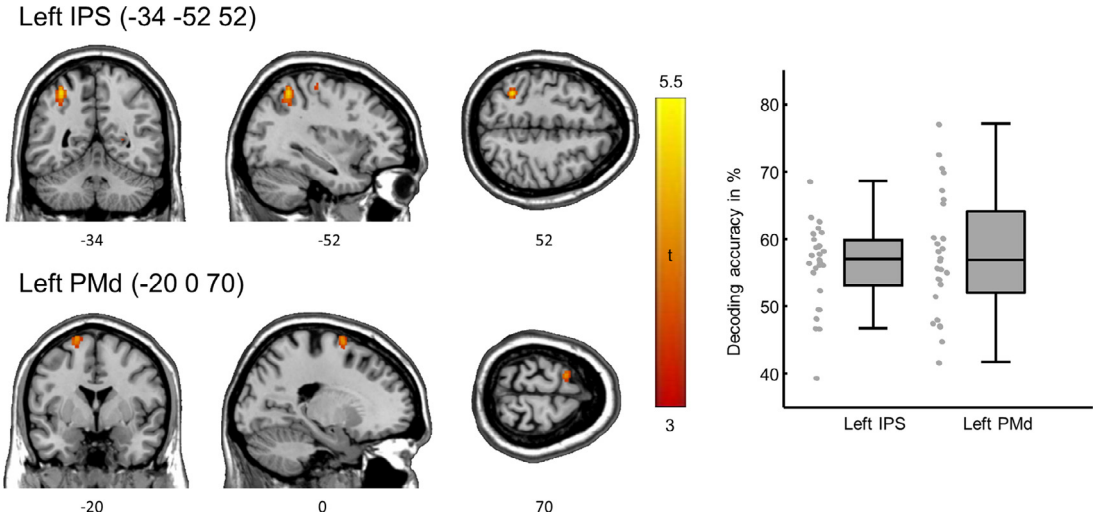

Fig. 5. FMRI control analysis result. The left panel displays significant clusters detected by the analysis controlling for motor-related confounds (displayed at $p < 0.001$, uncorrected). The unthresholded statistical map is available at https://www.neurovault.org/images/256,864/.The right panel shows box plots for IPS and PMd separately. Box edges indicate the 25th and 75th percentiles, central horizontal lines correspond to the median. Gray dots represent individual participants' decoding accuracies.

$p < 0.001$ uncorrected due to significantly reduced amount of data as compared to the main analysis), choice-related information was again found in the left IPS ([−34 −52 52], $t_{26} = 5.173$, cluster size = 128, mean = 56.157%, CI_{95} = [53.711% 58.603%]) and in the left PMd ([−20 0 72], $t_{26} = 4.443$, cluster size = 76, mean = 57.662%; CI_{95} = [54.117% 61.207%]). Altogether, the results of both behavioral and neuroimaging control analyses suggest that the main results were not driven by motor-related confounds.

Next, we compared the result of the present study with that of our previous study, in which decisions were communicated with saccades, instead of button presses (Wu et al., 2019, $n = 30$). Similar to the present study, choice-selective activity was found in premotor and intraparietal regions, with the difference that it was evident in both hemispheres. The previous study also reported choice-selective activity in the left prefrontal cortex (PFC), while it was absent in the current study. Notably, although both studies identified premotor and intraparietal regions as carrying choice-related information, there were no overlapping clusters. In particular, the premotor clusters identified in the previous study were located at the junction of precentral gyri and the caudal-most part of the superior frontal sulci ($peak_{left}$: [−32 10 62], $peak_{right}$: [34 4 52]), commonly referred to as the FEF (determined with the probabilistic maps by Wang et al., 2015; www.princeton.edu/~napl\vtpm.htm). In contrast, the premotor cluster detected in the current study lies in the adjacent PMd (−20 0 72), dorsocaudal to the FEF (determined with the SPM Anatomy toolbox version 3; Eickhoff et al., 2005), hinting that the location of choice-related information might shift between regions specialized for eye and hand movements depending on which response effector is used.

To further assess this possibility, we ran a set of regions of interest (ROI) analyses. First, we took the peak voxels in the bilateral FEF from the previous study as the ROI for the current data. For each participant, we extracted decoding accuracies from these voxels and averaged them. The averaged decoding accuracies were then submitted to a one-tailed, one-sample *t*-test against the chance level. Likewise, we used the peak voxel of the PMd cluster from the present study as the ROI for the previous study and tested whether choices could be reliably decoded from

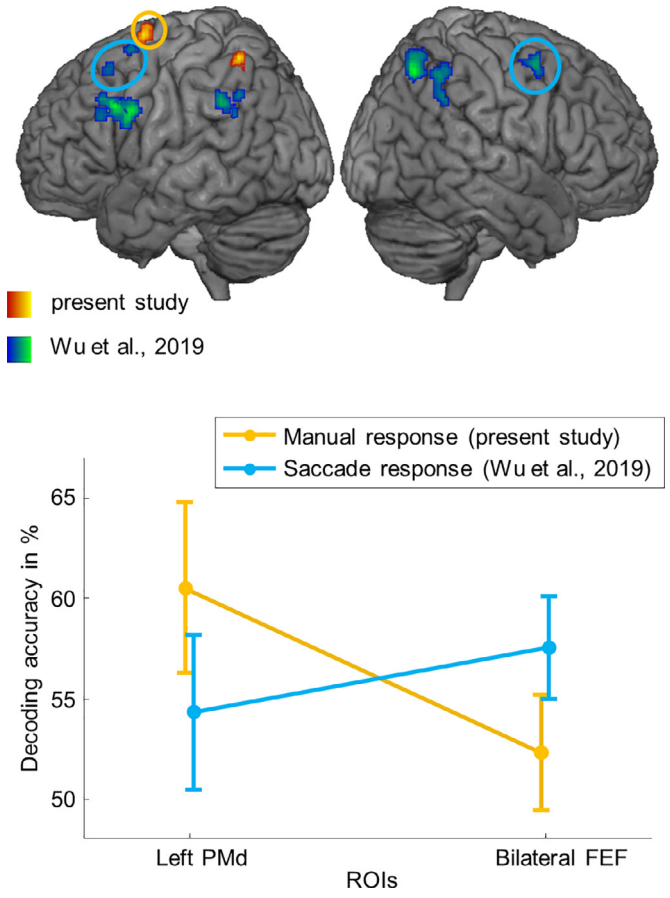

Fig. 6. Comparison with results from the saccade version of the task (Wu et al., 2019, n = 30). The upper panel displays brain regions carrying choice-related information as identified in the present study (in red-orange) and those detected in our previous work using saccades as decision reports (in blue-green, unthresholded statistical map available at https://www.neurovault.org/images/63,793/), both displayed at pFDR < 0.05, cluster corrected. The circles indicate the premotor and intraparietal clusters used for ROI analysis. The lower panel depicts mean decoding accuracies across participants collapsed across response modalities and effector-specific regions. Error bars indicate 95% CIs of the means.

the PMd. The results of these ROI analyses support the interpretation of an effector-dependent shift of choice representation within the premotor cortex (Fig. 6). Despite the higher sensitivity of ROI approach, the mean decoding accuracy computed from the bilateral FEF in the present study did not surpass the chance level (t_{26} = 1.534, mean = 52.272%; CI_{95} = [50.772% 55.315%], p = 0.137). Likewise, the mean decoding accuracy in the left PMd derived from the previous study did not differ significantly from the chance level (t_{29} = 2.172, mean = 54.301%; CI_{95} = [50.250% 58.352%], p = 0.076, Holm corrected). That is, when a manual response was used, the choice could only be reliably decoded from the left PMd, but not from the FEF. Conversely, the choice could only be read out from the FEF, but not from the PMd, when a saccadic response was required (Fig. 6).

4. Discussion

In the present study, we sought to identify human brain regions that represent categorical choices in the context of vibrotactile frequency comparisons. We used fMRI combined with a variant of the vibrotactile frequency discrimination task which allowed us to dissociate choice-selective BOLD signals from those related to the physical properties of stimulus orders and selection of specific manual responses. We identified the left IPS and PMd, contralateral to the response effector, as carrying choice-related information. With this result, we replicated the finding from our previous work using the same task, but with saccades as response effector (Wu et al., 2019). However, the informative premotor clusters identified with the previous oculomotor variant of the task were centered in the bilateral FEF rather than in the left PMd. Thus, the results of both studies suggest a response modality-specific organization of categorical choice representations for vibrotactile comparisons in humans.

The pivotal role of the premotor cortex in decision formation during vibrotactile comparisons has been established by the seminal work of Romo and colleagues using neurophysiological recordings in monkeys (reviewed in Romo and de Lafuente, 2013). The premotor cortex is strongly implicated in the computation of comparisons between the two sequentially presented stimuli, based on the consistent observation of choice-predictive signals before the initiation of manual responses (Hernández et al., 2002, 2010). In line with these reports, we identified the dorsal part of the premotor cortex as carrying choice-related information, with the crucial difference that choices in the present study were independent of stimulus order and selection of specific manual movements, while those in the above-mentioned monkey neurophysiological studies were inextricably linked with them. Taking this into account, the finding of such choice representations in a region that is primarily associated with the planning and preparation of manual actions may not appear straightforward. Indeed, results from a few human fMRI studies in the visual domain, wherein perceptual choices were disentangled from specific actions, are inconsistent. On the one hand, several studies failed to find evidence for decision-related BOLD signals in the premotor cortex when choices were decoupled from actions (e.g., Hebart et al., 2012; Filimon et al., 2013). On the other hand, premotor activity reflecting categorical choices regarding the stimulus identity independent of motor planning has been shown in other human fMRI studies (e.g., Hebart et al., 2014). With this study, we provide additional fMRI evidence for human premotor involvement in the representation of categorical choices which cannot be merely attributed to specific action selection.

Hereof, it is important to note that the analysis we used in the present study does not permit an inference about whether vibrotactile choices are indeed encoded in the PMd or generated elsewhere. Independent of whether this is the case, one possible explanation for our premotor finding is that the PMd serves as a node for short-term storage of categorical choice representations and its transformation into commands for concrete manual movements once all information required for the execution of specific actions are known. In other words, choice-related information in the PMd can be regarded as an instruction cue that needs to be maintained throughout the entire decision phase to enable the flexible association between the succeeding visual matching cues, spatial targets, and button presses (see Hoshi and Tanji, 2007; Wu et al., 2019). This interpretation agrees with a recent study showing a causal role of the premotor cortex in the flexible stimulus-response mapping in mice (Wu et al., 2020) and monkey neurophysiological studies implicating the PMd in the retrieval and integration of task-relevant information necessary for specification of particular actions (e.g., Nakayama et al., 2008; Yamagata et al., 2009, 2012).

While there is a vast amount of neurophysiological evidence for premotor involvement during vibrotactile comparisons, neural activities in the posterior parietal cortex (PPC) has remained largely unexplored in this context. Nevertheless, our finding of intraparietal choice representation was not surprising. Similar to the premotor area, posterior parietal regions are thought to be crucially involved in various decision-making tasks, most prominently when decisions are communicated by saccades (Gold and Shadlen, 2007). In particular, activity in the monkey LIP (homologous to the intraparietal subregions in humans) has been shown to mimic the presumed evidence accumulation toward one or the other saccade choices and thereupon regarded as the explicit neural representation of the evolving decisions (Shadlen and Kiani, 2013; but see

Huk et al., 2017 for a critical review). Moreover, evidence from recent studies on a wide range of decision-making tasks suggests that PPC's involvement is not confined to motor decisions but pertains to decisions at different levels of abstraction. For instance, both monkey and human PPC have been shown to represent choices that were independent of the planning of saccade responses (Bennur and Gold, 2011; Hebart et al., 2012). Among studies in the broader context of decision making, findings from monkey neurophysiological recordings using visual categorization tasks are particularly revealing (reviewed in Freedman and Assad, 2016). In these studies, monkeys were trained to perform delayed match-to-category tasks in which they decide whether the motion direction of the sample stimulus and the test stimulus belong to the same category based on a previously learned, arbitrarily defined boundary. After the test stimulus, monkeys indicated their decision on a match or mismatch with manual or saccadic responses. Using this task, LIP has been shown to exhibit signals reflecting the categorical choice which cannot be attributed to specific sensory stimulus properties nor action selection (Freedman and Assad, 2006; Swaminathan and Freedman, 2012; Swaminathan et al., 2013). Such categorical information is reminiscent of the choice-related information observed in our study as both are dissociated from the physical properties of stimuli as well as the selection of manual movements and are thus, represented at a similar level of abstraction. The similarity between them opens the possibility of a common mechanism and thereby boosts the notion of the PPC, and IPS more specifically, as a central node mediating cognitive computations (Freedman and Assad, 2016).

Given the above-mentioned functions ascribed to the PPC, one question which emerges from our results is whether the reported choice-related information is directly computed in the PPC via an evidence accumulation process or other mechanisms. Given our experimental design, we are not able to answer this question. In this study, we only used stimulus pairs with supra-threshold differences to facilitate the decodability of choice-related information. This is, however, problematic for assessing neural correlates of evidence accumulation as they would, according to the accumulation-to-bound model (Ratcliff et al., 2016), provide strong momentary evidence signals which are difficult to distinguish as such. As for the premotor cortex, it is possible that the IPS merely receives choice-related signals from elsewhere in the brain and thus, is not actively involved in the decision formation. However, there is evidence from several lines of research that warrants the IPS being a promising candidate region for decision formation during vibrotactile comparisons.

First, vibrotactile comparisons as implemented in the present study can be regarded as a process in which a choice is made based on the relation between two magnitudes. Combined evidence from monkey neurophysiology and human neuroimaging suggests that magnitudes and the relation between them are encoded by a network comprising the IPS and lateral PFC (Jacob, Vallentin and Nieder, 2012). Moreover, the IPS appears to be the first region within this network to process magnitude information (reviewed in Nieder, 2016). Second, Herding et al. (2019) showed that the centro-parietal positivity (CPP) in EEG signal, which has been suggested as a proxy for accumulated evidence across a variety of decision-making tasks (O'Connell et al., 2012; Kelly and O'Connell, 2013), also indexes the amount of sensory evidence during vibrotactile comparisons. More specifically, they identified the left IPS as the likely source of the CPP component reflecting the signed subjectively perceived difference between two frequencies. Notably, in this study, participants always compared f2 against f1. It would be interesting to explore whether and how this effect is modulated by comparisons in the reversed direction. Finally, using a reversible inactivation approach to investigate PPC's contribution to sensory evaluation and action selection, Zhou and Freedman (2019) revealed that monkeys' decisions were more severely affected when visual stimuli, rather than motor targets, were placed in the inactivated receptive fields of LIP neurons under investigation, providing compelling evidence for the causal role of the PPC in the sensory aspect of visual decisions. Given that the IPS is thought to have a similar role as a mediating node in the sensorimotor transformation across multiple sensory domains, it is intriguing to see whether a causal effect could also be demonstrated during vibrotactile comparisons.

With the present finding of premotor and intraparietal choice-selectivity, we have also replicated the finding of our previous study using the same task but with saccades as the response modality (Wu et al., 2019). When comparing both studies more closely, two differences are apparent. First, choice-related information was found in bilateral premotor and intraparietal regions when saccades were used. However, when manual responses were required, the premotor and intraparietal selectivity was only evident in the contralateral hemisphere. Moreover, we observed a relocation of choice-related information within the premotor area from the FEF to the PMd. Importantly, we did not assign these functional labels merely based on the response modalities required in the tasks. Both the FEF and the PMd were determined by means of well-established functional probability maps. In addition, the spatial arrangement of the FEF and the PMd clusters as identified by the spatially unbiased whole-brain searchlight routines in these two studies corresponds well to that reported in monkeys (e.g. Petrides, 1982; Halsband and Passingham, 1982; Bruce and Goldberg, 1985) and humans (Amiez et al., 2006), with saccade-related premotor region lying more anterior and ventral to premotor region exhibiting activities related to manual movements. It is unlikely that these differences were merely a by-product of idiosyncratic differences between samples. Rather, the results from these two studies suggest that categorical choice information during vibrotactile comparisons are represented in a response modality-dependent manner.

Intriguingly, our findings contrast with those derived from a number of human fMRI studies in the visual system using multiple response effectors (e.g., Heekeren et al., 2006; Ho et al., 2009; Liu and Pleskac, 2011; Filimon et al., 2013). These studies were able to identify brain regions showing decision-related BOLD signals in an effector-independent manner and implied the existence of a central decision-making hub in the brain, although with a wide variation of candidate brain regions across studies (e.g., the dorsolateral prefrontal cortex, insula, IPS, or inferior prefrontal sulcus). This discrepancy could be partially due to the methodological differences in disentangling decision-related from motor-related signals: The current study relied on a balanced experimental design and a multivariate technique that is sensitive to information encoded combinatorially in brain activity patterns. In contrast, the above-mentioned fMRI studies identified decision-related signals by elongating stimulus-response latencies while making specific assumptions about how sensory evidence is reflected in the average brain activity. Another possible, more intriguing reason for the discrepancy is that the response modality-dependent organization of choice information is confined to a specific level of abstraction. For instance, the dependency observed in our studies may result from the explicit foreknowledge of the required response effector, while such foreknowledge was lacking in some of the above-mentioned studies from the visual domain (Liu and Pleskac, 2011; Filimon et al., 2013). Taking this into account, one conceivable explanation for our findings is that effector-specific regions may only take over the computations of categorical choices, or at least reflect the outcomes of those computations before the actual action selection, if the response effector for decision reports is predictable to the observer. In addition, it is important to note that the above-mentioned studies in the visual system and our studies aimed at different types of decision-related BOLD signals. Using an univariate activation-based approach, the above-mentioned studies in the visual system targeted brain regions that represent the decision formation via sensory evidence accumulation, while we employed a multivariate approach to identify brain regions that carry information about the categorical outcomes of any potential computations. Thus, it raises the possibility that the computation of categorical choices during vibrotactile comparisons and sensory evidence accumulation in visual system are accommodated by different mechanisms.

In conclusion, our studies have shown that premotor and intraparietal regions carry information about categorical choice independent of stimulus order and specific action selection during vibrotactile comparisons. The results suggest that, when the response effector is prespecified, categorical choice information is represented in a response modality-dependent manner, with the PMd carrying information about categorical choices that are communicated by the manual movements and the FEF when saccades are utilized. Yet, it remains elusive whether such categorical choices are indeed computed in the identified regions and whether the modality-dependent organization holds when the required response effector is unpredictable. In this light, future studies combining a wide range of response modalities, response options for each effector, and task difficulties will provide essential insights into how categorical choices are computed and represented in different contexts.

Declaration of Competing Interest

The authors declare no competing financial interests.

Acknowledgments

This research was supported by the Deutsche Forschungsgemeinschaft (DFG) – project number 409180874. We thank Pia Schröder for many inspiring discussions and Sam Gijsen for proof reading a previous version of the manuscript.

Author contributions

Y.W. and F.B. designed the experiment and interpreted the results. Y.W. and L.A.V. conducted the experiment, Y.W. analyzed the data and wrote the manuscript. L.A.V. and F.B. reviewed and edited the manuscript.

Data and code availability statement

In accordance with EU's General Data Protection Regulation we are unable to share raw fMRI data. However, single subject decoding accuracy maps can be inspected on figshare (https://doi.org/10.6084/m9.figshare.9920111.v2) and group-level statistical maps are available at https://www.neurovault.org/collections/5936/. Furthermore, analysis codes have been uploaded to Github (https://github.com/yuanhaowu/DecodingAbstractChoices).

Supplementary materials

Supplementary material associated with this article can be found, in the online version, at doi:10.1016/j.neuroimage.2020.117592.

References

Amiez, C., Kostopoulos, P., Champod, A., Petrides, M., 2006. Local morphology predicts functional organization of the dorsal premotor region in the human brain. J. Neurosci. 26, 2724–2731. doi:10.1523/JNEUROSCI.4739-05.2006.

Behzadi, Y., Restom, K., Liau, J., Liu, T.T., 2007. A component based noise correction method (CompCor) for BOLD and perfusion based fMRI. Neuroimage 37, 90–101. doi:10.1016/j.neuroimage.2007.04.042.

Bennur, S., Gold, J.I., 2011. Distinct representations of a perceptual decision and the associated oculomotor plan in the monkey lateral intraparietal area. J. Neurosci. 31, 913–921. doi:10.1523/JNEUROSCI.4417-10.2011.

Brainard, D.H., 1997. The psychophysics toolbox. Spat. Vis. 10, 433–436. doi:10.1163/156856897x00357.

Bruce, C.J., Goldberg, M.E., 1985. Primate frontal eye fields. I. Single neurons discharging before saccades. J. Neurophysiol. 53, 603–635. doi:10.1152/jn.1985.53.3.603.

Chang, C.-C., Lin, C.-J., 2011. LIBSVM. ACM Trans. Intell. Syst. Technol. 2, 1–27. doi:10.1145/1961189.1961199.

Cisek, P., Kalaska, J.F., 2010. Neural mechanisms for interacting with a world full of action choices. Annu. Rev. Neurosci. 33, 269–298. doi:10.1146/annurev.neuro.051508.135409.

Ding, L., Gold, J.I., 2012. Neural correlates of perceptual decision making before, during, and after decision commitment in monkey frontal eye field. Cereb. Cortex 22, 1052–1067. doi:10.1093/cercor/bhr178.

Eickhoff, S.B., Stephan, K.E., Mohlberg, H., Grefkes, C., Fink, G.R., Amunts, K., Zilles, K., 2005. A new SPM toolbox for combining probabilistic cytoarchitectonic maps and functional imaging data. Neuroimage 25, 1325–1335. doi:10.1016/j.neuroimage.2004.12.034.

Freedman, D.J., Assad, J.A., 2006. Experience-dependent representation of visual categories in parietal cortex. Nature 443, 85–88. doi:10.1038/nature05078.

Filimon, F., Philiastides, M.G., Nelson, J.D., Kloosterman, N.A., Heekeren, H.R., 2013. How embodied is perceptual decision making ? Evidence for separate processing of perceptual and motor decisions. J. Neurosci. 33, 2121–2136. doi:10.1523/JNEUROSCI.2334-12.2013.

Freedman, D.J., Assad, J.A., 2016. Neuronal mechanisms of visual categorization: an abstract view on decision making. Annu. Rev. Neurosci. 39, 129–147. doi:10.1146/annurev-neuro-071714-033919.

Gold, J.I., Shadlen, M.N., 2007. The neural basis of decision making. Annu. Rev. Neurosci. 30, 535–574. doi:10.1146/annurev.neuro.29.051605.113038.

Görgen, K., Hebart, M.N., Allefeld, C., Haynes, J.D., 2018. The same analysis approach: practical protection against the pitfalls of novel neuroimaging analysis methods. Neuroimage 180, 19–30. doi:10.1016/j.neuroimage.2017.12.083.

Halsband, U., Passingham, R., 1982. The role of premotor and parietal cortex in the direction of action. Brain Res. 240, 368–372. doi:10.1016/0006-8993(82)90239-6.

Heekeren, H.R., Marrett, S., Ruff, D.A., Bandettini, P.A., Ungerleider, L.G., 2006. Involvement of human left dorsolateral prefrontal cortex in perceptual decision making is independent of response modality. Proc. Natl. Acad. Sci. U.S.A. 103, 10023–10028. doi:10.1073/pnas.0603949103.

Hebart, M.N., Baker, C.I., 2018. Deconstructing multivariate decoding for the study of brain function. Neuroimage 180, 4–18. doi:10.1016/j.neuroimage.2017.08.005.

Hebart, M.N., Donner, T.H., Haynes, J.D., 2012. Human visual and parietal cortex encode visual choices independent of motor plans. Neuroimage 63, 1393–1403. doi:10.1016/j.neuroimage.2012.08.027.

Hebart, M.N., Goergen, K., Haynes, J.-.D., 2015. The decoding toolbox (TDT): a versatile software package for multivariate analyses of functional imaging data. Front. Neuroinform. 8, 1–18. doi:10.3389/fninf.2014.00088.

Hebart, M.N., Schriever, Y., Donner, T.H., Haynes, J.-.D., 2014. The relationship between perceptual decision variables and confidence in the human brain. Cereb. Cortex BHU 181. doi:10.1093/cercor/bhu181.

Herding, J., Ludwig, S., Blankenburg, F., 2017. Response-modality-specific encoding of human choices in upper beta band oscillations during vibrotactile comparisons. Front. Hum. Neurosci. 1, 11. doi:10.3389/fnhum.2017.00118.

Herding, J., Ludwig, S., von Lautz, A., Spitzer, B., Blankenburg, F., 2019. Centro-parietal EEG potentials index subjective evidence and confidence during perceptual decision making. Neuroimage 201, 116011. doi:10.1016/j.neuroimage.2019.116011.

Herding, J., Spitzer, B., Blankenburg, F., 2016. Upper beta band oscillations in human premotor cortex encode subjective choices in a vibrotactile comparison task. J. Cogn. Neurosci. 28, 668–679. doi:10.1162/jocn_a_00932.

Hernández, A., Nácher, V., Luna, R., Zainos, A., Lemus, L., Alvarez, M., Vázquez, Y., Camarillo, L., Romo, R., 2010. Decoding a perceptual decision process across cortex. Neuron 66, 300–314. doi:10.1016/j.neuron.2010.03.031.

Hernández, A., Zainos, A., Romo, R., 2002. Temporal evolution of a decision-making process in medial premotor cortex 33, 959–972.

Ho, T.C., Brown, S., Serences, J.T., 2009. Domain general mechanisms of perceptual decision making in human cortex. J. Neurosci. 29, 8675–8687. doi:10.1523/JNEUROSCI.5984-08.2009.

Horwitz, G.D., Newsome, W.T., 1999. Separate signals for target selection and movement specification in the superior colliculus. Science 284, 1158–1161. doi:10.1126/science.284.5417.1158.

Hoshi, E., Tanji, J., 2007. Distinctions between dorsal and ventral premotor areas: anatomical connectivity and functional properties. Curr. Opin. Neurobiol. 17, 234–242. doi:10.1016/j.conb.2007.02.003.

Huk, A.C., Katz, L.N., Yates, J.L., 2017. The role of the lateral intraparietal area in (the study of) decision making. Annu. Rev. Neurosci. 40, 349–372. doi:10.1146/annurev-neuro-072116-031508.

Jacob, S.N., Vallentin, D., Nieder, A., 2012. Relating magnitudes: the brain's code for proportions. Trends Cogn. Sci. 16, 157–166. doi:10.1016/J.TICS.2012.02.002.

Kelly, S.P., O'Connell, R.G., 2013. Internal and external influences on the rate of sensory evidence accumulation in the human brain. J. Neurosci 33. doi:10.1523/JNEUROSCI.3355-13.2013, 19434 LP-19441.

Kim, J.-.N., Shadlen, M.N., 1999. Neural correlates of a decision in the dorsolateral prefrontal cortex of the macaque. Nat. Neurosci. 2, 176–185. doi:10.1038/5739.

Kriegeskorte, N., Goebel, R., Bandettini, P.A., 2006. Information-based functional brain mapping. Proc. Natl. Acad. Sci. U.S.A. 103, 3863–3868. doi:10.1073/pnas.0600244103.

Liu, T., Pleskac, T.J., 2011. Neural correlates of evidence accumulation in a perceptual decision task. J. Neurophysiol. 48824, 2383–2398. doi:10.1152/jn.00413.2011.

Nakayama, Y., Yamagata, T., Tanji, J., Hoshi, E., 2008. Transformation of a virtual action plan into a motor plan in the premotor cortex. J. Neurosci. 28, 10287–10297. doi:10.1523/JNEUROSCI.2372-08.2008.

Nieder, A., 2016. The neuronal code for number. Nat. Rev. Neurosci. 17, 366–382. doi:10.1038/nrn.2016.40.

Park, I.M., Meister, M.L.R., Huk, A.C., Pillow, J.W., 2014. Encoding and decoding in parietal cortex during sensorimotor decision-making. Nat. Neurosci. 17, 1395–1403. doi:10.1038/nn.3800.

O'Connell, R.G., Dockree, P.M., Kelly, S.P., 2012. A supramodal accumulation-to-bound signal that determines perceptual decisions in humans. Nat. Neurosci. 15, 1729.

Petrides, M., 1982. Motor conditional associative-learning after selective prefrontal lesions in the monkey. Behav. Brain Res. 5, 407–413. doi:10.1016/0166-4328(82)90044-4.

Ratcliff, R., Cherian, A., Segraves, M., 2003. A comparison of macaque behavior and superior colliculus neuronal activity to predictions from models of two-choice decisions. J. Neurophysiol. 90, 1392–1407. doi:10.1152/jn.01049.2002.

Ratcliff, R., Smith, P.L., Brown, S.D., McKoon, G., 2016. Diffusion decision model: current issues and history. Trends Cogn. Sci. 20, 260–281. doi:10.1016/j.tics.2016.01.007.

Roitman, J.D., Shadlen, M.N., 2002. Response of neurons in the lateral intraparietal area during a combined visual discrimination reaction time task. J. Neurosci. 22, 9475–9489. doi:10.1523/JNEUROSCI.22-21-09475.2002.

Romo, R., de Lafuente, V., 2013. Conversion of sensory signals into perceptual decisions. Prog. Neurobiol. 103, 41–75. doi:10.1016/j.pneurobio.2012.03.007.

Romo, R., Hernández, A., Zainos, A., 2004. Neuronal correlates of a perceptual decision in ventral premotor cortex. Neuron 41, 165–173. doi:10.1016/S0896-6273(03)00817-1.

Shadlen, M.N.N., Kiani, R., 2013. Decision making as a window on cognition. Neuron 80, 791–806. doi:10.1016/j.neuron.2013.10.047.

Shadlen, M.N., Newsome, W.T., 2001. Neural basis of a perceptual decision in the parietal cortex (area LIP) of the rhesus monkey. J. Neurophysiol. 86, 1916–1936. doi:10.1152/jn.2001.86.4.1916.

Swaminathan, S.K., Freedman, D.J., 2012. Preferential encoding of visual categories in parietal cortex compared with prefrontal cortex. Nat. Neurosci. 15, 315–320. doi:10.1038/nn.3016.

Swaminathan, S.K., Masse, N.Y., Freedman, D.J., 2013. A comparison of lateral and medial intraparietal areas during a visual categorization task. J. Neurosci. 33. doi:10.1523/JNEUROSCI.5723-12.2013, 13157 LP-13170.

Wang, L., Mruczek, R.E.B., Arcaro, M.J., Kastner, S., 2015. Probabilistic maps of visual topography in human cortex. Cereb. Cortex 25, 3911–3931. doi:10.1093/cercor/bhu277.

Wu, Y-h., Velenosi, L.A., Schröder, P., Ludwig, S., Blankenburg, F., 2019. Decoding vibrotactile choice independent of stimulus order and saccade selection during sequential comparisons. Hum. Brain Mapp. 1898–1907. doi:10.1002/hbm.24499.

Wu, Z., Litwin-Kumar, A., Shamash, P., Taylor, A., Axel, R., Shadlen, M., 2020. Context-dependent decision making in a premotor circuit. Neuron 106, 316–328. doi:10.1016/j.neuron.2020.01.034.

Yamagata, T., Nakayama, Y., Tanji, J., Hoshi, E., 2009. Processing of visual signals for direct specification of motor targets and for conceptual representation of action targets in the dorsal and ventral premotor cortex. J. Neurophysiol. 102, 3280–3294. doi:10.1152/jn.00452.2009.

Yamagata, T., Nakayama, Y., Tanji, J., Hoshi, E., 2012. Distinct information representation and processing for goal-directed behavior in the dorsolateral and ventrolateral prefrontal cortex and the dorsal premotor cortex. J. Neurosci. 32, 12934–12949. doi:10.1523/JNEUROSCI.2398-12.2012.

Zhou, Y., Freedman, D.J., 2019. Posterior parietal cortex plays a causal role in perceptual and categorical decisions. Science 365, 180–185. doi:10.1126/science.aaw8347.

Supplemental Information

B Attachments

Eidesstattliche Erklärung

Hiermit erkläre ich an Eides statt,

- dass ich die vorliegende Arbeit eigenständig und ohne unerlaubte Hilfe verfasst habe,
- dass Ideen und Gedanken aus Arbeiten anderer entsprechend gekennzeichnet wurden,
- dass ich mich nicht bereits anderwärtig um einen Doktorgrad beworben habe und keinen Doktorgrad in dem Promotionsfach Psychologie besitze, sowie
- dass ich die zugrundeliegende Promotionsordnung vom 08.08.2016 anerkenne.

BERLIN, 21.12.2023	LISA VELENOSI
Ort, Datum	Unterschrift

Erklärung gemäß § 7 Abs. 3 Satz 4 der Promotionsordnung über den Eigenanteil an den veröffentlichten oder zur Veröffentlichung vorgesehenen eingereichten wissenschaftlichen Schriften im Rahmen meiner publikationsbasierten Arbeit

I. **Name, Vorname:** Velenosi, Lisa Alexandria
Institut: Arbeitsbereich Neurocomputation and Neuroimaging
Promotionsfach: Psychologie
Titel: M.Sc.

II. **Nummerierte Aufstellung der eingereichten Schriften (Titel, Autoren, wo und wann veröffentlicht bzw. eingereicht)**:

1. Uluç I, **Velenosi LA**, Schmidt TT, Blankenburg F (2020). Parametric representation of tactile numerosity in working memory. *Eneuro*, *7*(1).

2. **Velenosi LA**, Wu YH, Schmidt TT, Blankenburg F (2020). Intraparietal sulcus maintains working memory representations of somatosensory categories in an adaptive, context-dependent manner. *NeuroImage*, *221*, 117146.

3. Wu YH, **Velenosi LA**, Schröder P, Ludwig S, Blankenburg F (2019). Decoding vibrotactile choice independent of stimulus order and saccade selection during sequential comparisons. *Human brain mapping*, *40(6)*, 1898 - 1907.

4. Wu YH, **Velenosi LA**, Blankenburg F (2021). Response modality-dependent categorical choice representations for vibrotactile comparisons. *NeuroImage*, *226*, 117592.

III. **Darlegung des eigenen Anteils an diesen Schriften:**

Die Bewertung des Eigenanteils richtet sich nach der Skala: “vollständig – überwiegend – mehrheitlich – in Teilen” und enthält nur für den jeweiligen Artikel relevante Arbeitsbereiche.

zu II. 1.: Konzeption (in Teilen), Versuchsdesign (in Teilen), Programmierung (in Teilen), Datenerhebung (in Teilen), Datenauswertung (in Teilen), Ergebnisdiskussion (in Teilen), Erstellen des Manuskriptes (in Teilen)

zu II. 2.: Konzeption (überwiegend), Versuchsdesign (überwiegend), Programmierung (vollständig), Datenerhebung (in Teilen), Datenauswertung (überwiegend), Ergebnisdiskussion (mehrheitlich), Erstellen des Manuskriptes (vollständig)

zu II. 3.: Konzeption (in Teilen), Versuchsdesign (in Teilen), Programmierung (in Teilen), Datenerhebung (in Teilen), Datenauswertung (in Teilen), Ergebnisdiskussion (in Teilen), Erstellen des Manuskriptes (in Teilen)

zu II. 4.: Konzeption (in Teilen), Versuchsdesign (in Teilen), Programmierung (in Teilen), Datenerhebung (in Teilen), Datenauswertung (in Teilen), Ergebnisdiskussion (in Teilen), Erstellen des Manuskriptes (in Teilen)

IV. **Die Namen und Anschriften nebst E-Mail oder Fax der jeweiligen Mitautorinnen oder Mitautoren:**

zu II. 1.: Dr. Isil Uluç, Athinoula A. Martinos Center for Biomedical Imaging, Department of Radiology, Massachusetts General Hospital, Charlestown, MA, 02129, USA & Harvard Medical School, Boston, MA, 02115, USA
E-Mail: http://iuluc@mgh.harvard.edu

Dr. Timo Torsten Schmidt, Neurocomputation and Neuroimaging Unit, Department of Education and Psychology, Freie Universität Berlin, 14195 Berlin, Germany
E-Mail: timo.t.schmidt@fu-berlin.de

Prof. Dr. med. Felix Blankenburg, Neurocomputation and Neuroimaging Unit, Department of Education and Psychology, Freie Universität Berlin, 14195 Berlin, Germany
E-Mail: felix.blankenburg@fu-berlin.de

zu II. 2.: Dr. Yuan-hao Wu, Neuroscience Institute, New York University Grossman School of Medicine, NY, 10016, USA
E-Mail: yuanhao.wu@nyulangone.org

Dr. Timo Torsten Schmidt, s.o.

Prof. Dr. med. Felix Blankenburg, s.o.

zu II. 3.: Dr. Yuan-hao Wu, s.o.

Dr. Pia Schröder, Former Member of Neurocomputation and Neuroimaging Unit, Department of Education and Psychology, Freie Universität Berlin, 14195 Berlin, Germany
E-Mail: pia-schroeder@web.de

Dr. Simon Ludwig, Former Member of Neurocomputation and Neuroimaging Unit, Department of Education and Psychology, Freie Universität Berlin, 14195 Berlin, Germany
E-Mail: simonludwig.sl@gmail.com

Dr. Felix Blankenburg, s.o.

zu II. 4.: Dr. Yuan-hao Wu, s.o.

Dr. Felix Blankenburg, s.o.

_____

Datum, Unterschrift der Doktorandin/ des Doktoranden

Ich bestätige die von Lisa Alexandria Velenosi unter III. abgegebene Erklärung:

Name: Prof. Dr. med. Felix Blankenburg Unterschrift _____

Name: Dr. Yuan-hao Wu Unterschrift _____

Name: Dr. Timo Torsten Schmidt Unterschrift _____

Name: Dr. Isil Uluç Unterschrift _____

Name: Dr. Pia Schröder Unterschrift _____

Name: Dr. Simon Ludwig Unterschrift _____